

**ADAPTIVE MODEL PREDICTIVE CONTROL WITH
GENERALIZED ORTHONORMAL BASIS FUNCTIONS**

Submitted in partial fulfillment of the requirements for

the degree of

Doctor of Philosophy

in

Chemical Engineering

Juan E. Morinelly Sanchez

B.S., Chemical Engineering, Michigan Technological University

M.S., Chemical Engineering, Michigan Technological University

Carnegie Mellon University

Pittsburgh, PA

October, 2017

Adaptive Model Predictive Control with Generalized Orthonormal Basis Functions, Ph.D. Thesis

© 2017 Juan E. Morinelly Sanchez

*“I have always believed, and I still believe, that whatever good or bad fortune may come our way
we can always give it meaning and transform it into something of value.”*

— Hermann Hesse

Siddartha (1922)

ACKNOWLEDGMENTS

I would like to start by recognizing several people that shaped my academic career prior to my time at Carnegie Mellon. I have the greatest memories from Michigan Tech, where it first occurred to me that I would, one day, pursue a PhD degree. I greatly appreciate the personal and professional guidance that Tomas Co and Faith Morrison gave me as an undergraduate student. I am thankful for the opportunity to be mentored by David Shonnard during my Masters at Michigan Tech, and David Miller, during my research appointment at NETL. Both of them always motivated my growth as a researcher and were personally invested in helping me succeed.

My advisor, Erik Ydstie, deserves a special mention for all the academic and personal support he has provided me during my PhD studies. Erik always has something valuable to say, I will certainly miss our conversations. I greatly appreciate the comments and observations he has made throughout the completion of this work. His ability to keep a good attitude is another teaching that I will take with me. I would also like to thank Professors Biegler, Sahinidis, and Ilic for being a helpful and accommodating committee.

Having two fellow Colombians, Pablo and German, around to guide me through the first year at Carnegie Mellon was a blessing. In our research group, Blake, Zixi, and Dana were always available to discuss an idea, or to have a friendly chat. My neighbors in the office from the Sahinidis group, Sree, Yash, Satya, Mustafa, Nick and others have always been a pleasure to be around. In general, I want to thank the CAPD student members as a group for creating such a motivating environment. Outside the department, my friends Sarah, Elliot, Alejandra, Irene, Manu and Leo were always supportive and this experience would not have been the same without having great times in between my studies.

My wife Christi has been the best partner in supporting this endeavor, I feel very fortunate to have her by my side. My parents Hector and Cecilia and my brothers Felipe and David have been far away during this period of my life but have remained my best friends. I would not have made it very far without the love and support I always find in our family.

I am grateful to the ACS Petroleum Research Fund and the Huang Family Foundation for their financial support.

ABSTRACT

An adaptive model predictive control (MPC) method using models derived from orthonormal basis functions is presented. The defining predictor dynamics are obtained from state-space realizations of finite truncations of generalized orthonormal basis functions (GOBF). A structured approach to define multivariable system models with customizable, open-loop stable linear dynamics is presented in Chapter 2. Properties of these model objects that are relevant to the adaptation component of the overall scheme, are also discussed. In Chapter 3, non-adaptive model predictive control policies are presented with the definition of extended state representations through filter operations that enable output feedback. An infinite horizon set-point tracking policy which always exists under the adopted modeling framework is presented. This policy and its associated cost are included as the terminal stage elements for a more general constrained case. The analysis of robust stability guarantees for the non-adaptive constrained formulation is presented, under the assumption of small prediction errors. In Chapter 4, adaptation is introduced and the certainty equivalence constrained MPC policy is formulated under the same framework of its non-adaptive counterpart. Information constraints that induce the excitation of the signals relevant to the adaptation process are formulated in Chapter 5. The constraint generation leverages the GOBF model structure by enforcing a sufficient richness condition directly on the state elements relevant to the control task. This is accomplished by the definition of a selection procedure that takes into account the characteristics of the most current parameter estimate distribution. Throughout the manuscript, illustrative simulation examples are provided with respect to minimal plant models. Concluding remarks and general descriptions for potential future work are outlined in Chapter 6.

CONTENTS

1	INTRODUCTION	1
1.1	Dual Control	3
1.2	Reinforcement Learning	4
1.3	Generalized Orthonormal Basis Functions and Adaptive MPC	5
1.4	Thesis Outline	7
2	PREDICTIVE MODELS WITH ORTHONORMAL BASIS FUNCTIONS	9
2.1	Plant Structure Preliminaries	9
2.1.1	MIMO Linear Plant	10
2.2	Rational Orthonormal Basis Functions	11
2.2.1	Generating Poles & Model Order	13
2.2.2	Common OBF Expansions	16
2.3	State-Space Realizations of OBF Models	18
2.3.1	All-Pass Cascade Decomposition	20
2.3.2	MISO Structure	30
2.4	GOBF Model Properties	31
2.4.1	Infinite Expansion	31
2.4.2	Asymptotic Properties of the Least-Squares Estimate	33
2.4.3	MIMO Model Error	35
2.5	Minimal GOBF Example	36

CONTENTS

2.6	Conclusions	43
3	GOBF MODEL PREDICTIVE CONTROL	45
3.1	Model Error Preliminaries	46
3.2	Tracking MPC Objective	48
3.2.1	Predictor Models with Backward Difference Filters	49
3.2.2	Infinite-Horizon Constant Reference Tracking	52
3.3	Extended Model	54
3.3.1	Input Record Model	55
3.3.2	Reference Signal Model	56
3.3.3	Optimal Control Problem	57
3.4	MPC Properties	58
3.4.1	Unconstrained Optimal Linear Controller	60
3.4.2	Constraints	62
3.4.3	Perfect Model & Constant Reference Disturbance	63
3.5	Robust Reformulation	66
3.5.1	Constraint Tightening	68
3.5.2	Artificial Steady-State	71
3.5.3	Reformulation	72
3.5.4	Input to State Stability	77
3.6	Summarizing Example	81
3.6.1	Experiment Definition	81
3.6.2	Output Feedback	81
3.6.3	Robust Reformulation	84
4	CERTAINTY EQUIVALENCE ADAPTIVE GOBF-MPC	91

4.1	Parameter Adaptation	92
4.1.1	Conditional Parameter Distribution	93
4.1.2	Recursive Least Squares Estimator	96
4.2	CE Adaptive Infinite-Horizon Tracking	97
4.2.1	SISO Mass-Spring Example	98
4.3	Certainty Equivalence Adaptive MPC	109
4.3.1	Optimal Control Problem	110
4.3.2	Quadruple Tank MIMO Plant Example	114
4.3.3	Quad-Tanks CE Adaptive MPC Results	117
4.4	Conclusions	125
5	INFORMATION CONSTRAINTS FOR GOBF MODELS	127
5.1	Information Preliminaries	128
5.1.1	Anticipated Information	128
5.1.2	Information Matrix	130
5.1.3	Information Maximization	131
5.1.4	Persistent Excitation	134
5.2	Review of Informative MPC Formulations	134
5.2.1	Dual Adaptive MPC (Heirung et al. 2017)	135
5.2.2	MPC with Experiment Constraint (Larsson et al. 2016)	137
5.2.3	Persistently Exciting MPC (Marafioti et al. 2014)	141
5.3	Informative GOBF MPC	143
5.3.1	SR GOBF State Constraint	145
5.3.2	Informative Optimal control Problem	149
5.3.3	Parameter Selection Heuristic	151

CONTENTS

5.3.4	Initialization	152
5.4	Implementation	153
5.4.1	Quad-Tank Simulation Results	155
5.5	Conclusions	164
6	CONCLUSIONS AND FUTURE WORK	165
6.1	Conclusions	165
6.1.1	Publications	166
6.2	Future work	167
6.2.1	Integration with Robust Controller	167
6.2.2	MIQP Reformulation	168
6.2.3	Further Experimental Validation	168
6.2.4	Adaptive Control with Physical Constraints	169
	BIBLIOGRAPHY	171

LIST OF FIGURES AND ILLUSTRATIONS

Figure 1.1	Thesis Overview Diagram	7
Figure 2.1	OBF SISO Model Structure	17
Figure 2.2	All-Pass Decomposition	22
Figure 2.3	GOBF Step Response	29
Figure 2.4	Model Error Diagram	35
Figure 2.5	Connected Mass-Spring System	37
Figure 2.6	Mass-Spring Laguerre ($n = 4$) Step Response	38
Figure 2.7	Mass-Spring Laguerre ($n = 4$) Sine Input Response	39
Figure 2.8	GOBF Pole Locations	41
Figure 2.9	Mass-Spring GOBF ($n = 4$) Step Response	41
Figure 2.10	Mass-Spring GOBF ($n = 4$) Sine Input Response	42
Figure 2.11	Mass-Spring GOBF ₃ ($n = 4$) Step Response State Decomposition	42
Figure 3.1	Structural Model Error	46
Figure 3.2	Output Feedback in MPC with GOBF Models	50
Figure 3.3	Bounded Disturbance Cost	75
Figure 3.5	Infinite-Horizon Tracking Policy, Approximate Model	83
Figure 3.4	Unfiltered LQ Policy, Approximate Model	83
Figure 3.6	Extended State Tracking Policy, Approximate Model	84
Figure 3.7	Robust Tracking Policy, Perfect Model	85

LIST OF FIGURES AND ILLUSTRATIONS

Figure 3.8	Robust Tracking Policy, Approximate Model	86
Figure 3.9	Lyapunov Descent and Output Disturbance, Approximate Model	87
Figure 3.10	Robust Tracking Policy with Higher Offset Cost, Approximate Model	87
Figure 3.11	Robust Tracking Policy Constraint Enforcement, Approximate Model	88
Figure 4.1	Adaptive GOBF MPC	92
Figure 4.2	FIR Control	99
Figure 4.3	FIR Estimation	100
Figure 4.4	Laguerre Control with $n = 4$	100
Figure 4.5	Laguerre Estimation with $n = 4$	101
Figure 4.6	Laguerre Control with $\xi = 0.8$	102
Figure 4.7	Laguerre Estimation with $\xi = 0.8$	102
Figure 4.8	Laguerre Higher Order Estimation with $\xi = 0.8$	103
Figure 4.9	GOBF Pole Locations	104
Figure 4.10	GOBF Control with $n = 4$	104
Figure 4.11	GOBF Estimation with $n = 4$	105
Figure 4.12	Fixed Denominator Control	107
Figure 4.13	Fixed Denominator Estimation	107
Figure 4.14	Information Inverse Conditioning	109
Figure 4.15	Quad-Tank System Diagram	114
Figure 4.16	Linearized Quad-Tank Model Pole Locations	117
Figure 4.17	Quad-Tank Model 1 Output Profiles	119
Figure 4.18	Quad-Tank Model 1 Input Profiles	120
Figure 4.19	Quad-Tank Model 2 Output Profiles	120
Figure 4.20	Quad-Tank Model 2 Input Profiles	121

Figure 4.21	Quad-Tank Model 3 Output Profiles	121
Figure 4.22	Quad-Tank Model 3 Input Profiles	122
Figure 4.23	Quad-Tank Filtered Error for Models 1-3	123
Figure 4.24	Quad-Tank Parameter Estimation	124
Figure 5.1	Ellipsoidal Parameter Confidence Region Transient	132
Figure 5.2	Quad-Tank Adapted Parameter Covariance with SR Constraints	157
Figure 5.3	Quad-Tank Regulation SR Input Detailed Profiles	158
Figure 5.4	Quad-Tank Regulation SR Parameter Estimation	158
Figure 5.5	Quad-Tank Output Profile Reference Intervals 1-2	159
Figure 5.6	Quad-Tank Input Profile Reference Intervals 1-2	160
Figure 5.7	Quad-Tank SR Activation	160
Figure 5.8	Quad-Tank Control Output Profiles	161
Figure 5.9	Quad-Tank Control Input Profiles	161
Figure 5.10	Off-Diagonal SISO Filters Parameter Estimation	163

LIST OF TABLES

Table 2.1	Common OBF expansions	17
Table 2.2	All-Pass Building Blocks	28
Table 3.1	Standard Nominal Stability Conditions	64
Table 4.1	Quad-Tank Model Nominal Parameters	115
Table 4.2	Initial Model Parameterization for CE Adaptive Control Experiments	118
Table 5.1	SR GOBF State Selection Index	162

INTRODUCTION

There has been a great deal of progress in the field of Model Predictive Control (MPC) over the last couple of decades. Advances in dynamic optimization allow current non-linear MPC formulations to solve problems with hundreds of thousands of variables in the order of seconds ([Biegler et al. 2015](#)). Other recent significant developments include the extension of the objective function to more general forms with Economic MPC formulations ([Griffith et al. 2017](#)) and the inclusion of discrete actuators in the problem formulation ([Rawlings & Risbeck 2017](#)). A summarizing overview of notable achievements and promising new directions can be found in ([Mayne 2014](#)). Meanwhile, meaningful advances in the specific field of adaptive MPC have been less common over the same period. This has been mainly caused by the loss of feasibility guarantees that can often be claimed for the non-adaptive case. As a direct consequence, assertions derived from Lyapunov theory with respect to closed-loop stability and robustness using classical approaches ([Goodwin & Sin 1984](#)) are no longer applicable.

Nonetheless, some adaptive MPC formulations that integrate linear model estimation attributes in their design have emerged in the literature. A defining distinction that can be

INTRODUCTION

made with respect to the proposed methods is whether the formulation *actively* engages in the generation of signals that enable adaptation or this is done *passively* through the modification of the estimator. An example of the passive approach is the set-membership identification formulation by [Tanaskovic et al. \(2014\)](#). In this method, a bounded number of models, belonging to a fixed finite impulse response (FIR) model structure, is updated recursively. The receding horizon problem is defined to satisfy constraints over all the members of the model ensemble.

The approach to be presented here belongs to the active learning class. A common feature found in this type of methods, is the incorporation of the evolution of information into the constraint set of the optimal control problem. The most relevant approaches to our work are the dual adaptive MPC by [Heirung et al. \(2017\)](#), the experiment design constrained formulation by [Larsson et al. \(2016\)](#), and, most notably, the persistent excitation formulation by [Marafioti et al. \(2014\)](#). The theoretical basis and practical implications for these three approaches are reviewed in detail in Chapter 5. Another notable recent contribution with a similar structure, is the information matrix maximization approach of [Rathouský & Havlena \(2013\)](#). Instead of constraining the problem directly, the information maximization feature is defined by a second stage optimization. The original idea of including persistent excitation constraints to a predictive controller can be attributed to [Genceli & Nikolaou \(1996\)](#). Their method is based an iterative semidefinite programming approach to induce simultaneous model identification in an MPC problem for Single-Input Single-Output (SISO) FIR systems.

1.1 DUAL CONTROL

A conceptual framework for the inclusion of active exploration in the control of uncertain systems was proposed by [Feldbaum \(1960\)](#) as Dual Control Theory. In this seminal work, the conflicting aspects of control and estimation are formalized as action and investigation risks. The former is characterized as the loss incurred by probing the system for identification, steering it away from the desired or best attainable state. The latter, is its counterpart from the estimation point of view. It represents the loss incurred by trying to reach the desired state with no regard for the quality of the information generated in the closed loop. Therefore, it is argued, the input to the system should be defined by an optimal trade-off of these risks. A purely *exploitative* control would not lead to the concentration of the probability densities of the uncertainty of the system. On the other hand, a purely *explorative* control would deviate the system dynamics unnecessarily away from its desired state.

As it will be shown, an adaptive MPC optimal control problem offers the opportunity to express these risks as components of the objective function and the constraint set. In our approach, the optimal trade-off of Dual Control will be determined by parameters in the design that enforce the recursive generation of a desired level of information which in turn lead to a reduction of the uncertainty of the parameter estimate.

1.2 REINFORCEMENT LEARNING

1.2 REINFORCEMENT LEARNING

Approximate Dynamic Programming (ADP) and Reinforcement Learning (RL) methods have been an increasingly active research area in many engineering disciplines (Lewis & Liu 2013). These methods provide a similar structure for feedback control of complex, uncertain systems. Sutton & Barto (1998) define the theoretical basis of RL under three characteristics of the problem to be solved: the *closed-loop* nature of the interaction between an agent and its environment, an agent that must *discover* which actions yield the most rewards, and a performance evaluation that considers *extended* periods. In the RL context, the agent can be viewed as the MPC algorithm itself, which computes actions adaptively by solving an optimal control problem defined by the environment's response in the form of output measurements.

Most of the research in this field is applicable to systems with discrete action and state spaces. The solutions to these problems often involve different mathematical approaches than those of MPC. A notable exception is Q-learning for uncertain discrete linear systems with an infinite quadratic cost (Bradtke et al. 1994). An adaptive policy iteration scheme is defined by the parametrization of the state-action Q-function in terms of bilinear features formed by the state and input elements of the system. Convergence to an optimal policy is achieved by the addition of an exploratory component to the current estimate of the optimal linear policy.

1.3 GENERALIZED ORTHONORMAL BASIS FUNCTIONS AND ADAPTIVE MPC

The backbone of MPC methods is the ability of the model structure to make accurate predictions. Adaptation is introduced with the specific purpose of interacting with the model structure towards this objective. This is not always accomplished in an efficient manner. One could argue that conventional linear modeling approaches that have attractive properties for their offline *identification* may not have the appropriate structure for their adjustment online in an adaptive scheme. For example, consider the Autoregressive Exogenous (ARX) model form,

$$y_t + a_1 y_{t-1} + \dots + a_{n_a} y_{t-n_a} = b_1 u_{t-1} + \dots + b_{n_b} u_{t-n_b} + e_t. \quad (1.1)$$

This linear structure is at the heart of the most defining contributions to the field of adaptive control in the twentieth century. Its coefficients may be determined with least squares methods and the direct use of elements of the input-output data record. The formulation of the self tuning regulator by [Åström & Wittenmark \(1973\)](#) and the later generalization to multivariable systems by [Goodwin et al. \(1980\)](#) were originally framed around this type of model. The issues may not be evident when computing dead-beat control actions with ARX estimates. However, when considering multi-step predictions required in the receding horizon approach inherent of MPC, significant challenges may surface. Most notably, the lack of stabilizability guarantees of a particular realization provided by the online estimator. This leads to the so called admissibility problem which can be solved by parallel estimation ([Middleton et al. 1988](#)) or non-convex optimization ([Staus et al. 1996](#)). These methods are still computationally expensive and hard to apply for multivariable

1.4 THESIS OUTLINE

systems. Moreover, model (1.1) can lead to ill-conditioned problems when there are close pole-zero cancellations. These challenges also emerge for identification approaches with state-space models. For this case, in general, the linearity of the estimation is also lost.

Beyond addressing the limitations described above, a good modeling alternative must facilitate the incorporation of plant knowledge into the model, making accurate predictions more plausible, while facilitating the parallel adaptation component. In this manuscript, we propose the Generalized Orthonormal Basis Functions (GOBF) modeling approach, as a compelling framework to study. This choice limits the applicability to systems that can be accurately approximated with open-loop stable linear models. This scope still covers many interesting control problems encountered in process systems. A comprehensive compilation of contributions to the identification and modeling aspects of GOBF expansions can be found in (Heuberger et al. 2005).

The use of orthonormal expansions in predictive control was originally proposed by the non-adaptive MPC formulation of Finn et al. (1993). The model structure considered in this work is referred to as Markov-Laguerre functions. It consists of the arrangement of two blocks in which the leading component has the FIR structure and the second portion has an all pass component derived from a first order orthonormal element. Sbarbaro et al. (1999) proposed a variety of unconstrained active strategies with different modifications to the objective function using orthonormal basis models. Both formulations are applied to SISO systems.

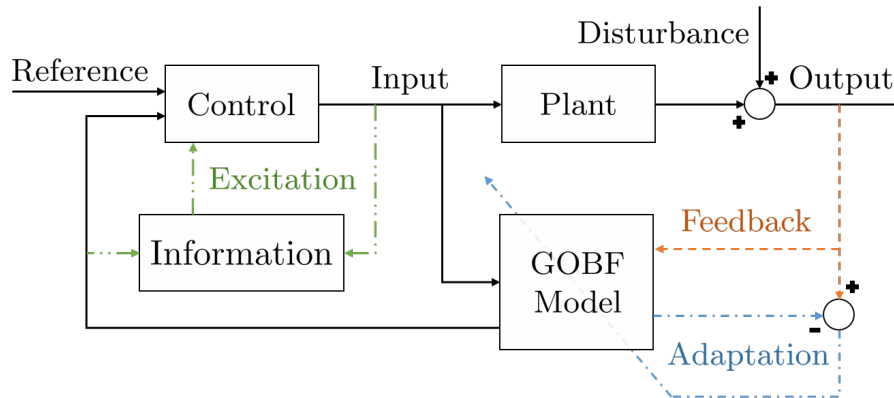


Figure 1.1: Thesis Overview Diagram

1.4 THESIS OUTLINE

In the subsequent chapters, we will disaggregate the exposition of the overall method according to the block components illustrated in Figure 1.1. As a first logical step, the relevant properties of the GOBF approach as well as a construction method for Multi-Input Multi-Output (MIMO) state-space model objects will be presented in Chapter 2. The Markov-Laguerre block structure of Finn et al. (1993) will be generalized by more detailed structures with irreducible orthonormal contributions.

Provided with fixed linear dynamic models, the formulation of output feedback MPC policies will be provided in Chapter 3. The feedback feature is an important element to the overall framework since the state vectors associated with a GOBF models are filtered versions of the input record. This is accomplished by the modification of the state-space models defined in Chapter 2 with backwards difference filters. This model adjustment leads to an alternative predictor representation that incorporates output measurements and previous inputs as elements of an extended state.

1.4 THESIS OUTLINE

The Certainty Equivalence (CE) adaptive MPC algorithm with GOBF models is specified in Chapter 4. It leverages the feedback component and other useful elements from the fixed model formulations in the preceding chapter. The effect of different orthonormal expansions in the adaptive control performance is analyzed. A method to obtain suitable generating poles with available linear model representations is outlined and demonstrated in an illustrative quadruple tank MIMO system.

Chapter 5 presents a modification to the CE problem that induces an active learning strategy consistent with Dual Control Theory. Excitation is introduced throughout the SISO subcomponents of the MIMO model by defining information constraints specific to each input channel. This is accomplished by extending the ideas of Marafiori et al. (2014) in terms of the scalar state elements that constitute the GOBF system representation. The approach is demonstrated in a scenario that extends the analysis of the illustrative MIMO plant example from Chapter 4. The dissertation is concluded with a set of summarizing conclusions and proposed future work in Chapter 6.

2

PREDICTIVE MODELS WITH ORTHONORMAL BASIS FUNCTIONS

This chapter provides a general introduction to Generalized Orthonormal Basis Functions (GOBFs) models. In addition, a method to construct Multi-Input, Multi-Output (MIMO) state-space models, suitable for Model Predictive Control (MPC) within this framework is presented. The MIMO model is generated by the decomposition of the plant into scalar transfer function elements for each input-output pair. An algorithm to obtain Single-Input, Single-Output (SISO) filters of arbitrarily high order and customizable dynamics is presented. The desired MIMO structure is obtained through the appropriate arrangement of these components. The SISO modeling approach is illustrated through a minimal mass-spring example.

2.1 PLANT STRUCTURE PRELIMINARIES

Since we are ultimately interested in the modeling of a MIMO system, we begin by stating the assumptions on the structure of the plant to be modeled.

2.1 PLANT STRUCTURE PRELIMINARIES

2.1.1 MIMO Linear Plant

The plant of interest is assumed to have stable, linear dynamics for each SISO pair. The output signal $\mathbf{y} \in \mathbb{R}^{n_y}$ is related to the input $\mathbf{u} \in \mathbb{R}^{n_u}$ with n_u by

$$\mathbf{y}_t = \mathbf{G}_p(q)\mathbf{u}_t + \mathbf{v}_t \quad (2.1)$$

where

- $\mathbf{G}_p(q)$ is a $n_y \times n_u$ matrix filter in the shift operator q

$$\mathbf{G}_p(q) = \begin{bmatrix} G_{11}(q) & G_{12}(q) & \cdots & G_{1n_u}(q) \\ G_{21}(q) & G_{22}(q) & \cdots & G_{2n_u}(q) \\ \vdots & \vdots & \ddots & \vdots \\ G_{n_y1}(q) & G_{n_y2}(q) & \cdots & G_{n_y n_u}(q) \end{bmatrix}$$

- The disturbance signal is bounded, $\mathbf{v}_t \in \mathbb{R}^{n_y}$, $\|\mathbf{v}_t\|^2 \leq k_v$

The indexing ij specifies a given input-output pair. The shift operator and its inverse, are defined to act on a discrete time signal x_t according to

$$q^{-1}x_t = x_{t-1}$$

$$qx_{t-1} = x_t.$$

A detailed account of this model description and other related concepts can be found in standard system identification literature (Ljung 1999). The disturbance signal, v_t , is modeled as a stationary process with $\mathbf{v}_t = \mathbf{H}_v(q)\boldsymbol{\nu}_t$, $\boldsymbol{\nu}_t \sim \mathcal{N}(\mathbf{0}, \boldsymbol{\Lambda})$. \mathbf{H}_v is a $n_y \times n_y$ matrix transfer function, under the assumption of stable, monic diagonal elements and zeros

everywhere else. It is further assumed that it is independently parametrized with respect to \mathbf{G}_p . The model approach to be developed in the subsequent sections, focuses on the input-output dynamics and satisfies these assumptions with the simplest fixed output error model, $\mathbf{H}_v(q) = \mathbf{I}$.

The assumed linearity and stability of the elements of \mathbf{G}_p imply that they can be represented by a rational scalar transfer function and its corresponding infinite impulse response,

$$G_{ij}(q) = \sum_{k=0}^{\infty} g_{ij,k} q^{-k} \quad (2.2)$$

This characterization corresponds to proper transfer function elements. It is further assumed that these are strictly proper. Therefore,

$$\lim_{|z| \rightarrow \infty} G_{ij}(z) = 0 \implies g_{ij,0} = 0.$$

Which follows from the equivalence of expressions for filters in the shift operator q and transfer functions in the complex variable z . Combining the assumed stability and the previous condition,

$$\sum_{k=0}^{\infty} |g_{ij,k}| < \infty \implies \sum_{k=1}^{\infty} |g_{ij,k}| < \infty$$

which is equivalent to bounded-input bounded-output (BIBO) stability.

2.2 RATIONAL ORTHONORMAL BASIS FUNCTIONS

The Laurent expansion elements that define the sum in equation (2.2) (i.e. $\{z^{-k}\}_{k=1}^{\infty}$) constitute the simplest case of a more structured general class of transfer functions that

define a rational orthonormal basis. As their name indicates, there are three properties for a specific set of functions to constitute such set. First, they can be expressed as the ratio of polynomial filters. Second, every subset of the basis must be orthonormal, as defined by the inner product of the defining function space. Lastly, the elements of the basis must form a structured basis which define a complete infinite expansion for any function in this space.

The space of interest is defined in the complex plane as the Hardy space of square integrable linear functions on the unit circle, (\mathbb{T}) , analytic on its exterior, denoted by \mathcal{H}_2 . Under the stated assumptions, this space contains the stable scalar transfer function components of $\mathbf{G}_p(q)$, the matrix-value filter in equation (2.1). The discussion will be limited to the subset of transfer functions in \mathcal{H}_2 with real-valued impulse responses. Under this restriction, the inner product and its corresponding norm for two functions $G_1, G_2 \in \mathcal{H}_2$ is given by¹

$$\begin{aligned}\langle G_1, G_2 \rangle &:= \frac{1}{2\pi i} \oint_{\mathbb{T}} G_1(z) G_2(z^{-1}) \frac{dz}{z} \\ \|G\| &:= \sqrt{\langle G, G \rangle}\end{aligned}$$

A similar operation, can be defined for matrix-valued transfer functions. In particular, it will be useful to define the outer product for real-valued vector functions $\mathbf{F}, \mathbf{G} \in \mathcal{H}_2^n$,

$$[[\mathbf{F}, \mathbf{G}]] := \frac{1}{2\pi i} \oint_{\mathbb{T}} \mathbf{F}(z) \mathbf{Y}^\top(z^{-1}) \frac{dz}{z}.$$

¹ In general, for functions with complex-valued impulse responses the second function in the integrand is replaced by its complex conjugate.

Definition 1. *Orthonormal Set in \mathcal{H}_2 .* A set of scalar transfer functions, $\mathbf{F} = \{F_1, F_2, \dots\}$, with scalar components in \mathcal{H}_2 is orthonormal if it satisfies

$$\langle F_i, F_j \rangle = \delta_{ij} = \begin{cases} 0, & \text{for } i = j \\ 1, & \text{for } i \neq j \end{cases}$$

for any i and j that define an element in the set.

Note that for a vector-valued function with n entries from an orthonormal set \mathbf{F} , $\mathbf{F}_n \in \mathcal{H}_2^n$, the outer product gives the identity matrix, *i.e.* $[\mathbf{F}_n, \mathbf{F}_n] = \mathbf{I}$. It follows from Cauchy's Residue Theorem that the impulse response functions satisfy orthonormality as defined above.

Definition 2. *Complete Orthonormal Basis.* If the error obtained from a finite truncation defined by the elements from an orthonormal basis, $\mathbf{F} = \{F_1, F_2, \dots\}$, is bounded and can be made arbitrarily small uniformly across all frequencies for any $G(z) \in \mathcal{H}_2$, \mathbf{F} is said to be complete.

$$\left| \sum_{k=1}^n g_k F_k(z) - G(z) \right| < \infty, \quad \sum_{k=n+1}^{\infty} |g_k| \rightarrow 0, \quad \text{as } n \rightarrow \infty \quad (2.3)$$

where the expansion coefficients are defined by $g_k := \langle G, F_k \rangle$.

2.2.1 Generating Poles & Model Order

An orthonormal basis can be defined in terms of its generating poles contained on a complex-valued set, ξ . Following standard transfer function notation, the poles corre-

spond to the roots of the denominator polynomials for all the transfer function elements in the basis. For example, a finite impulse response (FIR) model is generated by a basis defined by a singleton with a pole located at the origin of the complex plane, $\xi = 0$. This choice is attractive due to its generality and simplicity. Since it is also complete, a desired level of accuracy can be achieved with a truncation of sufficiently high order.

In terms of an identification, the associated regression problem is defined by a finite sequence of past inputs. If one could afford extensive experimentation, unlimited flexibility in input design, and no regard for model order, FIR models would be an excellent choice. This is obviously not the case in control design for process systems. Nevertheless, the step response model, which inherits the same limitations, is used in most commercial applications of model predictive control². A better choice would be to select generating poles that reflect available information with respect to the system to be modeled. The FIR and step response model choices corresponds to the situation of knowing nothing beyond the fact that the plant can be accurately described by a model object in \mathcal{H}_2 .

The most prominent feature of the GOBF modeling approach is the ability to retain some of the generality and simplicity of the FIR approach while reducing the order of the parameter space required for a comparable level of accuracy (Heuberger et al. 2005). In general, accurate locations of the poles may not be available. However, as long as the model is generated from a complete basis with approximate pole locations, the error is bounded according to the expressions in (2.3). This idea can be expressed more exactly for any basis that adheres to the general Takenaka-Malmquist (TM) form,

$$F_k(q) = \frac{\sqrt{1 - |\xi_k|^2}}{q - \xi_k} \prod_{i=1}^k \left(\frac{1 - \bar{\xi}_i q}{q - \xi_i} \right)$$

² e.g. Emerson's DeltaV, Aspen DMC

Completeness can be shown to hold for any TM basis (Ninness & Gómez 1996) if and only if the associated infinite sequence of generating poles $\{\xi_k\}_{k=1}^{\infty}$ satisfies

$$\sum_{k=1}^{\infty} (1 - |\xi_k|) = \infty \quad (2.4)$$

From equation (2.4) it is clear that a complete TM basis is restricted to generating poles in the unit disk, $|\xi_k| < 1$. For the purpose of obtaining models suitable for control design, the generating poles and the expansion order are treated as higher order parameters that remain fixed. These structural properties are meant to be maintained based on the monitoring of appropriate measures of the data record, and known changes of the underlying plant processes.

With a fixed basis and truncation order, the identification task reduces to specifying the coefficients for the model structure denoted by the subscript m . Recall that the values for the infinite expansion coefficients are determined by the inner product of the system and a basis function element, $\langle G, F_k \rangle$. Since the plant is not known exactly, these are uncertain. Therefore, the model must be parametrized with the aid of system identification routines.

In terms of the SISO decomposition of the model for (2.1), a parameter vector, θ_{ij} , must be estimated for each scalar filter element in the model. The corresponding SISO and MIMO predictor filters are defined by,

$$\hat{y}_{ij,t} := G_{ij,m}(q; \theta_{ij}) u_{j,t} \quad (2.5a)$$

$$\hat{\mathbf{y}}_t := \mathbf{G}_m(q; \boldsymbol{\theta}) \mathbf{u}_t. \quad (2.5b)$$

This scalar contribution architecture allows flexibility in the control design to only include the relevant dynamics among all input-output pairs and customize their generating pole set and estimator order. The MIMO model \mathbf{G}_m in equation (2.5b) is parameterized by a vector, $\boldsymbol{\theta} \in \boldsymbol{\Theta} \subset \mathbb{R}^n$, that contains all the SISO contributions to be identified. It is therefore desirable to reduce the MIMO model parameter dimension,

$$n = \sum_{i=1}^{n_y} \sum_{j=1}^{n_u} n_{ij},$$

for a given level of truncation error. As demonstrated by the illustrative example in the last section, this is enabled by the appropriate selection of the generating poles.

2.2.2 Common OBF Expansions

Consider an individual SISO predictor (2.5a) generated with orthonormal elements of a complete basis and drop the ij index for simplicity. The parametrization, just like in the FIR case, is linear in the parameters with respect to an information vector. Instead of being defined directly by the input record, this vector is obtained from the application of a vector-valued linear filter. This follows from the decomposition of the associated scalar filter, $G_m(q; \boldsymbol{\theta})$,

$$\begin{aligned} G_m(q; \boldsymbol{\theta}) &= \sum_{k=1}^n \theta_k F_k(q) \\ &= \boldsymbol{\theta}^\top \mathbf{F}_n(q). \end{aligned}$$

The elements of \mathbf{F}_n define the information vector at each time t as shown in equation (2.6). The linear structure for a given SISO predictor is illustrated in Figure 2.1. From

this illustration, it is clear that truncation coefficients that lead to accurate predictor structures depend on the fixed vector-valued filter. Therefore, they are also functions of the generating pole and order specified in the model structure.

$$\varphi_t := \mathbf{F}_n(q)u_t, \quad \mathbf{F}_n = \begin{bmatrix} F_1(q) \\ F_2(q) \\ \vdots \\ F_n(q) \end{bmatrix} \quad (2.6)$$

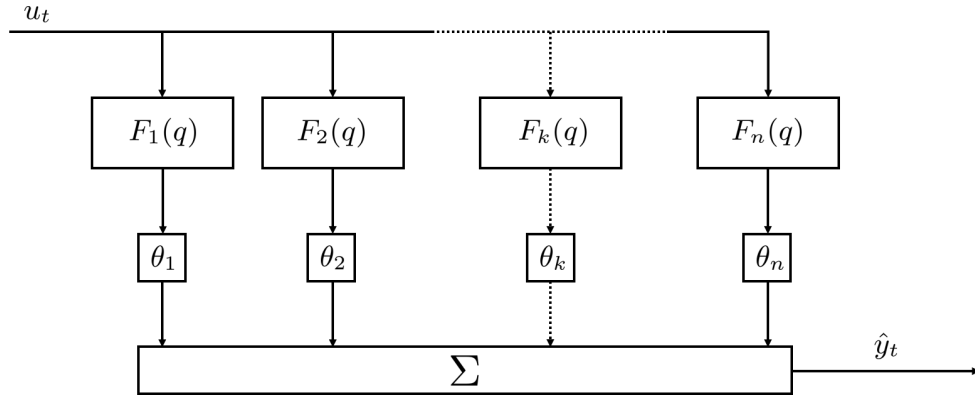


Figure 2.1: OBF SISO Model Structure

Table 2.1 lists common choices for OBF expansions suitable for the definition of linear process models.

Table 2.1: Common OBF expansions

Name	Generating Poles	Scalar Filter	All-Pass Filter
FIR	$\xi_k = 0$	$F_k(q) = \frac{1}{q} \Gamma_{k-1}(q)$	$\Gamma_k(q) = \frac{1}{q^k}$
Laguerre	$\xi_k = \xi \in \mathbb{R}$	$F_k(q) = \frac{\sqrt{1-\xi^2}}{q-\xi} \Gamma_{k-1}(q)$	$\Gamma_k(q) = \left(\frac{1-\xi q}{q-\xi}\right)^k$
TM	$\xi_k \in \mathbb{C}$	$F_k(q) = \frac{\sqrt{1- \xi_k ^2}}{q-\xi_k} \Gamma_{k-1}(q)$	$\Gamma_k(q) = \prod_{i=1}^k \left(\frac{1-\bar{\xi}_i q}{q-\xi_i}\right)$

2.3 STATE-SPACE REALIZATIONS OF OBF MODELS

Note that the FIR and Laguerre functions are special cases of the TM expansion. One could conclude that this choice is sufficiently rich for control design for any function in \mathcal{H}_2 . An obvious caveat to this approach is that the information vector would, in general, contain complex-valued signals. This would not be an issue if the design is limited to real-valued poles, forcing $\varphi_t \in \mathbb{R}^n$. However, this restriction impedes the efficient representation of systems dominated by under-damped dynamics. To address this challenge, we follow a generalized construction method derived from state-space realizations of TM all-pass filters (Bodin et al. 2000), displayed in the bottom right corner in Table 2.1. In particular, the minimal Kautz all-pass filter, defined by a conjugate pair of poles will provide an important component to the approach.

2.3 STATE-SPACE REALIZATIONS OF OBF MODELS

The objective of this section is to specify a systematic approach to define a MIMO state-space representation,

$$\begin{aligned}\varphi_{t+1} &= \mathbf{A}_\xi \varphi_t + \mathbf{B}_\xi \mathbf{u}_t \\ \hat{\mathbf{y}}_t &= \mathbf{C}_\theta \varphi_t,\end{aligned}\tag{2.7}$$

for the predictor filter $\mathbf{G}_m(q)$ in equation (2.5). In the subsequent chapter, this linear relationship will define the profiles to be optimized as a function of a finite sequence of control actions in the MPC framework. The subscript ξ indicates that the matrices in model (2.7) are defined by the set of generating poles used in the construction of the predictor structure based on prior information. On the other hand, the state-output predictor matrix, \mathbf{C}_θ , is parametrized by the vector θ .

A flexible state-space model generation method that allows the inclusion of the following relevant features for process control is desired:

- Multi-Input Multi-Output (MIMO)
- Delays, first and second order contributions
- Systems with right half plane zeros (inverse response)
- Under-damped (oscillatory) dynamics
- Embedded stabilizability

With respect to the last point, a very useful property that is automatically satisfied by any OBF expansion choice for the predictor model, is the inherent stability of the dynamics. This property holds independently of the realization of the uncertain parameter, θ , since any OBF choice only spans functions in \mathcal{H}_2 . This in turn leads to the ability to specify convex regions for the admissible parameters in the estimation process. This is not necessarily the case for other linear modeling approaches, such as auto-regressive exogenous (ARX) filters and general state-space models identified with a subspace method.

Following the SISO decomposition presented above, we begin by the simplified treatment for this case. Consider first a design with a single generating pole, $\xi \in \mathbb{R}$, and a given order, n , as shown by the middle row of Table 2.1. The resulting information vector dynamics can be expressed with the following one-pole Laguerre state-transition model,

$$\mathbf{A}_\xi = \begin{bmatrix} \xi & 0 & \cdots & 0 \\ (1 - \xi^2) & \xi & \ddots & \vdots \\ \vdots & \ddots & \ddots & 0 \\ (-\xi)^{n-2}(1 - \xi^2) & \cdots & (1 - \xi^2) & \xi \end{bmatrix}, \quad \mathbf{b}_\xi = \sqrt{1 - \xi^2} \begin{bmatrix} 1 \\ -\xi \\ \vdots \\ (-\xi)^{n-1} \end{bmatrix}.$$

Note that with the generating pole at the origin, these pair collapses to an FIR model. Simple approaches as the one-pole Laguerre are limited with respect to some of the features listed above.

Based on the properties discussed thus far, it should be apparent that customized OBF expansions can offer much more. For obvious reasons, the design of predictive controllers should include as much available prior information as the modeling framework can afford. In an OBF model, this information is contained in the set of generating poles. A generalized OBF (GOBF) model is simply defined by the inclusion of as many distinct pole locations in the unit disk as required. The specification of the corresponding infinite expansion elements is given in the next section. As discussed previously, from the perspective of identification of the MIMO model, variety in the generating pole set could be favorable, as long as the locations of the poles is selected in a way that reduces the required order of the vector that parametrizes the predictor matrix filter in equation (2.5b).

2.3.1 *All-Pass Cascade Decomposition*

We adopt the cascading of all-pass filters with known state-space realizations (Bodin et al. 2000) as the method of choice to build model (2.7). This approach is efficient in obtaining the desired difference equations since it circumvents the specification of the vector-valued filter structure in equation (2.6) and provides a single input state-transition pair $\{\mathbf{A}_\xi, \mathbf{b}_\xi\}$ directly. An all-pass filter is defined by the property of having a unit-gain for all frequencies. This holds if the filter satisfies

$$\Gamma(q)\Gamma(q^{-1}) = 1.$$

The last column of Table 2.1 includes some examples of orthogonal all-pass filters. Orthogonality of the filter is also given by an input balanced state-space realization. That is, the scalar all-pass filter $\Gamma(q)$ can be parametrized with $\{\mathbf{A}, \mathbf{b}, \mathbf{c}, d\}$ such that for $y_t = \Gamma(q)u_t$,

$$y_t = \left(d + \mathbf{c}(q\mathbf{I} - \mathbf{A})^{-1}\mathbf{b} \right) u_t, \quad \mathbf{A}\mathbf{A}^\top + \mathbf{b}\mathbf{b}^\top = \mathbf{I} \quad (2.8)$$

In general, a scalar filter has both properties (all-pass and orthogonality) if and only if its state-space realization satisfies

$$\begin{bmatrix} \mathbf{A} & \mathbf{b} \\ \mathbf{c} & d \end{bmatrix} \begin{bmatrix} \mathbf{A} & \mathbf{b} \\ \mathbf{c} & d \end{bmatrix}^\top = \mathbf{I} \quad (2.9)$$

Furthermore, the connection in series of all-pass orthogonal filters retains both properties (Mullis & Roberts 1976). The state-transition pair for the cascade, defines a vector-valued transfer function that can be used as the defining object to generate a GOBF infinite expansion.

The restriction of dealing with real-valued vectors φ requires that complex poles are included in conjugate pairs. The first step in generating the model is ordering the set of poles to be included in a given SISO predictor filter (2.5a) with complex pairs adjacent to each other. Such an ordered set allows the definition of a TM all-pass filter that decomposes into first order Laguerre and second order Kautz blocks that are themselves all-pass. In addition to these elemental units, fixed order FIR blocks can be included in the structure by setting sequences of zeros of the corresponding size in the ordered generating set (Finn et al. 1993).

2.3 STATE-SPACE REALIZATIONS OF OBF MODELS

The result is a blueprint for a TM all-pass filter with \tilde{n} elemental components and a state-space realization of order n , equal to the sum of the order of all contributions. The derivation of the irreducible real-valued blocks suitable for the cascading operation depicted in Figure 2.2 is shown next.

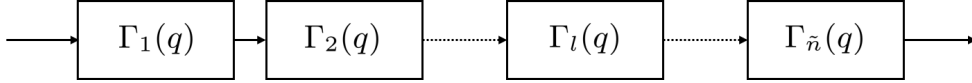


Figure 2.2: All-Pass Decomposition

2.3.1.1 Laguerre Block State-Space

Note that a FIR block of any order can be cast as a cascade of multiple first-order Laguerre blocks with all poles at the origin. Therefore, it is sufficient to derive the latter case. A first order transfer function,

$$F_L(z) = \frac{k_L}{z - \xi} \quad (2.10)$$

with $\xi \in \mathbb{R}$, constitutes an orthonormal Laguerre singleton if it is normal, *i.e.*,

$$\begin{aligned} 1 &= \langle F_L, F_L \rangle \\ &= \frac{1}{2\pi i} \oint_{\mathbb{T}} F_L(z) F_L(1/z) \frac{dz}{z}. \end{aligned}$$

The normalizing constant, k_L , is determined by applying the residue theorem,

$$\begin{aligned} 1 &= k_L^2 \operatorname{Res}_{\xi} \left(\frac{1}{(z - \xi)(1 - \xi z)} \right) \\ &= k_L^2 \lim_{z \rightarrow \xi} \frac{z - \xi}{(z - \xi)(1 - \xi z)} \\ &= \frac{k_L^2}{1 - \xi^2}. \end{aligned}$$

By selecting the positive root, the first order Laguerre block in (2.10) is defined by,

$$F_L(z) := \frac{\sqrt{1-\xi^2}}{z-\xi}. \quad (2.11)$$

The corresponding scalar state transition (2.12a) obtained from the equivalent filter expression is input balanced as a result. The remaining elements of the state-space, c_L and d_L , are defined by the relationships implicit in (2.9).

$$\varphi_{t+1} = a_L \varphi_t + b_L u_t \quad (2.12a)$$

$$y_t = c_L \varphi_t + d_L u_t \quad (2.12b)$$

$$\begin{aligned} a_L &= \xi \\ b_L &= \sqrt{1-\xi^2} \\ 0 &= a_L c_L + b_L d_L \\ 1 &= c_L^2 + d_L^2 \end{aligned} \implies \begin{bmatrix} a_L & b_L \\ c_L & d_L \end{bmatrix} = \begin{bmatrix} \xi & \sqrt{1-\xi^2} \\ \sqrt{1-\xi^2} & -\xi \end{bmatrix}$$

2.3.1.2 Kautz Block State-Space

Similarly to the Laguerre case, the first step of the derivation is to determine the required conditions on the state filter structure imposed by orthonormality. A set of two scalar functions, generated by a pair of complex poles, ξ_1 and ξ_2 , such that $\xi_2 := \bar{\xi}_1$, is orthonormal if the associated pair of filters

$$F_{K1}(z) = \frac{k_{K1}z}{(z-\xi_1)(z-\xi_2)}, \quad F_{K2}(z) = \frac{k_{K2}(1-\alpha_K z)}{(z-\xi_1)(z-\xi_2)} \quad (2.13)$$

satisfy,

$$\begin{aligned} 1 &= \langle F_{K_i}, F_{K_i} \rangle \\ &= \frac{1}{2\pi i} \oint_{\mathbb{T}} F_{K_i}(z) F_{K_i}(1/z) \frac{dz}{z} \end{aligned}$$

for $i = 1, 2$, and

$$\begin{aligned} 0 &= \langle F_{K_1}, F_{K_2} \rangle \\ &= \frac{1}{2\pi i} \oint_{\mathbb{T}} F_{K_1}(z) F_{K_2}(1/z) \frac{dz}{z}. \end{aligned}$$

Note that the form of the scalar elements in equation (2.13) is not unique to represent an orthonormal pair. For example, F_{K_2} could have been specified as a function with no zeros. We pick this pair as it yields a convenient state-space representation.

Applying the residue theorem to the normality condition for F_{K_1} , the following equality is obtained,

$$\begin{aligned} 1 &= (k_{K_1})^2 \left(\lim_{z \rightarrow \xi_1} \frac{z}{(z - \xi_2)(1 - \xi_1 z)(1 - \xi_2 z)} + \lim_{z \rightarrow \xi_2} \frac{z}{(z - \xi_1)(1 - \xi_1 z)(1 - \xi_2 z)} \right) \\ &= (k_{K_1})^2 \left(\frac{\xi_1(1 - \xi_2^2) - \xi_2(1 - \xi_1^2)}{(\xi_1 - \xi_2)(1 - \xi_1^2)(1 - \xi_2^2)(1 - \xi_1 \xi_2)} \right), \end{aligned}$$

after some simplifying algebra,

$$(k_{K_1})^2 = \left(1 - \left(\frac{\xi_1 + \xi_2}{1 + \xi_1 \xi_2} \right)^2 \right) (1 - (\xi_1 \xi_2)^2). \quad (2.14)$$

From orthogonality of the pair, we get

$$0 = k_{K_1} k_{K_2} \left(\lim_{z \rightarrow \xi_1} \frac{z(z - \alpha_K)}{(z - \xi_2)(1 - \xi_1 z)(1 - \xi_2 z)} + \lim_{z \rightarrow \xi_2} \frac{z(z - \alpha_K)}{(z - \xi_1)(1 - \xi_1 z)(1 - \xi_2 z)} \right).$$

Evaluation of the limit expressions followed by the multiplication of both sides by,

$$\frac{(\xi_1 - \xi_2)(1 - \xi_1\xi_2)}{k_{K1}k_{K2}},$$

gives

$$0 = \frac{\xi_1(\xi_1 - \alpha_K)}{1 - \xi_1^2} - \frac{\xi_2(\xi_2 - \alpha_K)}{1 - \xi_2^2}.$$

Leading to the following expression for the numerator coefficient in terms of the poles,

$$\alpha_K = \frac{\xi_1 + \xi_2}{1 + \xi_1\xi_2}. \quad (2.15)$$

The normalizing constant for F_{K2} is determined equivalently, by evaluating

$$\begin{aligned} 1 &= (k_{K2})^2 \left(\lim_{z \rightarrow \xi_1} \frac{(1 - \alpha_K z)(z - \alpha_K)}{(z - \xi_2)(1 - \xi_1 z)(1 - \xi_2 z)} + \lim_{z \rightarrow \xi_2} \frac{(1 - \alpha_K z)(z - \alpha_K)}{(z - \xi_1)(1 - \xi_1 z)(1 - \xi_2 z)} \right) \\ &= (k_{K2})^2 \left(\frac{(1 - \alpha_K \xi_1)(\xi_1 - \alpha_K)(1 - \xi_2^2) - (1 - \alpha_K \xi_2)(\xi_2 - \alpha_K)(1 - \xi_1^2)}{(\xi_1 - \xi_2)(1 - \xi_1^2)(1 - \xi_2^2)(1 - \xi_1\xi_2)} \right) \end{aligned}$$

which simplifies to

$$(k_{K2})^2 = 1 - (\xi_1\xi_2)^2. \quad (2.16)$$

In general, for a conjugate pair $\{\xi, \bar{\xi}\}$, the vector-valued function of interest, $\mathbf{F}_K(z)$, is obtained by inserting the expressions for the numerator coefficient and normalizing constants in (2.13),

$$\mathbf{F}_K(z) = \begin{bmatrix} \frac{\sqrt{(1 - p_K^2)(1 - \alpha_K^2)}z}{z^2 - s_K z + p_K} \\ \frac{\sqrt{1 - p_K^2}(1 - \alpha_K z)}{z^2 - s_K z + p_K} \end{bmatrix} \quad (2.17)$$

2.3 STATE-SPACE REALIZATIONS OF OBF MODELS

where the positive roots have been selected, and

$$p_K := \xi \bar{\xi}, s_K := \xi + \bar{\xi}, \alpha_K := \frac{s_K}{1 + p_K}.$$

The top scalar element yields the following difference equation,

$$\varphi_{1,t+1} = s_K \varphi_{1,t} - p_K \varphi_{1,t-1} + \sqrt{(1 - p_K^2)(1 - \alpha_K^2)} u_t.$$

Noting that the scalar filter elements are related by,

$$F_{K1}(q) = \sqrt{1 - \alpha_K^2} \frac{q}{1 - \alpha_K q} F_{K2}(q)$$

a second difference equation is obtained,

$$\sqrt{1 - \alpha_K^2} \varphi_{2,t+1} = -\alpha_K \varphi_{1,t+1} + \varphi_{1,t}.$$

The combination of the difference equations above yield the orthonormal state transition dynamics, $\boldsymbol{\varphi}_{t+1} = \mathbf{A}_K \boldsymbol{\varphi}_t + \mathbf{b}_K u_t$, for the Kautz block,

$$\boldsymbol{\varphi}_{t+1} = \begin{bmatrix} \alpha_K & -p_K \sqrt{1 - \alpha_K^2} \\ \sqrt{1 - \alpha_K^2} & \alpha_K p_K \end{bmatrix} \boldsymbol{\varphi}_t + \sqrt{1 - p_K^2} \begin{bmatrix} \sqrt{1 - \alpha_K^2} \\ -\alpha_K \end{bmatrix} u_t.$$

Finally, with the input balanced state transition pair $\{\mathbf{A}_K, \mathbf{b}_K\}$ above, the missing elements for the state-space, \mathbf{c}_K and d_K , are given by (2.9),

$$\begin{aligned} \mathbf{0} &= \mathbf{A}_K \mathbf{c}_K^\top + \mathbf{b}_K d_K & \Rightarrow & \mathbf{c}_K = \begin{bmatrix} 0 & \sqrt{1 - p_K^2} \end{bmatrix} \\ 1 &= \mathbf{c}_K \mathbf{c}_K^\top + d_K^2 & & d_K = p_K \end{aligned} \quad (2.18)$$

2.3.1.3 State-Space Construction

A summary of the state-space realizations for the elemental orthogonal all-pass building blocks is given in Table 2.2. These contributions allow the construction of state-transition dynamics for an ordered set of generating poles, obtained with the sequence of matrix operations specified by Algorithm 2.1.

Algorithm 2.1 All-Pass Cascading

Require:

Ordered pole set $\boldsymbol{\xi} = \{\xi_1, \xi_2, \dots, \xi_n\}$ \triangleright Adjacent conjugate pairs, FIR blocks

Ensure:

$\{\mathbf{A}_\xi, \mathbf{b}_\xi\}$

1: Generate $\{\mathbf{A}_l, \mathbf{b}_l, \mathbf{c}_l, d_l\}$ for $l = 1, 2, \dots, \tilde{n}$ \triangleright Building blocks in Table 2.2

2: $\mathbf{A}_c \leftarrow \mathbf{A}_1, \mathbf{b}_c \leftarrow \mathbf{b}_1, \mathbf{c}_c \leftarrow \mathbf{c}_1, d_c \leftarrow d_1$

3: **for** $l = 2, \dots, m$ **do**

4: $\mathbf{A}_c \leftarrow \begin{bmatrix} \mathbf{A}_c & \mathbf{0} \\ \mathbf{b}_l \mathbf{c}_c & \mathbf{A}_l \end{bmatrix}, \mathbf{b}_c \leftarrow \begin{bmatrix} \mathbf{b}_c \\ \mathbf{b}_l d_c \end{bmatrix}, \mathbf{c}_c \leftarrow \begin{bmatrix} d_l \mathbf{c}_c & \mathbf{c}_l \end{bmatrix}, d_c \leftarrow d_l d_c$

5: **end for**

6: $\mathbf{A}_\xi \leftarrow \mathbf{A}_c, \mathbf{b}_\xi \leftarrow \mathbf{b}_c$

2.3 STATE-SPACE REALIZATIONS OF OBF MODELS

Table 2.2: All-Pass Building Blocks

Name ($\xi \in \mathbb{D}$)	All-Pass SISO State-Space $\begin{bmatrix} \mathbf{A} & \mathbf{b} \\ \mathbf{c} & d \end{bmatrix}$
FIR ($\{0, 0, \dots, 0\}$)	$\begin{bmatrix} \begin{bmatrix} \mathbf{0} & 0 \\ \mathbf{I} & \mathbf{0} \end{bmatrix} & \begin{bmatrix} 1 \\ \mathbf{0} \end{bmatrix} \\ \begin{bmatrix} 1 & \mathbf{0} \end{bmatrix} & [0] \end{bmatrix}$
Laguerre ($\{\xi\} \in \mathbb{R}$)	$\begin{bmatrix} [\xi] & [\sqrt{1-\xi^2}] \\ [\sqrt{1-\xi^2}] & [-\xi] \end{bmatrix}$
Kautz ($\{\xi, \bar{\xi}\} \in \mathbb{C}$)	$\begin{bmatrix} \begin{bmatrix} \alpha_K & -p_K \sqrt{1-\alpha_K^2} \\ \sqrt{1-\alpha_K^2} & \alpha_K p_K \end{bmatrix} & \sqrt{1-p_K^2} \begin{bmatrix} \sqrt{1-\alpha_K^2} \\ -\alpha_K \end{bmatrix} \\ \begin{bmatrix} 0 & \sqrt{1-p_K^2} \end{bmatrix} & [p_K] \end{bmatrix}$

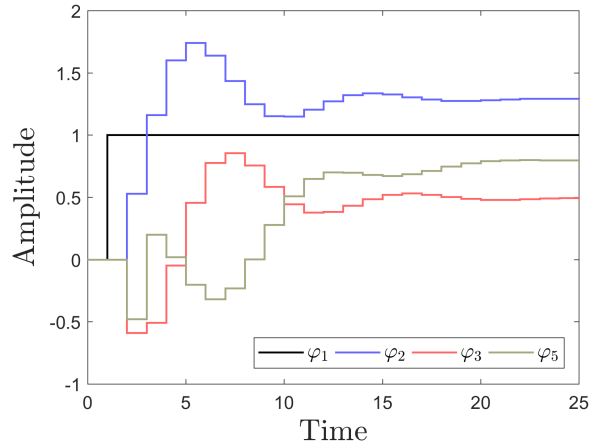


Figure 2.3: GOBF Step Response

All-Pass Cascade Example

Consider the ordered generating pole set given by

$$\xi = \{0, 0.6 + 0.5i, 0.6 - 0.5i, 0.8, -0.2\},$$

A state-transition pair, $\{\mathbf{A}_\xi, \mathbf{b}_\xi\}$, with model with order $n = 5$, is constructed by cascading the corresponding all-pass building blocks according to Algorithm 2.1. The unit step response for the states corresponding to four scalar function elements is illustrated in Figure 2.3.

The model contains FIR, Laguerre, and Kautz features. The delay caused by the first feature affects all the states as the leading element. The complex pair contribution to ξ defines a Kautz block that is reflected in the oscillatory profiles for φ_2 , φ_3 , and φ_5 . This last one is dominated by the slower Laguerre contribution but still contains oscillations as the preceding complex pair elements in the cascade also affect its dynamics.

2.3.2 MISO Structure

Note that, according to the defined MIMO model structure, each output predictor channel can be expressed as

$$\hat{y}_{i,t} = \sum_{j=1}^{n_u} G_{ij,m}(q)u_{j,t}, \quad G_{ij,m}(q) = \boldsymbol{\theta}_{ij}^\top (q\mathbf{I} - \mathbf{A}_{ij,\xi})^{-1} \mathbf{b}_{ij,\xi}$$

where its multi-input single-output (MISO) state-space representation, is given by

$$\begin{aligned} \boldsymbol{\varphi}_{i,t+1} &= \underbrace{\begin{bmatrix} \mathbf{A}_{i1,\xi} & \mathbf{0} & \cdots & \mathbf{0} \\ \mathbf{0} & \mathbf{A}_{i2,\xi} & \ddots & \vdots \\ \vdots & \ddots & \ddots & \mathbf{0} \\ \mathbf{0} & \cdots & \mathbf{0} & \mathbf{A}_{in_u,\xi} \end{bmatrix}}_{\mathbf{A}_{i,\xi} :=} \boldsymbol{\varphi}_{i,t} + \underbrace{\begin{bmatrix} \mathbf{b}_{i1,\xi} & \mathbf{0} & \cdots & \mathbf{0} \\ \mathbf{0} & \mathbf{b}_{i2,\xi} & \ddots & \vdots \\ \vdots & \ddots & \ddots & \mathbf{0} \\ \mathbf{0} & \cdots & \mathbf{0} & \mathbf{b}_{in_u,\xi} \end{bmatrix}}_{\mathbf{B}_{i,\xi} :=} \mathbf{u}_t \\ \hat{y}_{i,t} &= \underbrace{\begin{bmatrix} \boldsymbol{\theta}_{i1}^\top & \boldsymbol{\theta}_{i2}^\top & \cdots & \boldsymbol{\theta}_{in_u}^\top \end{bmatrix}}_{\boldsymbol{\theta}_i^\top :=} \boldsymbol{\varphi}_{i,t} \end{aligned}$$

for $i = 1, 2, \dots, n_y$. Finally, the MIMO state-space in (2.7), $\{\mathbf{A}_\xi, \mathbf{B}_\xi, \mathbf{C}_\theta\}$, is obtained by the appropriate arrangement of the MISO systems,

$$\mathbf{A}_\xi := \begin{bmatrix} \mathbf{A}_{1,\xi} & \mathbf{0} & \cdots & \mathbf{0} \\ \mathbf{0} & \mathbf{A}_{2,\xi} & \ddots & \vdots \\ \vdots & \ddots & \ddots & \mathbf{0} \\ \mathbf{0} & \cdots & \mathbf{0} & \mathbf{A}_{n_y,\xi} \end{bmatrix}, \quad \mathbf{B}_\xi := \begin{bmatrix} \mathbf{B}_{1,\xi} \\ \mathbf{B}_{2,\xi} \\ \vdots \\ \mathbf{B}_{n_y,\xi} \end{bmatrix}, \quad \mathbf{C}_\theta := \begin{bmatrix} \boldsymbol{\theta}_1^\top & \mathbf{0} & \cdots & \mathbf{0} \\ \mathbf{0} & \boldsymbol{\theta}_2^\top & \ddots & \vdots \\ \vdots & \ddots & \ddots & \mathbf{0} \\ \mathbf{0} & \cdots & \mathbf{0} & \boldsymbol{\theta}_{n_y}^\top \end{bmatrix}.$$

This MIMO model construction reduces to the incorporation of pole locations and model order for each input-output pair into individual state transition dynamics $\{\mathbf{A}_{ij,\xi}, \mathbf{b}_{ij,\xi}\}$ and their subsequent concatenation according to the expressions above.

2.4 GOBF MODEL PROPERTIES

2.4.1 Infinite Expansion

Consider the vector-valued function defined by the ordered pole set, $\boldsymbol{\xi} = \{\xi_1, \xi_2, \dots, \xi_n\}$, its state-transition pair as described in the previous section,

$$\mathbf{F}_\xi(z) := (z\mathbf{I} - \mathbf{A}_\xi)^{-1} \mathbf{b}_\xi.$$

and its all-pass filter,

$$\Gamma_\xi(z) := \prod_{i=1}^n \frac{1 - \bar{\xi}_i z}{z - \xi_i}.$$

A structured infinite expansion, that in turn defines a complete basis, can be constructed with these two objects such that, any scalar function, $G(z) \in \mathcal{H}_2$, has an infinite expansion,

$$G(z) = \sum_{k=1}^{\infty} \boldsymbol{\vartheta}_k^\top \mathbf{V}_k(z), \quad \mathbf{V}_k(z) := \mathbf{F}_\xi(z) (\Gamma_\xi(z))^{k-1}. \quad (2.19)$$

Note that this sum of vector-valued elements can also be expressed in terms of an infinite expansion of the scalar elements of \mathbf{V}_k . Equivalently to an scalar expansion, the exact

2.4 GOBF MODEL PROPERTIES

coefficient vector with n elements, $\boldsymbol{\vartheta}_k$, is defined by the plant dynamics and the matching set of scalar transfer functions,

$$\boldsymbol{\vartheta}_k = \begin{bmatrix} \langle G, F_{k+1} \rangle \\ \langle G, F_{k+2} \rangle \\ \vdots \\ \langle G, F_{k+n} \rangle \end{bmatrix}$$

where the functions $\{F_{k+1}, F_{k+2}, \dots, F_{k+n}\}$ are the scalar elements of \mathbf{V}_k .

The expansion expressed in equation (2.19) can be decomposed into the leading finite contribution of order n and the infinite remainder,

$$G(z) = G_m(z) + G_v(z) \quad (2.20)$$

where,

$$G_m(z) := \boldsymbol{\theta}_o^\top \mathbf{F}_\xi(z), \quad \boldsymbol{\theta}_o := \boldsymbol{\vartheta}_1, \quad G_v(z) := \sum_{k=2}^{\infty} \boldsymbol{\vartheta}_k^\top \mathbf{V}_k(z). \quad (2.21)$$

Without loss of generality, a finite order model obtained with any of the pole structures discussed thus far, can be equivalently expressed using this vector-valued expansion. Therefore, it is assumed, that the model with order n , constructed by the cascading of an arbitrary number of elemental blocks, defines a GOBF expansion in the general form of equation (2.19).

2.4.2 Asymptotic Properties of the Least-Squares Estimate

An estimate, $\hat{\theta}$, that parametrizes an uncertain SISO plant G with a fixed GOBF expansion can be obtained via least squares with respect to the available data record,

$$\mathbf{Y}_N = \{y_N, y_{N-1}, \dots, y_0, u_{N-1}, u_{N-2}, \dots, u_0\},$$

by minimizing the observed model error.

$$\hat{\theta}_N := \arg \min_{\theta} \sum_{k=0}^N \left(y_k - \varphi_k^\top \theta \right)^2 \quad (2.22)$$

The well known solution of the unconstrained least-squares estimation problem is given analytically by

$$\hat{\theta}_N = \left(\sum_{k=0}^N \varphi_k \varphi_k^\top \right)^{-1} \left(\sum_{k=0}^N \varphi_k y_k \right)$$

with $\varphi_k = \mathbf{F}_\xi u_k$. As shown in (Heuberger et al. 2005), for an input with constant unit mean spectrum, the asymptotic limit of the matrix,

$$\mathbf{R}_N := \frac{1}{N} \left(\sum_{k=0}^N \varphi_k \varphi_k^\top \right),$$

is given by

$$\mathbf{R}^* := \lim_{N \rightarrow \infty} \mathbf{R}_N = \frac{1}{2\pi i} \oint_{\mathbb{T}} \mathbf{F}_\xi(z) \mathbf{F}_\xi^\top(z^{-1}) \frac{dz}{z}.$$

Which follows from Parseval's Relation. From the definition of the vector outer product and the orthonormality of the elements of \mathbf{F}_ξ , this expression gives $\mathbf{R}^* = \mathbf{I}$. As a

result, the equations above are perfectly conditioned and the corresponding asymptotic parameter estimate is,

$$\boldsymbol{\theta}^* := \lim_{N \rightarrow \infty} \frac{1}{N} \sum_{k=0}^N \boldsymbol{\varphi}_k \mathbb{E}[y_k]$$

it follows from the Gaussian noise assumption that $\mathbb{E}[v_k] = 0$. Using the infinite expansion in (2.19), Parseval's relation, and the definition of the vector outer product,

$$\boldsymbol{\theta}^* = \boldsymbol{\theta}_o + \sum_{l=2}^{\infty} [\mathbf{F}_\xi, \mathbf{V}_l] \boldsymbol{\vartheta}_l$$

The infinite sum term above corresponds to the tail of the expansion that is not included in the model. This term equals zero as a result of orthonormality. In conclusion, under the ideal conditions for the input described above, the orthonormal output error structure delivers a consistent asymptotic parameter estimate, $\boldsymbol{\theta}^* = \boldsymbol{\theta}_o$ (Heuberger et al. 2005).

In terms of convergence, a more general asymptotic result that follows from the central limit theorem (Ljung 1999) is stated,

$$\lim_{N \rightarrow \infty} \sqrt{N} (\hat{\boldsymbol{\theta}}_N - \boldsymbol{\theta}^*) \sim \mathcal{N}(\mathbf{0}, \sigma^2 \mathbf{R}_N^{-1})$$

where σ^2 is the variance of the scalar measurement noise signal, and $\hat{\boldsymbol{\theta}}^*$ is the asymptotic estimate obtained from an arbitrary input spectrum. With these definitions, the difference between the model (with its parameter estimate, $\hat{\boldsymbol{\theta}}$), and the system is conveniently decomposed,

$$G(q) - G_m(q; \hat{\boldsymbol{\theta}}) = \left(G_m(q; \boldsymbol{\theta}_o) - G_m(q; \hat{\boldsymbol{\theta}}) \right) + \left(G(q) - G_m(q; \boldsymbol{\theta}_o) \right)$$

The first term is the variance with respect to model parametrized by the first n infinite expansion coefficients, while the second term is the structural bias contribution generated by the tail that follows the finite truncation.

2.4.3 MIMO Model Error

To conclude the section, we return to the expression for the MIMO plant. Since the finite subset of infinite expansion coefficients for each SISO model element are uncertain, we parametrize the predictor filter with an estimate, $\hat{\theta}$. From the perspective of this parametrization and the actual measured output, the plant can be decomposed into the model and the error dynamics, as illustrated in Figure 2.4, and expressed in equation (2.23).

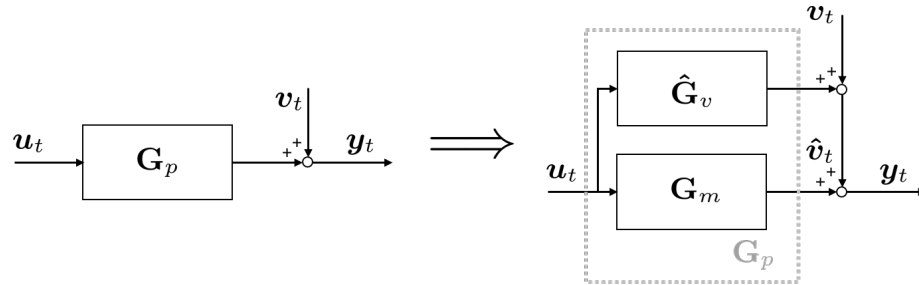


Figure 2.4: Model Error Diagram

$$\begin{aligned}
 \mathbf{y}_t &= \left(\mathbf{G}_m(q; \hat{\theta}) + \hat{\mathbf{G}}_v(q; \hat{\theta}) \right) \mathbf{u}_t + \mathbf{v}_t \\
 &= \mathbf{G}_m(q; \hat{\theta}) \mathbf{u}_t + \hat{\mathbf{v}}_t.
 \end{aligned} \tag{2.23}$$

2.5 MINIMAL GOBF EXAMPLE

The model error vector is defined accordingly by

$$\hat{\mathbf{v}}_t := \hat{\mathbf{G}}_v(q)\mathbf{u}_t + \mathbf{v}_t, \quad (2.24)$$

with scalar elements, $\hat{v}_{i,t} = \sum_{j=1}^{n_u} \hat{G}_{ij,v}(q)u_{j,t} + v_{i,t}$, for $i = 1, 2, \dots, n_y$.

Perfect knowledge of the true coefficients of the underlying GOBF infinite expansion, $\boldsymbol{\theta}_o$, has not been assumed. Therefore, each scalar model error transfer function must be decomposed in two parts,

$$\hat{G}_v(q) = \tilde{\boldsymbol{\theta}}^\top \mathbf{F}_\xi(q) + G_v(q)$$

where $\tilde{\boldsymbol{\theta}} = \boldsymbol{\theta}_o - \hat{\boldsymbol{\theta}}$ and G_v is defined in equation (2.21). The first term in the expression above vanishes as the value of the parameter estimate approaches the expansion coefficients. Since both terms in the right hand side are defined by orthonormal elements that span functions in \mathcal{H}_2 . It follows that the input to error transfer function is always stable, for any bounded $\tilde{\boldsymbol{\theta}}$.

2.5 MINIMAL GOBF EXAMPLE

A SISO model is constructed for a system of two masses connected by springs as illustrated in Figure 2.5. The continuous time dynamics are given by the damped harmonic oscillator equations. The model is written in terms of a state vector containing the displacement and acceleration, d and a respectively, of each block with mass m . The subscript h denotes the hidden mass that is indirectly related to the input-output structure. The input is a force acting on the outer mass, while the output is a noisy measurement

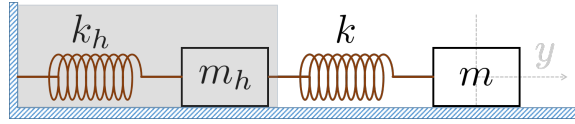


Figure 2.5: Connected Mass-Spring System

of its displacement. It is assumed that the damping force due to friction, f_F , is linearly proportional to acceleration, such that $f_F = -\beta a$, $\beta = 1$.

A balance of forces for both masses, yields the following continuous time state-space description,

$$\dot{\mathbf{x}} = \begin{bmatrix} 0 & 1 & 0 & 0 \\ -k/m & -1/m & k/m & 0 \\ 0 & 0 & 0 & 1 \\ k/m_h & 0 & -(k+k_h)/m_h & -1/m_h \end{bmatrix} \mathbf{x} + \begin{bmatrix} 0 \\ 1/m \\ 0 \\ 0 \end{bmatrix} u$$

$$y = \begin{bmatrix} 1 & 0 & 0 & 0 \end{bmatrix} \mathbf{x} + v$$

where $\mathbf{x} = \begin{bmatrix} d & a & d_h & a_h \end{bmatrix}^\top$. The mass values are set to $m = m_h = 2$ while the spring constants are set to $k = 0.1$, $k_h = 1$. Assume the system parameters yield units of time in seconds. These values were chosen to specify the combination of under and over-damped dynamics for the connected system.

A discretization with zero-order hold for the input and a sampling time of one second results on a stable transfer function with the following poles, rounded to the nearest second decimal place,

$$\{0.89, 0.68, 0.59 + 0.50i, 0.59 + 0.50i\}.$$

2.5 MINIMAL GOBF EXAMPLE

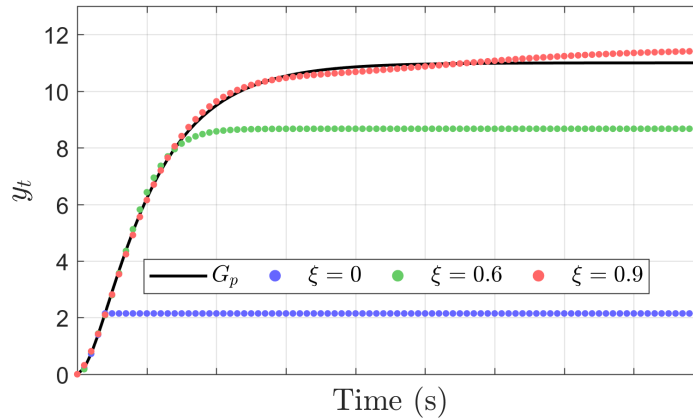
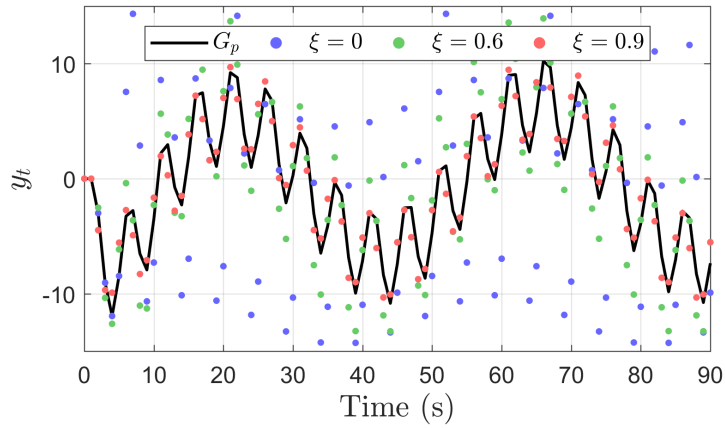


Figure 2.6: Mass-Spring Laguerre ($n = 4$) Step Response

To illustrate the ideas presented in this chapter, the output profiles for a unit step and a sinusoidal wave input sequence were simulated. The sine wave input signal is composed by two simple sine contributions with different period and amplitude. The undisturbed response ($v = 0$) is simulated to remove this effect from the analysis. The same pair of input profiles was applied to the transfer functions obtained from a finite truncation of the first 4 elements of different OBF expansions. The results are split in two groups of three distinct cases each. The first, with one-pole Laguerre expansions, and a second, obtained with the GOBF approach. In all cases, the expansion coefficients were computed from the inner product of the discrete plant dynamics and the respective basis function element. The first group is generated with an FIR expansion ($\xi = 0$) and two real pole locations, $\xi = 0.6$ and $\xi = 0.9$. These latter two, were chosen from the nearest decimal approximation for the real part of the system poles, located closest and furthest to the origin, respectively. The results are displayed in Figures 2.6 and 2.7.

As expected, due to the defining plant poles location in the complex plane, the FIR truncation with exact expansion coefficients can only represent the true dynamics for a

Figure 2.7: Mass-Spring Laguerre ($n = 4$) Sine Input Response

short period corresponding to the truncation order. An accurate representation with this approach would require roughly 50 parameters. Moving the generating pole location along the real axis towards the plant poles provides better approximations. The green dotted profile, for the intermediately accurate pole location, yields acceptable sinusoidal response matching. On the other hand, the steady-state gain, shown in the step response in Figure 2.6, provides a closer match to the system than the FIR case, but still grossly misrepresented. Overall, the one-pole Laguerre expansion can be tuned to match the mass-spring system simulated responses to the studied inputs only by the last case. A pole location that is inconsistent with the system may require higher order truncations as demonstrated by the limiting behavior of the FIR case.

The second set of simulations were made with model structures that belong to the broader GOBF class, where multiple pole locations for a given expansion are specified.

2.5 MINIMAL GOBF EXAMPLE

Three different model instances, with $n = 4$, are constructed according to the following generating sets,

$$\begin{aligned}\xi_1 &= \left\{ 0.9, \quad 0.6 + 0.2i, \quad 0.6 - 0.2i, \quad 0 \right\} \\ \xi_2 &= \left\{ 0.9, \quad 0.6 + 0.2i, \quad 0.6 - 0.2i, \quad 0.9 \right\} \\ \xi_3 &= \left\{ 0.9, \quad 0.6 + 0.5i, \quad 0.6 - 0.5i, \quad 0.7 \right\}.\end{aligned}\tag{2.25}$$

Their location in the complex plane is illustrated in Figure 2.8 for a visual reference. The truncation responses, for the same step and sine wave input profiles described above, are shown in Figures 2.9 and 2.10. It is observed that even for the generating set that includes a pole at the origin, the truncation obtained is capable of matching the simulated system profiles accurately. In fact, the performance is comparable to the most accurate GOBF basis. This indicates that as long as the pole choices are partially accurate with respect to the system, good representations can be obtained. This is enabled by the dynamic diversity expressed by the varying pole locations.

It is noted that the small steady-state gain offsets are observed in Figure 2.9. An additional advantage of the GOBF framework, is that it offers the flexibility to address this type of issue by the inclusion of tailored functions to the existing set. The new function element can be derived from the existing set or with a new pole location. The Laguerre expansion with the outer-most pole is capable of representing the system with acceptable accuracy. This is possible because the pole corresponding to this location dominates the dynamics as shown by the orthonormal component step response decomposition of GOBF_3 in Figure 2.11. For a system with a dominating feature that is oscillatory, this would no longer be the case.

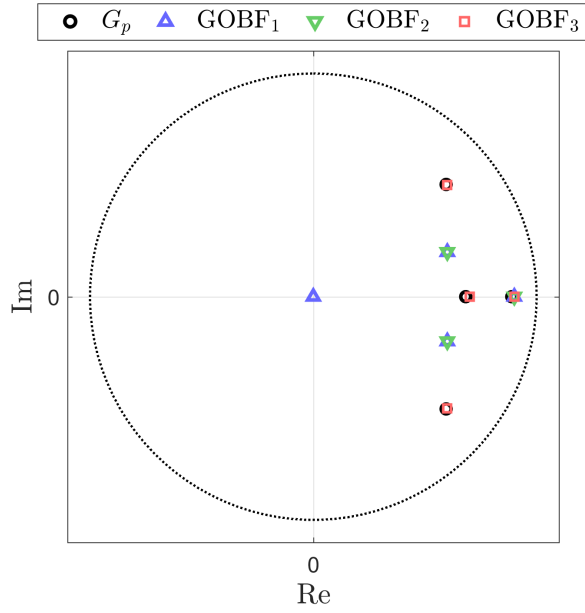


Figure 2.8: GOBF Pole Locations

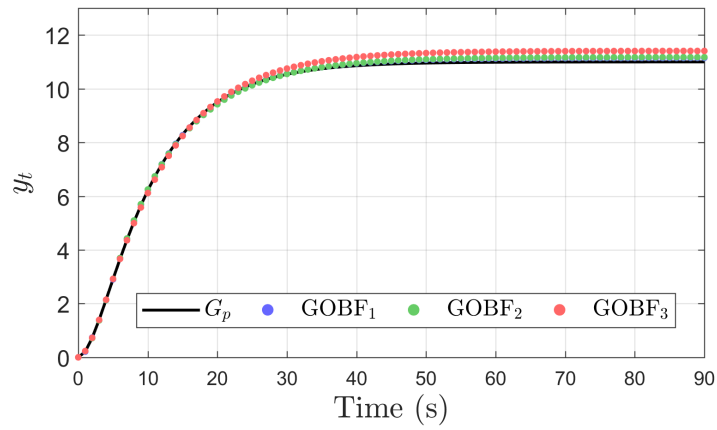


Figure 2.9: Mass-Spring GOBF ($n = 4$) Step Response

2.5 MINIMAL GOBF EXAMPLE

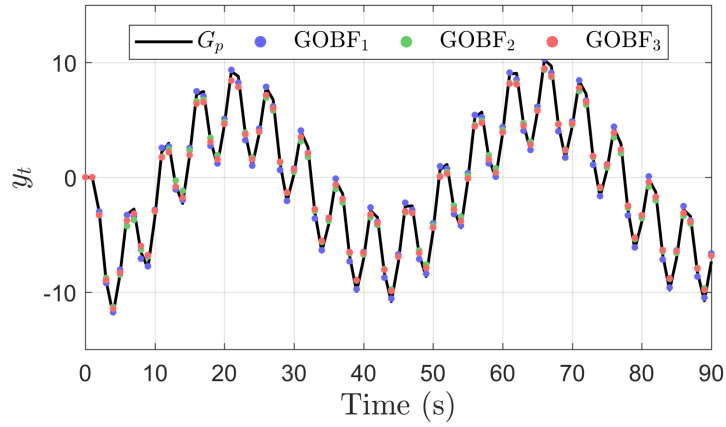


Figure 2.10: Mass-Spring GOBF ($n = 4$) Sine Input Response

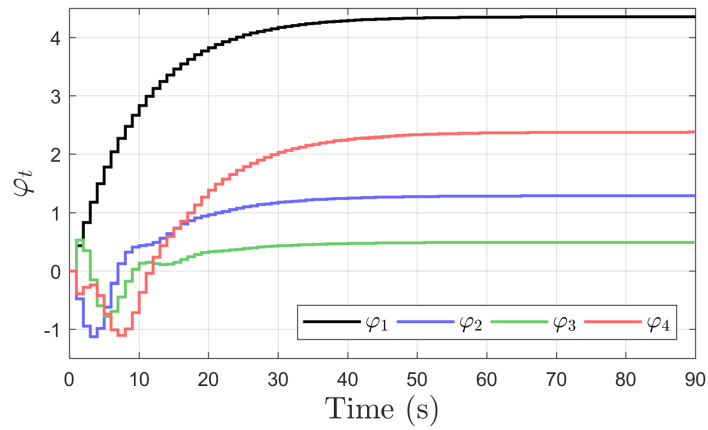


Figure 2.11: Mass-Spring GOBF_3 ($n = 4$) Step Response State Decomposition

2.6 CONCLUSIONS

The modeling approach³ to be followed in the subsequent chapters has been introduced. The scope is limited to plants that can be usefully approximated with stable MIMO linear filters. Different OBF structures have been presented along with general properties that follow from the orthonormal expansion definition. A multivariable input-output model is generated component-wise for each SISO filter under the generalized orthonormal basis functions framework. A cascading method for the customized construction of state transition models with varying elemental, real-valued contributions is summarized in Algorithm 2.1. The detailed derivation of these components from the defining orthonormality condition was provided. Lastly, in section 2.5 we present a set of simulations with a minimal mass-spring example that outlines the key properties of interest for the proposed modeling framework.

³ The interested reader may find the detailed description of modeling and identification concepts in the compilation of contributions in (Heuberger et al. 2005) and the references therein.

3

GOBF MODEL PREDICTIVE CONTROL

In this chapter, we are interested in leveraging the GOBF modeling approach to define output feedback model predictive tracking control algorithms. This will require the adjustment of the models obtained through the systematic approach given in the previous chapter. This adjustment is defined by the application of backward difference filters that, in turn, enable output feedback. Once all modeling elements of the problem are properly outlined, a series of MPC policies are provided. In particular, a robust MPC formulation that takes into account the error dynamics associated with the filtered model is outlined in detail.

In the interest of brevity, it is assumed that the reader is familiar with the receding horizon approach inherent of all MPC methods. This allows us to direct our attention immediately to the features of the standard components of the associated optimal control problem. Before diving into these details, a contextualizing discussion of the associated assumptions for an accurate model is provided. This will enable the application of standard MPC stability theory later in the chapter.

3.1 MODEL ERROR PRELIMINARIES

3.1 MODEL ERROR PRELIMINARIES

Recall that, under the plant assumptions stated in Chapter 2, the overall MIMO state-space model, constructed from a fixed underlying generating pole structure, allows the following system description,

$$\varphi_{t+1} = \mathbf{A}(\boldsymbol{\xi})\varphi_t + \mathbf{B}(\boldsymbol{\xi})\mathbf{u}_t, \quad \varphi_0 \quad (3.1a)$$

$$\mathbf{y}_t = \mathbf{C}(\boldsymbol{\theta}, \boldsymbol{\xi})\varphi_t + \hat{\mathbf{v}}_t(\boldsymbol{\theta}, \boldsymbol{\xi}). \quad (3.1b)$$

where φ_o denotes the initial condition for the information state. The notational significance of $\boldsymbol{\xi}$ is extended to indicate the collection of pole generating sets and truncation orders for all the SISO relationships in the model. Also, note that instead of using subscripts, as in the previous chapter, we have written the matrices and disturbance signal in (3.1) explicitly as functions of the model parameters. These relationships are implied by the system decomposition illustrated in Figure 3.1.

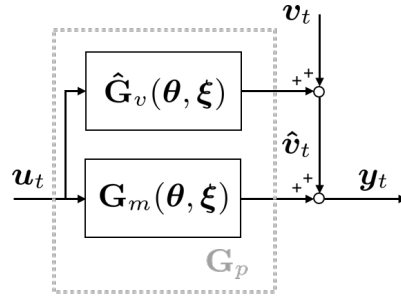


Figure 3.1: Structural Model Error

The system characterization above unveils the composition of the model error signal. First of all, it is desired that the SISO generating pole sets and model orders can re-

semble the dynamic components inherent to the system. Once this is accomplished, a parametrization specified by θ , weight the built-in basis functions for suitable approximations. Both of these items were discussed in the previous chapter. Specifically, it was shown how the GOBF approach offers flexible structures that reduce the effect of the unmodeled dynamics, \hat{G}_v , on the error when the model poles are close to those of the real system.

In this chapter, we assume that a GOBF model that satisfies these structural requirements has been defined such that the composite disturbance in Figure 3.1 is bounded by some constant, *i.e.* $\|\hat{v}_t\| < \bar{k}_v \forall t$. We will then focus on the ability of the optimal feedback action, provided by MPC algorithms, to handle the remaining uncertain disturbance signal.

Three important assumptions are usually made on the defining linear state-space model such as (3.1) and its initial state:

- Stabilizability of the pair $\{A, B\}$
- Detectability of the pair $\{C, A\}$
- Initial feasibility of the optimal control problem

We note that due to the defining characteristic of generating poles inside the unit disk, a GOBF model state-space realization will automatically satisfy the first two items. This property extends to the related filtered models to be introduced below. The last item applies for any modeling approach. Therefore, we will continue under this assumption.

3.2 TRACKING MPC OBJECTIVE

3.2 TRACKING MPC OBJECTIVE

We aim to formulate a scalar MPC objective cost function, to be minimized, that adheres to the following standard form,

$$J_N(\hat{\mathbf{x}}_0, \mathbf{u}) := \sum_{k=0}^{N-1} \ell(\hat{\mathbf{x}}_k, \hat{\mathbf{u}}_k) + J_f(\hat{\mathbf{x}}_N), \quad \hat{\mathbf{x}}_0 = \mathbf{x}_t. \quad (3.2)$$

The functions $\ell(\cdot, \cdot)$ and $J_f(\cdot)$ are referred to as the stage and terminal costs respectively. The state variable, \mathbf{x}_t , represents a signal that defines the process dynamics of interest. Conventionally, its elements correspond to variables with physical significance. In our development, these are defined by the control design structure and the GOBF information vector, φ_t , as specified in the previous chapter. The receding horizon control vector, \mathbf{u} , concatenates N input elements. The hat accents on the state, \mathbf{x} , and control, \mathbf{u} , variables indicate the evaluation in the receding horizon window, which is made with respect to a nominal model parametrized θ .

For a tracking control problem, the stage cost is defined with respect to the output reference signal, \mathbf{y}_t^r . In contrast to \mathbf{u} , beyond the N elements for each stage, this vector includes an additional one, to be used in the definition of the terminal cost.

$$\mathbf{u} := \begin{bmatrix} \hat{\mathbf{u}}_0 \\ \hat{\mathbf{u}}_1 \\ \vdots \\ \hat{\mathbf{u}}_{N-1} \end{bmatrix} \in \mathbb{R}^{Nn_u}, \quad \mathbf{y}_t^r := \begin{bmatrix} \mathbf{y}_t^r \\ \mathbf{y}_{t+1}^r \\ \vdots \\ \mathbf{y}_{t+N}^r \end{bmatrix} \in \mathbb{R}^{(N+1)n_y}.$$

With some abuse of notation, the reference signal time index, t , is excluded when making statements with regards to the MPC problem, *e.g.*, $\hat{\mathbf{y}}_k - \mathbf{y}_k^r = \hat{\mathbf{y}}_k - \mathbf{y}_{t+k}^r$.

We proceed with the definition of the tracking control stage cost function with respect to a predictor model,

$$\ell(\hat{\mathbf{y}}, \hat{\mathbf{u}}) := \|\hat{\mathbf{y}} - \mathbf{y}^r\|_{\mathbf{Q}}^2 + \|\Delta\hat{\mathbf{u}}\|_{\mathbf{R}}^2. \quad (3.3)$$

Where the symmetric cost matrices, $\mathbf{Q} \succeq 0$ and $\mathbf{R} \succ 0$, specify the relative importance of tracking for different output channels and the magnitude of the control moves respectively. The backward difference operator, Δ , in the second term, is given in terms of the shift operator as

$$\Delta := 1 - q^{-1}. \quad (3.4)$$

Note that the stage cost has been defined directly in terms of the output prediction. The modifications to be introduced in the section 3.2.1 will allow its formulation in the standard form of equation (3.2). In general, linear-quadratic (LQ) controllers include a contribution that penalizes the energy of the control directly (*i.e.* $\|\mathbf{u}\|^2$). However, this is not explicit in the analysis below, mostly for compactness of the exposition. Its inclusion is trivial and would not affect the results. Furthermore, under the tracking objective of interest, a cost for $\Delta\mathbf{u}$ is arguably more applicable as it does not penalize nonzero control actions required to reach arbitrary, stationary reference signals.

3.2.1 Predictor Models with Backward Difference Filters

By construction, the information state vector φ_t in (3.1) is simply a filtered version of the input record as defined in section 2.3. Therefore, using the state-space defined by the triad

3.2 TRACKING MPC OBJECTIVE

$\{A_\xi, B_\xi, C_\theta\}$ as the predictor directly, would not permit the inclusion of the information provided by output measurements in the control design.

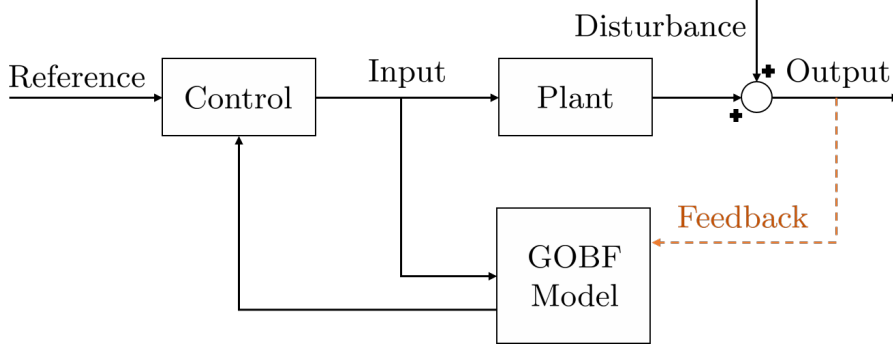


Figure 3.2: Output Feedback in MPC with GOBF Models

As shown in Figure 3.2, in the absence of a further modification, the output signal is completely decoupled from the controller. In order to address this limitation, the model is modified with a low-order backwards difference filter, Δ^{n_d} ,

$$\begin{aligned}\Delta^{n_d} &= (1 - q^{-1})^{n_d} \\ &= 1 + d_1 q^{-1} + \dots + d_{n_d} q^{-n_d}.\end{aligned}$$

The filter is applied to predictions made with the nominal GOBF model (3.1), such that

$$\begin{aligned}\Delta^{n_d} \hat{\varphi}_{k+1} &= A_\xi \Delta^{n_d} \hat{\varphi}_k + B_\xi \Delta^{n_d} \hat{u}_k, & \Delta^{n_d} \hat{\varphi}_0 &= \Delta^{n_d} \varphi_t \\ \Delta^{n_d} \hat{y}_k &= C_\theta \Delta^{n_d} \hat{\varphi}_k.\end{aligned}$$

This system can be equivalently expressed in terms of the state-space triad $\{\mathbf{A}_m, \mathbf{B}_m, \mathbf{C}_m\}$, as

$$\hat{\mathbf{x}}_{m,k+1} = \underbrace{\begin{bmatrix} \mathbf{A}_\xi & \mathbf{0} & \cdots & \cdots & \mathbf{0} \\ \mathbf{C}_\theta \mathbf{A}_\xi & -d_1 \mathbf{I} & \cdots & \cdots & -d_{n_d} \mathbf{I} \\ \mathbf{0} & \mathbf{I} & \mathbf{0} & \cdots & \mathbf{0} \\ \vdots & \ddots & \ddots & \ddots & \vdots \\ \mathbf{0} & \cdots & \cdots & \mathbf{I} & \mathbf{0} \end{bmatrix}}_{\mathbf{A}_m :=} \hat{\mathbf{x}}_{m,k} + \underbrace{\begin{bmatrix} \mathbf{B}_\xi \\ \mathbf{C}_\theta \mathbf{B}_\xi \\ \mathbf{0} \\ \vdots \\ \mathbf{0} \end{bmatrix}}_{\mathbf{B}_m :=} \Delta^{n_d} \mathbf{u}_k \quad (3.5)$$

$$\hat{\mathbf{y}}_k = \underbrace{\begin{bmatrix} \mathbf{0} & \mathbf{I} & \mathbf{0} & \cdots & \mathbf{0} \end{bmatrix}}_{\mathbf{C}_m :=} \hat{\mathbf{x}}_{m,k}$$

where

$$\hat{\mathbf{x}}_{m,k} := \left[\Delta^{n_d} \hat{\varphi}_k^\top \quad \hat{\mathbf{y}}_k^\top \quad \hat{\mathbf{y}}_{k-1}^\top \quad \cdots \quad \hat{\mathbf{y}}_{k-n_d+1}^\top \right]^\top.$$

Output feedback has been introduced by updating the state vector with the corresponding output measurements in the data record, $\{\mathbf{y}_t, \mathbf{y}_{t-1}, \dots, \mathbf{y}_{t-n_d+1}\}$, prior to the computation of the optimal control.

The filtering feature is a control design tool and it is meant to remain independent of the parameter estimation process when dealing with the adaptive formulations presented in the following chapter. In addition to introducing output feedback, the filter reduces the correlation with respect to the output noise signal (Finn et al. 1993). From (3.5), it is clear that higher order filters imply additional elements of the data record in the state update which could be useful when dealing with periodic disturbances. The backwards

3.2 TRACKING MPC OBJECTIVE

difference choice presents a couple of useful properties. First, it facilitates the recovery of the unfiltered input signals with alternating sign coefficients given by Pascal's triangle.

$$\begin{aligned}
 \Delta &= 1 - q^{-1} \\
 \Delta^2 &= 1 - 2q^{-1} + q^{-2} \\
 \Delta^3 &= 1 - 3q^{-1} + 3q^{-2} - q^{-3} \\
 &\vdots \\
 \Delta^{n_d} &= 1 - \dots \dots \dots + (-1)^{n_d} q^{-n_d}.
 \end{aligned}$$

More importantly, as the system approaches any steady state, $\Delta^{n_d} \varphi_t \rightarrow 0$. For example, with $n_d = 3$, at steady state, $\varphi_t = \varphi_{t-1} = \varphi_{t-2} = \varphi_{t-3}$,

$$\begin{aligned}
 \Delta^3 \varphi_t &= \varphi_t - 3\varphi_{t-1} + 3\varphi_{t-2} - \varphi_{t-3} \\
 &= (1 - 3 + 3 - 1)\varphi_t \\
 &= 0
 \end{aligned}$$

3.2.2 Infinite-Horizon Constant Reference Tracking

Due to the inherent controllability of the input-output elements used in the construction of $\{\mathbf{A}_\xi, \mathbf{B}_\xi\}$, stabilizability for the corresponding state transition pair for the filtered model, $\{\mathbf{A}_m, \mathbf{B}_m\}$, in equation (3.5) follows. As a result, for any bounded parameter estimate, $\hat{\theta}$, the solution of an unconstrained infinite horizon LQ problem for a constant ref-

erence signal, \mathbf{y}^r , is possible in principle. For a model generated with the first backwards difference filter, Δ , the objective function reduces to the following regulation problem,

$$J_\infty(\mathbf{x}_{tr}, \Delta \hat{\mathbf{u}}_k = \kappa(\hat{\mathbf{x}}_{tr,k})) := \lim_{N \rightarrow \infty} \sum_{k=0}^{N-1} \|\hat{\mathbf{x}}_{tr,k}\|_{\mathbf{Q}_{tr}}^2 + \|\Delta \hat{\mathbf{u}}_k\|_{\mathbf{R}}^2, \quad \hat{\mathbf{x}}_{tr,0} = \mathbf{x}_{tr}. \quad (3.6)$$

Here, the policy κ is to be followed in the infinite horizon. The applicable state transition dynamics and corresponding state, according to (3.5), are given by

$$\hat{\mathbf{x}}_{tr,k+1} = \mathbf{A}_m \hat{\mathbf{x}}_{tr,k} + \mathbf{B}_m \Delta \hat{\mathbf{u}}_k \quad (3.7)$$

$$\mathbf{A}_m = \begin{bmatrix} \mathbf{A}_\xi & \mathbf{0} \\ \mathbf{C}_\theta \mathbf{A}_\xi & \mathbf{I} \end{bmatrix}, \quad \mathbf{B}_m = \begin{bmatrix} \mathbf{B}_\xi \\ \mathbf{C}_\theta \mathbf{B}_\xi \end{bmatrix}, \quad \text{and } \hat{\mathbf{x}}_{tr,k} := \begin{bmatrix} \Delta \hat{\phi}_k \\ \hat{\mathbf{y}}_k - \mathbf{y}^r \end{bmatrix}$$

The tracking state cost matrix \mathbf{Q}_{tr} is obtained from the model output matrix, \mathbf{C}_m , and, \mathbf{Q} , in (3.3),

$$\mathbf{Q}_{tr} = \mathbf{C}_m^\top \mathbf{Q} \mathbf{C}_m \succeq 0, \quad \mathbf{C}_m = [\mathbf{0} \quad \mathbf{I}].$$

Equivalent expressions for higher order filtered models are obtained in a similar fashion. The solution to this LQR problem is obtained from the associated Discrete Algebraic Riccati Equation (DARE),

$$\mathbf{P}_\infty = \mathbf{A}_m^\top \mathbf{P}_\infty \mathbf{A}_m - \mathbf{A}_m^\top \mathbf{P}_\infty \mathbf{B}_m \left(\mathbf{B}_m^\top \mathbf{P}_\infty \mathbf{B}_m + \mathbf{R} \right)^{-1} \mathbf{B}_m^\top \mathbf{P}_\infty \mathbf{A}_m + \mathbf{Q}_{tr}. \quad (3.8)$$

The symmetric matrix solution, $\mathbf{P}_\infty \succeq 0$, defines the minimal cost, J_∞^* , for the unconstrained minimization with objective (3.6), under the model structure parametrized by $\{\mathbf{A}_\xi, \mathbf{B}_\xi, \mathbf{C}_\theta\}$,

$$J_\infty^*(\mathbf{x}_{tr}) := \min_{\kappa} J_\infty(\mathbf{x}_{tr}, \kappa(\mathbf{x}_{tr})) = \mathbf{x}_{tr}^\top \mathbf{P}_\infty \mathbf{x}_{tr}, \quad \forall \mathbf{x}_{tr}$$

3.3 EXTENDED MODEL

This cost is achieved by the minimizing policy, $\kappa_\infty^*(\mathbf{x}_{tr}) = \mathbf{K}_\infty \mathbf{x}_{tr}$,

$$\mathbf{K}_\infty := - \left(\mathbf{B}_m^\top \mathbf{P}_\infty \mathbf{B}_m + \mathbf{R} \right)^{-1} \mathbf{B}_m^\top \mathbf{P}_\infty \mathbf{A}_m.$$

For a time varying reference signal and a finite receding horizon, the terminal cost, J_f , is defined by the last element of the reference signal \mathbf{y}_t^r and the infinite horizon cost matrix,

$$J_f(\hat{\mathbf{x}}_m) := \|\hat{\mathbf{x}}_m - \mathbf{x}_m^r\|_{\mathbf{P}_\infty}^2 \quad (3.9)$$

where reference state signal, \mathbf{x}_m^r , for Δ , is defined by the terminal cost reference, \mathbf{y}^r

$$\hat{\mathbf{x}}_{tr} = \hat{\mathbf{x}}_m - \mathbf{x}_m^r, \quad \mathbf{x}_m^r := \begin{bmatrix} \mathbf{0} \\ \mathbf{y}^r \end{bmatrix} \quad (3.10)$$

This terminal cost choice implies that the objective function is computed assuming that the optimal policy κ_∞^* is followed beyond the receding horizon window.

3.3 EXTENDED MODEL

Combining the stage and terminal cost definitions from the previous section, a general time-varying reference tracking objective function is defined by

$$\sum_{k=0}^{N-1} \left(\|\mathbf{C}_m \hat{\mathbf{x}}_{m,k} - \mathbf{y}_k^r\|_{\mathbf{Q}}^2 + \|\Delta \hat{\mathbf{u}}_k\|_{\mathbf{R}}^2 \right) + \|\hat{\mathbf{x}}_{m,N} - \mathbf{x}_{m,N}^s\|_{\mathbf{P}_\infty}^2.$$

As expressed above, under a fixed model, this function depends on other signals in addition to the filtered model initial condition, $\hat{\mathbf{x}}_{m,0}$, and the receding horizon control vector,

u. The purpose of this section is to introduce model extensions that allow a compact problem definition that adheres to the form of (3.2). In practical terms, these model extensions are entirely notational. However, they will be useful in the subsequent development.

3.3.1 Input Record Model

Appending a model for the control sequence is convenient for two reasons. First, it allows the computation of filtered inputs from the initial condition. Secondly, it facilitates the expression of input constraints in terms of the state. This is easily accomplished with the controllable state-transition dynamics corresponding to the inverse filtering operation, $\{\mathbf{A}_u, \mathbf{B}_u\}$. For example, for Δ^2 , from equation (3.5), and the filter coefficients $d_1 = -2$ and $d_2 = 1$,

$$\hat{\mathbf{x}}_{u,k+1} = \mathbf{A}_u \hat{\mathbf{x}}_{u,k} + \mathbf{B}_u \Delta^2 \hat{\mathbf{u}}_k \quad (3.11)$$

$$\mathbf{A}_u = \begin{bmatrix} 2\mathbf{I} & -\mathbf{I} \\ \mathbf{I} & \mathbf{0} \end{bmatrix}, \mathbf{B}_u = \begin{bmatrix} \mathbf{I} \\ \mathbf{0} \end{bmatrix}, \hat{\mathbf{x}}_{u,0} = \begin{bmatrix} \mathbf{u}_{t-1} \\ \mathbf{u}_{t-2} \end{bmatrix}$$

Input constraints can be specified directly in terms of $\hat{\mathbf{x}}_{u,k}$. On the other hand, inputs and input moves are expressed with linear combinations of the input record contained in the state and the filtered control,

$$\hat{\mathbf{u}} = \mathbf{L}_0 \hat{\mathbf{x}}_{u,k} + \Delta^{n_d} \hat{\mathbf{u}}_k$$

$$\Delta \hat{\mathbf{u}}_k = \mathbf{L}_1 \hat{\mathbf{x}}_{u,k} + \Delta^{n_d} \hat{\mathbf{u}}_k.$$

3.3 EXTENDED MODEL

For the particular case above, with $n_d = 2$, $L_0 = [2I \ -I]$, and $L_1 = [I \ -I]$. The control move cost in (3.3) can also be expressed in terms of the input record state and the filtered input,

$$\|\Delta\hat{\mathbf{u}}_k\|_{\mathbf{R}}^2 = \|\hat{\mathbf{x}}_{u,k}\|_{\mathbf{R}_u}^2 + \|\Delta^{n_d}\hat{\mathbf{u}}_k\|_{\mathbf{R}}^2 + 2\hat{\mathbf{x}}_{u,k}^\top \mathbf{S}_u \Delta^{n_d}\hat{\mathbf{u}}_k \quad (3.12)$$

where $\mathbf{R}_u = L_1^\top \mathbf{R} L_1$, and $\mathbf{S}_u = L_1^\top \mathbf{R}$.

3.3.2 Reference Signal Model

Similarly to the input record model, the reference signal can also be incorporated into the state (Bitmead et al. 1990). This is accomplished with the following unforced dynamics,

$$\hat{\mathbf{x}}_{r,k+1} = \underbrace{\begin{bmatrix} \mathbf{0} & \mathbf{I} & \mathbf{0} & \cdots & \mathbf{0} \\ \vdots & \ddots & \ddots & \ddots & \vdots \\ \vdots & \ddots & \ddots & \ddots & \mathbf{0} \\ \vdots & \ddots & \ddots & \ddots & \mathbf{I} \\ \mathbf{0} & \cdots & \cdots & \cdots & \mathbf{0} \end{bmatrix}}_{\mathbf{A}_r :=} \hat{\mathbf{x}}_{r,k}, \quad \hat{\mathbf{x}}_{r,0} = \mathbf{y}_t^r, \quad (3.13)$$

and

$$\mathbf{y}_k^r = \underbrace{\begin{bmatrix} \mathbf{I} & \mathbf{0} & \cdots & \cdots & \mathbf{0} \end{bmatrix}}_{\mathbf{C}_r :=} \hat{\mathbf{x}}_{r,k}.$$

The stability of the reference state follows trivially since \mathbf{A}_r is nilpotent. Also, we note that the tracking stage cost in (3.3) and the steady state signal in (3.9) can be equivalently expressed by

$$\begin{aligned} \mathbf{C}_m \hat{\mathbf{x}}_{m,k} - \mathbf{y}_k^r &= [\mathbf{C}_m \quad -\mathbf{C}_r] \begin{bmatrix} \hat{\mathbf{x}}_{m,k} \\ \hat{\mathbf{x}}_{r,k} \end{bmatrix}, \\ \hat{\mathbf{x}}_{m,N} - \mathbf{x}_{m,N}^s &= [\mathbf{I} \quad -\mathbf{C}_r^{n_d}] \begin{bmatrix} \hat{\mathbf{x}}_{m,N} \\ \hat{\mathbf{x}}_{r,N} \end{bmatrix}, \end{aligned} \quad \mathbf{C}_r^{n_d} := \begin{bmatrix} \mathbf{0} \\ \mathbf{C}_r \\ \vdots \\ \mathbf{C}_r \end{bmatrix} \quad (3.14)$$

3.3.3 Optimal Control Problem

An extended model state is obtained by concatenating the predictor model with the auxiliary models for the input record and the reference signal,

$$\hat{\mathbf{x}}_{k+1} = \mathbf{A} \hat{\mathbf{x}}_k + \mathbf{B} \Delta^{n_d} \hat{\mathbf{u}}_k \quad (3.15)$$

$$\mathbf{A} := \begin{bmatrix} \mathbf{A}_m & \mathbf{0} & \mathbf{0} \\ \mathbf{0} & \mathbf{A}_u & \mathbf{0} \\ \mathbf{0} & \mathbf{0} & \mathbf{A}_r \end{bmatrix}, \quad \mathbf{B} := \begin{bmatrix} \mathbf{B}_m \\ \mathbf{B}_u \\ \mathbf{0} \end{bmatrix}, \quad \text{and } \hat{\mathbf{x}}_k := \begin{bmatrix} \hat{\mathbf{x}}_{m,k} \\ \hat{\mathbf{x}}_{u,k} \\ \hat{\mathbf{x}}_{r,k} \end{bmatrix}.$$

In terms of the extended state, the time-varying reference tracking objective function reduces to regulation with state-input costs (Bitmead et al. 1990),

$$J_N(\hat{\mathbf{x}}_0, \mathbf{u}) := \sum_{k=0}^{N-1} \left(\|\hat{\mathbf{x}}_k\|_{\mathbf{Q}_\ell}^2 + \|\Delta^{n_d} \hat{\mathbf{u}}_k\|_{\mathbf{R}}^2 + 2\hat{\mathbf{x}}_k^\top \mathbf{S}_\ell \Delta^{n_d} \hat{\mathbf{u}}_k \right) + \|\hat{\mathbf{x}}_N\|_{\mathbf{P}_f}^2. \quad (3.16)$$

The extended model cost matrices, $\{\mathbf{Q}_\ell, \mathbf{S}_\ell, \mathbf{P}_f\}$, are defined by the original stage cost matrices, $\{\mathbf{Q}, \mathbf{R}\}$, and the infinite horizon tracking cost matrix, \mathbf{P}_∞ , related by the extended

3.4 MPC PROPERTIES

state definition and the expressions in (3.12) and (3.14). At a given time, t , the initial condition, $\hat{\mathbf{x}}_0$, is updated with the filtered GOBF vector, $\Delta^{n_d}\varphi_t$, the finite horizon reference signal, \mathbf{y}_t^r , and the relevant elements of the input-output data record. The optimal control problem is composed by the objective function above with the nominal extended model and a set of input/output and terminal constraints mapped onto the space of the control sequence, such that $\mathbf{u} \in \mathcal{U}_N$,

$$\mathcal{P}_N(\mathbf{x}) : J_N^*(\mathbf{x}) = \min_{\mathbf{u}} \{J_N(\hat{\mathbf{x}}_0, \mathbf{u}) \mid \mathbf{u} \in \mathcal{U}_N, \hat{\mathbf{x}}_0 = \mathbf{x}\}. \quad (3.17)$$

The optimizing argument is denoted by \mathbf{u}^* . The optimization above is performed over the filtered inputs, $\Delta^{n_d}\hat{\mathbf{u}}_k$ for $k \in \mathbb{I}_{0:N-1}$. However, the optimal receding horizon control, \mathbf{u}^* , can be recovered by the applying the inverse difference filter to the optimized filtered input sequence. Since this is already built in the extended state definition, the desired solution vector is equivalently recovered from the leading elements of $\hat{\mathbf{x}}_{u,k}$ for $k \in \mathbb{I}_{1:N}$. The MPC optimal policy obtained from applying the first element of \mathbf{u}^* at each time, t , is denoted by

$$\kappa_N^*(\mathbf{x}_t) := \hat{\mathbf{u}}_0^*. \quad (3.18)$$

3.4 MPC PROPERTIES

We are now interested in establishing the properties of MPC policies resulting from the online solution of the receding horizon problem (3.17) under different scenarios. In addition to the control design choices made thus far, this analysis requires the assumption of feasibility for the fixed horizon length. We start by defining the model error in terms of its

GOBF expansion. Next, the derivation of an analytic solution for the unconstrained case is presented. We compile the necessary ingredients for stability and optimality for the constrained case under ideal conditions. The section is closed with the outline of a robust constrained reformulation. As one would expect, these results follow from the predictive accuracy of the model and the characteristics of the constraint set.

We make use of a simplifying choice for the filter order, $n_d = 1$, below. All statements to be made hold in the general case, $n_d > 1$, with an equivalent treatment. As a result, $L_1 = \mathbf{0}$, and the objective function (3.16) simplifies to

$$J_N(\hat{\mathbf{x}}_0, \mathbf{u}^*) := \sum_{k=0}^{N-1} \left(\|\hat{\mathbf{x}}_k\|_{\mathbf{Q}_\ell}^2 + \|\Delta\hat{\mathbf{u}}_k\|_{\mathbf{R}}^2 \right) + \|\hat{\mathbf{x}}_N\|_{\mathbf{P}_f}^2. \quad (3.19)$$

The related state is, $\hat{\mathbf{x}}_k = [\Delta\hat{\varphi}_k^\top \quad \hat{\mathbf{y}}_k^\top \quad \hat{\mathbf{u}}_{k-1}^\top \quad \hat{\mathbf{x}}_{r,k}^\top]^\top$, with transition dynamics given by (3.15). Note that only the output signal elements are subject to unknown disturbances. The system state transitions are described accordingly,

$$\mathbf{x}_{t+1} = \underbrace{\mathbf{A}\mathbf{x}_t + \mathbf{B}\Delta\mathbf{u}_t}_{f(\mathbf{x}_t, \mathbf{u}_t)} + \mathbf{w}_t. \quad (3.20)$$

The disturbance signal, \mathbf{w}_t , has the following structure

$$\mathbf{x}_t = \begin{bmatrix} \Delta\varphi_t \\ \mathbf{y}_t \\ \mathbf{u}_{t-1} \\ \mathbf{y}_t^r \end{bmatrix}, \quad \mathbf{w}_t = \begin{bmatrix} \mathbf{0} \\ \mathbf{w}_{y,t} \\ \mathbf{0} \\ \mathbf{w}_{r,t} \end{bmatrix} \quad (3.21)$$

3.4 MPC PROPERTIES

where $\mathbf{w}_{y,t} = \Delta \hat{\mathbf{v}}_t$ is the filtered unmeasured signal with model error and measurement noise contributions as defined in the previous chapter. On the other hand, $\mathbf{w}_{r,t}$ is deterministic and known.

3.4.1 Unconstrained Optimal Linear Controller

In the absence of constraints there is no need for recursive optimizations as an equivalent analytical solution for the optimal control function can be obtained off-line via Dynamic Programming. The finite horizon control design is kept, allowing the incorporation of future output reference changes N steps ahead of time through the disturbance \mathbf{w}_r .

The elements of the finite horizon control vector, \mathbf{u}^* , minimize a sequence of action-state cost functions,

$$\min_{\hat{\mathbf{u}}_{N-i}} \begin{bmatrix} \hat{\mathbf{x}}_{N-i} \\ \Delta \hat{\mathbf{u}}_{N-i} \end{bmatrix}^\top \begin{bmatrix} \mathbf{A}^\top \mathbf{P}_{i-1} \mathbf{A} + \mathbf{Q}_\ell & \mathbf{A}^\top \mathbf{P}_{i-1} \mathbf{B} \\ \mathbf{B}^\top \mathbf{P}_{i-1} \mathbf{A} & \mathbf{B}^\top \mathbf{P}_{i-1} \mathbf{B} + \mathbf{R} \end{bmatrix} \begin{bmatrix} \hat{\mathbf{x}}_{N-i} \\ \Delta \hat{\mathbf{u}}_{N-i} \end{bmatrix}, \forall i \in \mathbb{I}_{1:N},$$

where the quadratic cost matrices \mathbf{P}_i are related by optimality, expressed by the following Riccati matrix difference equation (RDE),

$$\mathbf{P}_i = \mathbf{A}^\top \mathbf{P}_{i-1} \mathbf{A} - \mathbf{A}^\top \mathbf{P}_{i-1} \mathbf{B} (\mathbf{B}^\top \mathbf{P}_{i-1} \mathbf{B} + \mathbf{R})^{-1} \mathbf{B}^\top \mathbf{P}_{i-1} \mathbf{A} + \mathbf{Q}_\ell, \mathbf{P}_0 = \mathbf{P}_f$$

The optimal input for the first stage is computed from the stationary condition for the quadratic action-state cost with $i = N$,

$$\Delta \hat{\mathbf{u}}_0^* = -(\mathbf{B}^\top \mathbf{P}_{N-1} \mathbf{B} + \mathbf{R})^{-1} \mathbf{B}^\top \mathbf{P}_{N-1} \mathbf{A} \mathbf{x}$$

Due to the structure of the extended state and the definition of the terminal cost, the following equalities hold,

$$\begin{aligned} B^\top P_{N-1} B &= B_m^\top P_\infty B_m \\ B^\top P_{N-1} A x &= \begin{bmatrix} B_m^\top P_\infty A_m & \mathbf{0} & B_m^\top P_{r,N-1} A_r \end{bmatrix} x. \end{aligned}$$

These relationships allow us to obtain the optimal control law from (3.8) and the computation of the coupled model-reference cost matrix, $P_{r,N-1}$, which is given by a matrix recursion of lower dimension,

$$P_{r,i} = (A_m + B_m K_\infty)^\top P_{r,i-1} A_r - C_m^\top Q C_r, \quad P_{r,0} = -P_\infty C_m^\top C_r.$$

The result, conveniently decomposes into a linear gain policy with filtered model, input, and reference contributions that act on the corresponding elements of the extended model state,

$$\kappa_N^{\text{nc},*}(\mathbf{x}) := \begin{bmatrix} K_\infty & K_u & K_r \end{bmatrix} \begin{bmatrix} \mathbf{x}_m \\ \mathbf{x}_u \\ \mathbf{x}_r \end{bmatrix} \quad (3.22)$$

where,

$$\begin{aligned} K_u &= I \\ K_r &= -(B_m^\top P_\infty B_m + R)^{-1} B_m^\top P_{r,N-1} A_r \end{aligned}$$

For higher order difference filters, the DARE and matrix recursion above must include control-state contributions, while K_u is defined by the applicable linear combination of input record elements that compose this portion of the extended state.

3.4.2 Constraints

As noted earlier, the GOBF model state, does not necessarily have a direct interpretation with respect to all physical variables of the system. As such, this framework is limited to handle input and output signal constraints directly. More precisely, these can be expressed only for physical variables modeled as system inputs or outputs. Nonetheless, both constraint sets, $\hat{\mathbf{u}}_k \in \mathcal{U}$ and $\hat{\mathbf{y}}_k \in \mathcal{Y}$, are expressed in term of the extended state,

$$\mathcal{X} = \{\mathbf{x} \mid \mathbf{x}_u \in \mathcal{U}, \mathbf{C}_m \mathbf{x}_m \in \mathcal{Y}\}.$$

It is assumed that the resulting region is a bounded polyhedral set. We aim to characterize the properties that follow from the choices thus far. Note that with (3.10), we have implicitly defined the corresponding terminal policy in terms of the extended state,

$$\kappa_f(\mathbf{x}) := \mathbf{x}_u + \mathbf{K}_\infty(\mathbf{x}_m - \mathbf{x}_m^r), \quad \mathbf{x}_m^r = \begin{bmatrix} \mathbf{0} \\ \mathbf{y}^r \end{bmatrix}. \quad (3.23)$$

the infinite horizon policy, κ_∞^* , maps model states to filtered inputs. To be consistent with f in (3.20), and the definition for κ_N^* , the terminal policy is defined to map from extended states to inputs directly instead. Cases with higher order difference filters follow the same form with a gain acting on \mathbf{x}_u determined by the respective inverse filter coefficients. Next, the terminal region, \mathcal{X}_f , and reachable sets \mathcal{X}_j , for $j = 1, \dots, N$, are introduced. The former is defined to be a closed subset of \mathcal{X} . The latter, as the set of states from which \mathcal{X}_f is reachable by a sequence of j controls, or less, while the corresponding state trajectory remains in \mathcal{X} . In particular, \mathcal{X}_N , denotes the set of admissible initial conditions.

These elements are dependent on the polyhedral region \mathcal{X} and the horizon N and can be determined off-line with simulations.

By acknowledging the disturbance signal, w , we must include its effect in the analysis. First, the special case with zero model error and a constant reference disturbance is studied. This simplified development follows the formulation of ingredients for optimality and stability by [Mayne et al. \(2000\)](#). This is followed in the next section by the analysis of the general case assuming that the disturbance belongs to a bounded compact set. The problem reformulation is inspired by the work of [Limon et al. \(2010\)](#) and [Zeilinger et al. \(2014\)](#). Appropriate modifications that follow from the adopted modeling framework are made.

3.4.3 Perfect Model & Constant Reference Disturbance

With respect to its definition in (3.21), the disturbance signal in this case is given by

$$w^0 := \begin{bmatrix} \mathbf{0} \\ \mathbf{0} \\ \mathbf{0} \\ w_r \end{bmatrix},$$

where the nonzero portion of the disturbance appends a constant signal to the last element of the reference state, *i.e.* $w_r := \left[\mathbf{0} \ \dots \ \mathbf{0} \ y^r{}^\top \right]^\top$.

The effect of the output disturbance, \hat{v} , has been removed from the analysis. Given that \mathcal{P}_N is defined with a tracking objective in mind, we skip the nominal, undisturbed case. Nonetheless, the simplified description below covers it as a special case with $y^r = \mathbf{0}$.

The constant reference signal is set to equal to the last element of \mathbf{y}_0^r . Consequently, a time invariant terminal cost, policy, and set are obtained for $t \geq 0$. As time advances, the reference state vector elements are all equal and \mathcal{P}_N collapses to the constant reference tracking problem under a perfect model.

Table 3.1: Standard Nominal Stability Conditions

Condition	Comments
$\mathbf{C1}$ $\begin{aligned} &\mathcal{X}_r(\mathbf{y}^r) \cap \mathcal{X}_f \neq \emptyset, \\ &\mathcal{X}_f \text{ closed, } \mathcal{X}_f \subset \mathcal{X} \end{aligned}$	$\mathcal{X}_r(\mathbf{y}^r)$ is defined to contain the set of steady-state admissible inputs, with nominal output \mathbf{y}^r . For a given $\mathbf{x} \in \mathcal{X}_r(\mathbf{y}^r)$, the related infinite-horizon constant tracking model state (3.7) equals zero.
$\mathbf{C2}$ $\begin{aligned} &f(\mathbf{x}, \kappa_f(\mathbf{x})) + \mathbf{w}^0 \in \mathcal{X}_f, \\ &\forall \mathbf{x} \in \mathcal{X}_f \end{aligned}$	This condition implies that the control constraints are satisfied in the terminal region, <i>i.e.</i> $\kappa_f(\mathbf{x}) \in \mathcal{U}$, $\forall \mathbf{x} \in \mathcal{X}_f$, by construction of the extended state.
$\mathbf{C3}$ $\begin{aligned} &J_f(f(\mathbf{x}, \kappa_f(\mathbf{x})) + \mathbf{w}^0) \\ &-J_f(\mathbf{x}) \leq -\ell(\mathbf{x}, \kappa_f(\mathbf{x})), \\ &\forall \mathbf{x} \in \mathcal{X}_f \end{aligned}$	The terminal policy is a Lyapunov function in a neighborhood of the origin of (3.7) mapped onto the extended state space, for the closed loop system with constant disturbance \mathbf{w}_0^r .

Table 3.1 summarizes the sufficient conditions for stability of the closed-loop system under the optimal MPC policy, $f(\mathbf{x}, \kappa_N^*(\mathbf{x})) + \mathbf{w}^0$. In addition to meeting these criteria, \mathcal{P}_N must be feasible, with a horizon N large enough and constraints that yield a nonempty set of admissible initial conditions, \mathcal{X}_N . These properties are traditionally stated in terms of an equivalent system with its coordinates shifted such that the origin correspond to a steady state of interest. In that case, the first line of $\mathbf{C1}$ in Table 3.1 is replaced with $\mathbf{0} \in \mathcal{X}_f$. Assuming that the number of output and input channels allow for the existence

of such steady states, it follows from the controllability properties of the GOBF model components, that \mathcal{X}_r is nonempty. Furthermore, satisfaction of **C1** implies $\mathbf{y}^r \in \mathcal{Y}$. The set \mathcal{X}_r is a function of the constant reference and is formally defined by

$$\mathcal{X}_r(\mathbf{y}^r) := \{ \mathbf{x} \mid \exists \boldsymbol{\varphi}^s, (\mathbf{A}_\xi - \mathbf{I})\boldsymbol{\varphi}^s + \mathbf{B}_\xi \mathbf{x}_u = \mathbf{0}, \mathbf{C}_\theta \boldsymbol{\varphi}^s = \mathbf{y}^r \}.$$

The infinite-horizon terminal policy drives the tracking state in (3.7) asymptotically to zero. As a result, according to (3.23), $\mathbf{x}_m - \mathbf{x}_m^r \rightarrow 0$, and the policy approaches a steady state, $\kappa_f(\mathbf{x}) \rightarrow \mathbf{x}_u^s \in \mathcal{U}$, $\forall \mathbf{x} \in \mathcal{X}_f$ and $\forall \mathbf{y}^r \in \mathcal{Y}$, with the same rate. Therefore, **C2**, is also satisfied. **C3** is determined via induction.

Theorem 1. *Convergence under κ_N^* and \mathbf{w}^0 .* Assuming **C1** is satisfied, the closed loop system $f(\mathbf{x}, \kappa_N^*(\mathbf{x})) + \mathbf{w}^0$ approaches an admissible steady state, $\mathbf{x}^s \in \mathcal{X}_s$, asymptotically with region of attraction \mathcal{X}_N .

Proof. Let $\kappa_i^*, J_i^* \forall i \in \mathbb{I}_{1:N-1}$, denote a sequence of optimal policies, and corresponding costs. Each pair is defined equivalently to κ_N^* and J_N^* . Set $\kappa_0^* := \kappa_f$ and $J_0^* := J_f$. From optimality, it follows that

$$J_i^*(\mathbf{x}) = \ell(\mathbf{x}, \hat{\kappa}_i^*(\mathbf{x})) + J_{i-1}^*(f(\mathbf{x}, \hat{\kappa}_i^*(\mathbf{x})) + \mathbf{w}^0)$$

Noting that $\kappa_1^* = \kappa_f$, for $\mathbf{x} \in \mathcal{X}_0$ since $\mathcal{X}_0 = \mathcal{X}_f \subset \mathcal{X}$, the expression above gives

$$J_1^*(\mathbf{x}) = \underbrace{\ell(\mathbf{x}, \kappa_1^*(\mathbf{x})) + J_0^*(f(\mathbf{x}, \kappa_1^*(\mathbf{x})) + \mathbf{w}^0)}_{= J_f(\mathbf{x})}$$

3.5 ROBUST REFORMULATION

for $i = 1$. Therefore, $J_1^*(\mathbf{x}) = J_0^*(\mathbf{x})$, $\forall \mathbf{x} \in \mathcal{X}_0$.

Assume that, $J_{i+1}^*(\mathbf{x}) \leq J_i^*(\mathbf{x}) \forall \mathbf{x} \in \mathcal{X}_i$. Evaluating the difference, we get

$$\begin{aligned}
 0 &\geq J_{i+1}^*(\mathbf{x}) - J_i^*(\mathbf{x}) \\
 &= \ell(\mathbf{x}, \kappa_{i+1}^*(\mathbf{x})) - \ell(\mathbf{x}, \kappa_i^*(\mathbf{x})) + J_i^*(f(\mathbf{x}, \kappa_{i+1}^*(\mathbf{x})) + \mathbf{w}^0) - J_{i-1}^*(f(\mathbf{x}, \kappa_i^*(\mathbf{x})) + \mathbf{w}^0) \\
 &\geq \ell(\mathbf{x}, \kappa_i^*(\mathbf{x})) - \ell(\mathbf{x}, \kappa_i^*(\mathbf{x})) + J_i^*(f(\mathbf{x}, \kappa_i^*(\mathbf{x})) + \mathbf{w}^0) - J_{i-1}^*(f(\mathbf{x}, \kappa_i^*(\mathbf{x})) + \mathbf{w}^0) \\
 &= J_i^*(f(\mathbf{x}, \kappa_i^*(\mathbf{x})) + \mathbf{w}^0) - J_i^*(\mathbf{x}) + \ell(\mathbf{x}, \kappa_i^*(\mathbf{x}))
 \end{aligned}$$

By the principle of mathematical induction, monotonicity is established and

$$J_N^*(f(\mathbf{x}, \kappa_N^*(\mathbf{x})) + \mathbf{w}^0) - J_N^*(\mathbf{x}) \leq -\ell(\mathbf{x}, \kappa_N^*(\mathbf{x})), \forall \mathbf{x} \in \mathcal{X}_N.$$

This condition implies that the MPC objective cost for the closed-loop with constant disturbance, \mathbf{w}_0 , is a Lyapunov function in the shifted coordinates with the resulting steady state at the origin. The result follows. \square

This simplified analysis does not necessarily apply to the general disturbance with a nonzero model error and/or measurement noise. It is only possible due to the fact that the disturbance set has a single deterministic, known element. For the general case neither equality nor descent can be guaranteed for $J_1^*(\mathbf{x})$ with respect to $J_0^*(\mathbf{x})$.

3.5 ROBUST REFORMULATION

The robust linear MPC algorithms in (Limon et al. 2010; Zeilinger et al. 2014) for tracking piece-wise constant signals are adapted to the GOBF modeling approach. In order

to enforce equivalent conditions to those in Table 3.1 for the general case, \mathcal{P}_N must be reformulated. A more strict characterization of these conditions is covered by the concept of input-to-state stability (ISS) as described in Appendix B of (Rawlings & Mayne 2009).

Under the piece-wise constant output reference restriction, the associated elements of the extended model are unnecessary and cumbersome. Before the new problem is described, the state transition model for the system is simplified by excluding them,

$$\mathbf{x}_{t+1} = \mathbf{A}\mathbf{x}_t + \mathbf{B}\Delta\mathbf{u}_t + \mathbf{w}_t \quad (3.24)$$

$$\mathbf{A} := \begin{bmatrix} \mathbf{A}_m & \mathbf{0} \\ \mathbf{0} & \mathbf{I} \end{bmatrix}, \mathbf{B} := \begin{bmatrix} \mathbf{B}_m \\ \mathbf{I} \end{bmatrix}.$$

Where the state and disturbance vectors have the following notational structure,

$$\mathbf{x} := \begin{bmatrix} \mathbf{x}_m \\ \mathbf{x}_u \end{bmatrix}, \mathbf{x}_m := \begin{bmatrix} \mathbf{x}_\varphi \\ \mathbf{x}_y \end{bmatrix}, \text{ and } \mathbf{w} := \begin{bmatrix} \mathbf{w}_m \\ \mathbf{0} \end{bmatrix}, \mathbf{w}_m := \begin{bmatrix} \mathbf{0} \\ \mathbf{w}_y \end{bmatrix}$$

with $\mathbf{x}_\varphi := \Delta\boldsymbol{\varphi}$, $\mathbf{x}_y := \mathbf{y}$. The optimal control problem is designed for the tracking of a reference signal, \mathbf{y}_t^r , subject to step changes that occur at a much lower frequency than the control action.

There are three main obstacles that make an adequate formulation with robust guarantees non-trivial. First, the disturbed closed-loop system may undergo constraint violations that yield inadmissible initial conditions due to the disturbance action. This issue is addressed by the tightening of the constraints with respect to a bounding set for the error dynamics and a subsequent adjustment to the optimal control that keeps the disturbed state in a region surrounding the stabilized nominal trajectory. Second, changes in the reference signal may also render the problem infeasible. There are no guarantees that

the shifted terminal region, associated to the new reference, remains reachable under the fixed horizon. Additional decision variables are introduced to define an artificial steady state. Third, the existence of an ISS Lyapunov function is desired in order to establish associated guarantees. This is resolved by appending a cost that penalizes the distance between the measurement and the optimization variables of the first stage cost that are disturbed. In the following subsections, the required modifications to the objective and the constraint set of the optimal control problem are introduced in detail.

3.5.1 Constraint Tightening

The key concept in this aspect of the reformulation is to split the optimal control action into two interrelated processes (Mayne et al. 2005). The optimization is performed with respect to the deterministic nominal system (3.24). The disturbed state is then steered towards the optimized nominal trajectory with a suitable stabilizing proportional control law. The robust design combines the effects of stabilization by the optimized nominal control, and the ancillary law to counteract the disturbance which steers the actual trajectory away from the optimized variables. In order to develop these ideas, the following model error definition is adopted,

$$e_m := x_m - \hat{x}_m$$

where,

$$\begin{aligned} x_m^+ &:= A_m x_m + B_m \Delta u + w_m, & \Delta u &= u - u^- \\ \hat{x}_m^+ &:= A_m \hat{x}_m + B_m \Delta \hat{u}, & \Delta \hat{u} &= \hat{u} - u^- \end{aligned} \tag{3.25}$$

Here we have adopted the superscripts $+/-$ to denote a single forward/backward sampling time move.

The proposed proportional law is specified by an optimized nominal input and state,

$$\mathbf{u} = \hat{\mathbf{u}}^* + \mathbf{K}_m \mathbf{e}_m^*. \quad (3.26)$$

The stabilizing gain \mathbf{K}_m , is chosen such that the closed loop matrix,

$$\mathbf{A}_K := \mathbf{A}_m + \mathbf{B}_m \mathbf{K}_m,$$

has all of its eigenvalues inside the unit circle. The optimized nominal state is constrained to $\hat{\mathbf{x}}_u = \mathbf{x}_u$ such that the input move expressions in (3.25) always hold. The following expression for the projected model error at the next sampling time is obtained,

$$\mathbf{e}_m^+ = \mathbf{A}_K \mathbf{e}_m^* + \mathbf{w}_m \quad (3.27)$$

Under the existence of a region around the nominal trajectory with the following characteristics with respect to (3.26), robust guarantees can be derived. First, the associated tightening must result in nonempty feasible regions for the nominal variables in the optimal control problem. This property is related to the magnitude of the error signal and the required stabilizing gain. Moreover, the set must be robustly positive invariant for the disturbed closed loop (Rawlings & Mayne 2009).

Definition 2. *Robust Positive Invariant (rPI) Set.* \mathcal{E}_m is a rPI set for the closed loop error system, $\mathbf{e}_m^+ = \mathbf{A}_K \mathbf{e}_m + \mathbf{w}_m$, $\mathbf{w}_m \in \mathcal{W}_m$, if $\mathbf{A}_K \mathcal{E}_m \oplus \mathcal{W}_m \in \mathcal{E}_m$.

A minimal region that reduces the tightening while meeting the invariance condition is desired. It follows that if the nominal state trajectory remains in the interior of the original constraints, \mathcal{X} , with a margin specified by a suitable rPI set, the disturbed system trajectory will satisfy $\mathbf{x} \in \mathcal{X}$. The tightened constraint sets are denoted with the subscript w . For example, the state tightened extended state constraint set, $\mathcal{X}_w \subseteq \mathcal{X}$, is defined with

$$\mathcal{X}_w := \{ \mathbf{x} \mid \mathbf{x}_y \in \mathcal{Y}_w, \mathbf{x}_u \in \mathcal{U}_w \}.$$

The tightening of the input/output constraints is performed with respect to the largest expected disturbance realization. Under the model structure, this is fixed by a lower-dimensional set. To make this observation explicit, we rewrite (3.27) with the stabilizing gain, $\mathbf{K}_m = [\mathbf{K}_\varphi \quad \mathbf{K}_y]$, in terms of the undisturbed GOBF vector and the disturbed output,

$$\begin{bmatrix} \mathbf{e}_\varphi^+ \\ \mathbf{e}_y^+ \end{bmatrix} = \begin{bmatrix} \mathbf{A}_\xi + \mathbf{B}_\xi \mathbf{K}_\varphi & \mathbf{B}_\xi \mathbf{K}_y \\ \mathbf{C}_\theta (\mathbf{A}_\xi + \mathbf{B}_\xi \mathbf{K}_\varphi) & \mathbf{I} + \mathbf{C}_\theta \mathbf{B}_\xi \mathbf{K}_y \end{bmatrix} \begin{bmatrix} \mathbf{e}_\varphi \\ \mathbf{e}_y \end{bmatrix} + \begin{bmatrix} \mathbf{0} \\ \mathbf{w}_y \end{bmatrix}$$

Noting that the filtered information state is deterministic, updated with the input record, the optimal nominal state is also constrained to give $\mathbf{e}_m^* = [\mathbf{0} \quad \mathbf{e}_y^{*\top}]^\top$. The following system of coupled equations is obtained

$$\mathbf{e}_\varphi^+ = \mathbf{B}_\xi \mathbf{K}_y \mathbf{e}_y^* \tag{3.28a}$$

$$\mathbf{e}_y^+ = (\mathbf{I} + \mathbf{C}_\theta \mathbf{B}_\xi \mathbf{K}_y) \mathbf{e}_y^* + \mathbf{w}_y. \tag{3.28b}$$

Both error systems are stable, by construction. It is then sufficient to specify a rPI set for the output error system (3.28b), $\mathcal{E}_y \in \mathbb{R}^{n_y}$, such that $\mathbf{e}_y^+ \in \mathcal{E}_y, \forall \mathbf{e}_y \in \mathcal{E}_y, \mathbf{w}_y \in \mathcal{W}_y$.

Assuming \mathcal{W}_y is a known compact set, the existence of a minimal rPI set is guaranteed and an arbitrarily accurate outer approximation can be computed (Rakovic et al. 2005). The model error rPI set is specified in (3.29).

$$\mathcal{E}_m = \mathbf{B}_\xi \mathbf{K}_y \mathcal{E}_y \times \mathcal{E}_y. \quad (3.29)$$

The tightened input/output constraints, that in turn define \mathcal{X}_w , are given by

$$\begin{aligned} \mathcal{Y}_w &:= \mathcal{Y} \ominus \mathcal{E}_y \\ \mathcal{U}_w &:= \mathcal{U} \ominus \mathbf{K}_y \mathcal{E}_y. \end{aligned} \quad (3.30)$$

where the operations \ominus and \oplus denote the Minkowski sum and difference respectively.

3.5.2 Artificial Steady-State

With the modified constraint set definition in hand, the artificial steady state and its role in the robust reformulation is presented. Consider the occurrence of a step change in the reference trajectory going from \mathbf{y}_t^r to \mathbf{y}_{t+}^r . Assume that the first reference is robustly admissible, i.e. $\mathbf{y}_t^r \in \mathcal{Y}_w$, and prior to time t , the system has been stabilized to an rPI region around a matching steady state. Once the step change is introduced, the MPC terminal set must be shifted accordingly. If the new reference is not admissible, the optimal problem is infeasible and the control action undefined. Even if this is not the case, there is no guarantee that the shifted terminal set can be reached within the limited number of steps, determined by the finite horizon, without constraint violations. The artificial steady state simply allows the problem to remain feasible by defining a terminal set, consistent with

3.5 ROBUST REFORMULATION

the model, as close as possible to the one corresponding to the intended reference. The stage and terminal costs are redefined accordingly,

$$\begin{aligned}\ell(\mathbf{x}, \mathbf{u}, \mathbf{x}_m^s) &:= \|\mathbf{x}_m - \mathbf{x}_m^s\|_{\mathbf{Q}_\ell}^2 + \|\mathbf{u} - \mathbf{x}_u\|_{\mathbf{R}}^2 \\ J_f(\mathbf{x}_m, \mathbf{x}_m^s) &:= \|\mathbf{x}_m - \mathbf{x}_m^s\|_{\mathbf{P}_f}^2\end{aligned}\tag{3.31}$$

where, $\mathbf{Q}_\ell = \mathbf{C}_m^\top \mathbf{Q} \mathbf{C}_m^\top$, $\mathbf{P}_f = \mathbf{P}_\infty$. The artificial steady state variable, $\hat{\mathbf{x}}^s$, must be consistent with the model,

$$\begin{aligned}\hat{\boldsymbol{\varphi}}^s &= \mathbf{A}_\xi \hat{\boldsymbol{\varphi}}^s + \mathbf{B}_\xi \hat{\mathbf{u}}^s \\ \hat{\mathbf{y}}^s &= \mathbf{C}_\theta \hat{\boldsymbol{\varphi}}^s\end{aligned}, \quad \hat{\mathbf{x}}^s = \begin{bmatrix} \hat{\mathbf{x}}_m^s \\ \hat{\mathbf{u}}^s \end{bmatrix}, \quad \hat{\mathbf{x}}_m^s = \begin{bmatrix} \mathbf{0} \\ \hat{\mathbf{y}}^s \end{bmatrix}$$

and should be as close to the steady state that results on the intended output reference signal, \mathbf{y}_t^r . The artificial steady state characterization is completed with the definition of the associated cost to be minimized,

$$J_s(\mathbf{y}^s, \mathbf{y}^r) := \|\mathbf{y}^s - \mathbf{y}^r\|_{\mathbf{T}}^2\tag{3.32}$$

where the offset cost matrix, \mathbf{T} , is symmetric and satisfies $\mathbf{T} \succeq c_T \mathbf{Q}$, for a scalar real constant, $c_T \in (0, 1]$.

3.5.3 Reformulation

The modifications introduced in relation to $\mathcal{P}_N(\mathbf{x})$ are briefly summarized. First, the output element of the nominal state at the first stage, $\hat{\mathbf{x}}_{y,0}$, is set as a decision variable

and constrained to a neighborhood of the current measured output, \mathbf{y} . A penalty cost to the deviation from the measurement is added to the objective. Second, an artificial steady state, that is also a decision variable, is defined with an associated offset cost to be appended to the objective and additional constraints. The stage and final costs are centered at the artificial steady state. The original input/output constraints are tightened proportionally to an associated rPI set. The terminal constraint set, $\mathcal{X}_{f,w}(\hat{\mathbf{x}}^s)$, is defined as an invariant set for tracking (Definition 2 in Limon et al. (2010)) and parametrized by the artificial steady state. The terminal cost is centered at $\hat{\mathbf{x}}^s$, implying that the stabilizing infinite horizon tracking policy is applied beyond the finite portion in the objective according to (3.23),

$$\kappa_f(\mathbf{x}, \mathbf{x}_m^s) = \mathbf{x}_u + \mathbf{K}_\infty(\mathbf{x}_m - \mathbf{x}_m^s).$$

The optimal nominal input and initial state pair, $\{\hat{\mathbf{u}}_0^*, \hat{\mathbf{x}}_0^*\}$, is subsequently used to compute a robust MPC policy (3.26).

The tracking invariance definition implies that the terminal set, $\mathcal{X}_{f,w}(\hat{\mathbf{x}}^s)$, parametrized by a robustly admissible steady state,

$$\hat{\mathbf{x}}^s \in \mathcal{X}_s = \{\hat{\mathbf{x}}^s \mid (3.33g) \text{ and } (3.33h) \text{ hold}\},$$

satisfies $\hat{\mathbf{x}}^s \oplus (\mathcal{E}_m \times \mathbf{K}_y \mathcal{E}_y) \subseteq \mathcal{X}_{f,w}(\hat{\mathbf{x}}^s) \subseteq \mathcal{X}$, and is positively invariant under the tracking terminal policy,

$$f(\hat{\mathbf{x}}, \kappa_f(\hat{\mathbf{x}}, \hat{\mathbf{x}}_m^s)) \in \mathcal{X}_{f,w}(\hat{\mathbf{x}}^s), \forall \hat{\mathbf{x}} \in \mathcal{X}_{f,w}(\hat{\mathbf{x}}^s) \text{ and } \forall \hat{\mathbf{x}}^s \in \mathcal{X}_s.$$

3.5 ROBUST REFORMULATION

At a given sampling instance, the optimal control problem is parametrized by the current reference signal and the measured state. The tracking objective is redefined with the new variables,

$$J_N(\hat{\mathbf{x}}_0, \mathbf{u}, \hat{\mathbf{x}}_m^s) := \sum_{k=0}^{N-1} \ell(\hat{\mathbf{x}}_k, \hat{\mathbf{u}}_k, \hat{\mathbf{x}}_m^s) + J_f(\hat{\mathbf{x}}_{m,N}, \hat{\mathbf{x}}_m^s)$$

The full robust MPC optimization problem obtained by appending the offset and measurement deviation costs, along with the related constraints, $\mathcal{P}_{w,N}(\mathbf{x}, \mathbf{y}^r)$, is stated below.

$$\mathcal{P}_{w,N}(\mathbf{x}, \mathbf{y}^r) : \min_{\hat{\mathbf{x}}_0, \mathbf{u}, \hat{\mathbf{x}}_m^s, \hat{\varphi}^s} J_N(\hat{\mathbf{x}}_0, \mathbf{u}, \hat{\mathbf{x}}_m^s) + J_s(\hat{\mathbf{y}}^s, \mathbf{y}^r) + J_f(\mathbf{x}_m, \hat{\mathbf{x}}_{m,0}) \quad (3.33)$$

$$\text{s.t.} \quad \hat{\mathbf{x}}_{k+1} = f(\hat{\mathbf{x}}_k, \hat{\mathbf{u}}_k), \quad k \in \mathbb{I}_{0:N-1} \quad (3.33a)$$

$$\hat{\mathbf{x}}_{\varphi,0} = \mathbf{x}_{\varphi} \quad (3.33b)$$

$$\mathbf{x}_y \in \hat{\mathbf{x}}_{y,0} \oplus \mathcal{E}_y \quad (3.33c)$$

$$\hat{\mathbf{x}}_{u,0} = \mathbf{x}_u \quad (3.33d)$$

$$\hat{\mathbf{x}}_k \in \mathcal{X}_w, \quad k \in \mathbb{I}_{1:N-1} \quad (3.33e)$$

$$\hat{\mathbf{x}}_N \in \mathcal{X}_{w,f}(\hat{\mathbf{x}}^s) \quad (3.33f)$$

$$\begin{bmatrix} \mathbf{A}_{\xi} - \mathbf{I} & \mathbf{B}_{\xi} \\ \mathbf{C}_{\theta} & \mathbf{0} \end{bmatrix} \begin{bmatrix} \hat{\varphi}^s \\ \hat{\mathbf{u}}^s \end{bmatrix} = \begin{bmatrix} \mathbf{0} \\ \hat{\mathbf{y}}^s \end{bmatrix} \quad (3.33g)$$

$$\hat{\mathbf{x}}^s \in \mathcal{X}_w \quad (3.33h)$$

Note that the terminal cost is used twice. Inside J_N to penalize deviations from the desired steady state at the end of the finite horizon, and a second time to penalize the deviation of the first stage extended model variables, $\hat{\mathbf{x}}_{m,0}$, from the measured states.

The associated optimal cost and robustly admissible set of measured states are implicitly defined accordingly by $J_{w,N}^*(\mathbf{x}, \mathbf{y}^r)$ and $\mathcal{X}_{w,N}$.

Two additional adjustments, that allow the use of the optimal objective as an ISS Lyapunov function, are required. First, if the measured error is sufficiently small, then the first stage state is no longer optimized. Instead, it is fixed at the measured state. This is achieved by enforcing the following condition,

$$\begin{aligned} &\text{if } \Delta(\mathbf{y} - \mathbf{C}_\theta \boldsymbol{\varphi}) \in c_y \mathcal{E}_y, \\ &\quad \text{replace (3.33b)-(3.33d)} \\ &\quad \text{with } \hat{\mathbf{x}}_0 = \mathbf{x}, \end{aligned} \tag{3.34}$$

where the real constant, c_y , satisfies $0 < c_y \ll 1$. This modification will be useful to show that the cost associated with the error is bounded. As shown in Figure 3.3, for a given optimized error, \mathbf{w}_m can make the subsequent error at the next sampling instance either greater or smaller, as measured by $\|\cdot\|_{\mathcal{P}_f}^2$, as shown by the dashed lines. If the error is fixed at zero by the adjustment above, the disturbance terminal cost is obtained. The error cost is then bounded from above on both sides of the vertical dotted line for any realization of the disturbance.

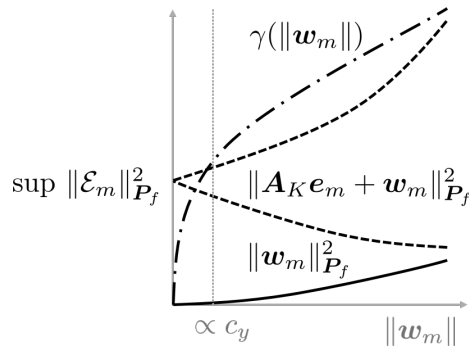


Figure 3.3: Bounded Disturbance Cost

3.5 ROBUST REFORMULATION

Second, the finite horizon control is determined by the terminal policy if the tracking is satisfied within a small region around the reference model state, \mathbf{x}_m^r , i.e.,

$$\begin{aligned}
 & \text{if } \|\mathbf{x}_m - \mathbf{x}_m^r\|_{\mathbf{P}_f}^2 \leq \epsilon \\
 & \hat{\mathbf{x}}_0^* = \mathbf{x}, \quad \hat{\mathbf{x}}_m^{s,*} = \mathbf{x}_m^r \\
 & \mathbf{u}^* = \begin{bmatrix} \kappa_f(\hat{\mathbf{x}}_0^*, \hat{\mathbf{x}}_m^{s,*}) \\ \vdots \\ \kappa_f(\hat{\mathbf{x}}_{N-1}, \hat{\mathbf{x}}_m^{s,*}) \end{bmatrix}
 \end{aligned} \tag{3.35}$$

where ϵ defines the region

$$\mathcal{E}_{m,\epsilon}(\mathbf{x}_m^r) := \{\mathbf{x}_m \mid \|\mathbf{x}_m - \mathbf{x}_m^r\|_{\mathbf{P}_f}^2 \leq \epsilon\} \subseteq \mathbf{x}_m^r \oplus \mathcal{E}_m.$$

All the elements of the robust MPC control strategy have been introduced. Omitting the dependence of the output reference, and noting that under the constraints imposed on the nominal state $\mathbf{K}_m \mathbf{e}_m^*$ simplifies to $\mathbf{K}_y \mathbf{e}_y^*$, the control law is

$$\kappa_N^{rc,*}(\mathbf{x}) := \hat{\mathbf{u}}_0^* + \mathbf{K}_y \mathbf{e}_y^* \tag{3.36}$$

The policy is summarized in the pseudo-code in Algorithm 3.1 below.

Algorithm 3.1 Robust Control Action

Require:Measured State, \mathbf{x} , and Disturbance \mathbf{w}_m rPI Set and Ancillary Gain $\mathcal{E}_m, \mathbf{K}_m$ GOBF Matrices \mathbf{A}, \mathbf{B} , and \mathbf{C}_θ Parameters $c_y, \mathbf{Q}, \mathbf{R}, \mathbf{T}$, and \mathbf{P}_f **Ensure:**Control action \mathbf{u}

- 1: Check (3.34), adjust constraints if necessary
 - 2: Solve (3.33)
 - 3: Check (3.35), update solution if necessary
 - 4: Extract $\hat{\mathbf{u}}_0^*, \hat{\mathbf{y}}_0^*$
 - 5: $\mathbf{u} \leftarrow \hat{\mathbf{u}}_0^* + \mathbf{K}_y(\mathbf{y} - \hat{\mathbf{y}}_0^*)$
-

3.5.4 *Input to State Stability*

Before a ISS result can be stated, a few preliminary definitions and results are required. Noting that for a fixed sequence of inputs, the objective function of $\mathcal{P}_{w,N}(\mathbf{x}, \mathbf{y}^r)$ is fully determined by the model portion of the state, \mathbf{x}_m , define the function $V^* : \mathbb{R}^{n_m} \rightarrow \mathbb{R}_+$,

$$V^*(\mathbf{x}_m - \mathbf{x}_m^r) := J_{w,N}^*(\mathbf{x}, \mathbf{y}^r),$$

and the projection of $\mathcal{X}_{w,N}$ onto \mathbb{R}^{n_m} , $\mathcal{M} := \text{Proj}_m(\mathcal{X}_{w,N})$. Also, consider the following shifted receding horizon control moves vector and initial condition,

$$\Delta \mathbf{u}^\circ := \begin{bmatrix} \Delta \hat{\mathbf{u}}_1^* \\ \vdots \\ \Delta \hat{\mathbf{u}}_{N-1}^* \\ \mathbf{K}_\infty(\hat{\mathbf{x}}_{m,N}^* - \hat{\mathbf{x}}_m^{s,*}) \end{bmatrix}, \quad \hat{\mathbf{x}}_{m,0}^\circ = \hat{\mathbf{x}}_{m,1}^*,$$

obtained from the optimal solution of $\mathcal{P}_{w,N}^*(\mathbf{x}, \mathbf{y}^r)$. Due to the tightened constraints and the assumed invariance of the terminal tracking target set, this vector along with the artificial steady state variables, $\hat{\mathbf{x}}^{s,*}$, $\hat{\mathbf{y}}^{s,*}$, parametrize a feasible solution of $\mathcal{P}_{w,N}^*(\mathbf{x}^+, \hat{\mathbf{y}}^r)$. Additionally, define $V^\circ(\mathbf{x}_m^+ - \mathbf{x}_m^r)$ as the associated suboptimal objective cost. Note that for any pair, $\mathbf{x}_m^a, \mathbf{x}_m^b \in \mathbb{R}^{n_m}$, it follows from the first order condition of convexity applied to $\frac{1}{2} \|\cdot\|_{\mathcal{Q}_\ell}^2$, that

$$\|\mathbf{x}_m^a\|_{\mathcal{Q}_\ell}^2 + \|\mathbf{x}_m^b\|_{\mathcal{Q}_\ell}^2 \geq \frac{1}{2} \|\mathbf{x}_m^a + \mathbf{x}_m^b\|_{\mathcal{Q}_\ell}^2. \quad (3.37)$$

Lastly, as shown in (R&M ref) the existence of an ISS Lyapunov function for a given constrained dynamic system implies input to state stability. We proceed to show that $V^*(\mathbf{x}_m - \mathbf{x}_m^r)$ satisfy the defining inequalities for an ISS Lyapunov function, that guarantee robust stability.

Theorem 3. *Constrained Input-to-State Stability under $\kappa_N^{rc,*}$ and $w_y \in \mathcal{W}_y$.* Assuming a nonempty compact set \mathcal{M} , the closed-loop system trajectory for $\mathbf{x}_m - \mathbf{x}_m^r$ under the policy $\kappa_N^{rc,*}$ is ISS in \mathcal{M} .

Proof. First note that, $\forall \mathbf{x}_m \in \mathcal{M}$,

$$\begin{aligned}
V^*(\mathbf{x}_m - \mathbf{x}_m^r) &\geq \|\hat{\mathbf{x}}_{m,0}^* - \hat{\mathbf{x}}_m^{s,*}\|_{\mathbf{Q}_\ell}^2 + \|\mathbf{x}_m - \hat{\mathbf{x}}_{m,0}^*\|_{\mathbf{P}_f}^2 + \|\hat{\mathbf{x}}_m^{s,*} - \mathbf{x}_m^r\|_{\mathbf{T}_s}^2 \\
&\geq \|\hat{\mathbf{x}}_{m,0}^* - \hat{\mathbf{x}}_m^{s,*}\|_{\mathbf{Q}_\ell}^2 + \|\mathbf{x}_m - \hat{\mathbf{x}}_{m,0}^*\|_{\mathbf{Q}_\ell}^2 + c_T \|\hat{\mathbf{x}}_m^{s,*} - \mathbf{x}_m^r\|_{\mathbf{Q}_\ell}^2 \\
&\geq \frac{1}{2} c_T \|\mathbf{x}_m - \hat{\mathbf{x}}_m^{s,*}\|_{\mathbf{Q}_\ell}^2 + \frac{1}{2} c_T \|\mathbf{x}_m^* - \hat{\mathbf{x}}_{m,0}^*\|_{\mathbf{Q}_\ell}^2 \\
&\geq \frac{1}{4} c_T \|\mathbf{x}_m - \mathbf{x}_m^r\|_{\mathbf{Q}_\ell}^2.
\end{aligned}$$

where $\mathbf{T}_s = \mathbf{C}_m^\top \mathbf{T} \mathbf{C}_m$. The second line holds since the choice of matrices guarantee $\|\cdot\|_{\mathbf{P}_f}^2 \geq \|\cdot\|_{\mathbf{Q}_\ell}^2$ and $\|\cdot\|_{\mathbf{T}_s}^2 \geq c_T \|\cdot\|_{\mathbf{Q}_\ell}^2$. The lines below follow from applying the inequality in (3.37) and multiplying by positive constants less than one. It can be shown that there exist a \mathcal{K}_∞ -class function, $\underline{\alpha}(\|\mathbf{x}_m - \mathbf{x}_m^r\|)$ that bounds the right hand side from below since $\mathbf{Q}_\ell \succeq 0$. Therefore, $V^*(\mathbf{x}_m - \mathbf{x}_m^r) \geq \underline{\alpha}(\|\mathbf{x}_m - \mathbf{x}_m^r\|)$. On the other hand, an upper bound can be obtained for $\mathbf{x}_m \in \mathcal{E}_{m,\epsilon}(\mathbf{x}_m^r)$, since it follows from the assignments in (3.35) that $V^*(\mathbf{x}_m - \mathbf{x}_m^r) \leq \|\mathbf{x}_m - \mathbf{x}_m^r\|_{\mathbf{P}_f}^2 \leq \bar{\alpha}_\epsilon(\|\mathbf{x}_m - \mathbf{x}_m^r\|)$. This upper bound can be extended to the set \mathcal{M} by another \mathcal{K}_∞ -class function, $\bar{\alpha}(\|\mathbf{x}_m - \mathbf{x}_m^r\|)$ as long as $\mathcal{E}_{m,\epsilon}(\mathbf{x}_m^r) \subseteq \mathcal{M}$, which was assumed to hold for all robustly admissible references. From optimality, it follows that

$$V^*(\mathbf{x}_m^+ - \mathbf{x}_m^r) - V^*(\mathbf{x}_m - \mathbf{x}_m^r) \leq V^\circ(\mathbf{x}_m^+ - \mathbf{x}_m^r) - V^*(\mathbf{x}_m - \mathbf{x}_m^r).$$

3.5 ROBUST REFORMULATION

Expanding the right hand side,

$$\begin{aligned}
V^\circ(\mathbf{x}_m^+ - \mathbf{x}_m^r) - V^*(\mathbf{x}_m - \mathbf{x}_m^r) &= -\|\hat{\mathbf{x}}_{m,0}^* - \hat{\mathbf{x}}_m^{s,*}\|_{\mathbf{Q}_\ell}^2 - \|\Delta \hat{\mathbf{u}}_0^*\|_{\mathbf{R}}^2 \\
&\quad + \|\mathbf{x}_m^+ - \hat{\mathbf{x}}_{m,1}^*\|_{\mathbf{P}_f}^2 - \|\mathbf{x}_m - \hat{\mathbf{x}}_{m,0}^*\|_{\mathbf{P}_f}^2 \\
&\leq -(\|\hat{\mathbf{x}}_{m,0}^* - \hat{\mathbf{x}}_m^{s,*}\|_{\mathbf{Q}_\ell}^2 + \|\mathbf{x}_m - \hat{\mathbf{x}}_{m,0}^*\|_{\mathbf{Q}_\ell}^2) \\
&\quad + \|\mathbf{x}_m^+ - \hat{\mathbf{x}}_{m,1}^*\|_{\mathbf{P}_f}^2 \\
&\leq -\frac{1}{2}\|\mathbf{x}_m - \hat{\mathbf{x}}_m^{s,*}\|_{\mathbf{Q}_\ell}^2 + \|\mathbf{A}_K \mathbf{e}_m^* + \mathbf{w}_m\|_{\mathbf{P}_f}^2
\end{aligned}$$

The equality is obtained after the elimination of terms given by the shifted input sequence and the optimality of the terminal cost. The first inequality holds since $\|\cdot\|_{\mathbf{R}}^2 \geq 0$ and $\|\cdot\|_{\mathbf{P}_f}^2 \geq \|\cdot\|_{\mathbf{Q}_\ell}^2$. The application of the inequality in (3.37), and the definition of the model error dynamics (3.27) yield the last line. It can be shown that for the optimal artificial steady state at each sampling instance, there exists a scalar constant $c_s^* \in (0, 1]$, such that $\|\mathbf{x}_m - \hat{\mathbf{x}}_m^{s,*}\|_{\mathbf{Q}_\ell}^2 = c_s^* \|\mathbf{x}_m - \mathbf{x}_m^r\|_{\mathbf{Q}_\ell}^2$. In particular, if the assignments (3.35) apply, $c_s^* = 1$. Therefore, there exists a \mathcal{K}_∞ -class function, $\alpha(\|\mathbf{x}_m - \mathbf{x}_m^r\|)$ such that $-\frac{1}{2}c_s^* \|\mathbf{x}_m - \mathbf{x}_m^r\|_{\mathbf{Q}_\ell}^2 \leq -\alpha(\|\mathbf{x}_m - \mathbf{x}_m^r\|)$. As shown above, (3.34) enables the definition of a \mathcal{K} -class function, $\gamma(\|\mathbf{w}_m\|)$, that satisfies,

$$\|\mathbf{A}_K \mathbf{e}_m^* + \mathbf{w}_m\|_{\mathbf{P}_f}^2 \leq \gamma(\|\mathbf{w}_m\|).$$

Combining these inequalities with the previous observations, it is determined that $\forall \mathbf{x}_m \in \mathcal{M}$, and $\forall \mathbf{w}_y \in \mathcal{W}_y$,

$$V^*(\mathbf{x}_m^+ - \mathbf{x}_m^r) \geq \underline{\alpha}(\|\mathbf{x}_m - \mathbf{x}_m^r\|)$$

$$V^*(\mathbf{x}_m^+ - \mathbf{x}_m^r) \leq \bar{\alpha}(\|\mathbf{x}_m - \mathbf{x}_m^r\|)$$

$$V^*(\mathbf{x}_m^+ - \mathbf{x}_m^r) \leq V^*(\mathbf{x}_m - \mathbf{x}_m^r) - \alpha(\|\mathbf{x}_m - \mathbf{x}_m^r\|) + \gamma(\|\mathbf{w}_m\|)$$

which define an ISS Lyapunov function and the result follows. \square

3.6 SUMMARIZING EXAMPLE

The control design elements, presented throughout the chapter, will be illustrated with their application to the minimal mass-spring example from Chapter 2. The intention is to follow incremental levels of sophistication in the control design, allowing us to draw conclusions for each particular case in a didactic manner.

3.6.1 *Experiment Definition*

The stage cost parameters, $\mathbf{Q} = 0.1$, $\mathbf{R} = 1$, and a measurement noise sequence with known bounds remain the same for all the cases presented. Two GOBF models are generated. First, an exact model with the poles and expansion coefficients that match the physical system. Second, an approximate model with the generation pole set ξ_3 from the preceding chapter and the parameter output matrix $\mathbf{C}_\theta = \begin{bmatrix} 2.25 & 1.00 & 0.00 & 0.75 \end{bmatrix}$ is specified.

3.6.2 *Output Feedback*

The first aspect to be discussed is the effect of output feedback, enabled by the model obtained after implementing a backwards difference filter on the GOBF dynamics. In or-

3.6 SUMMARIZING EXAMPLE

der to assess its value, a baseline is defined with an LQ controller applied to the following unfiltered dynamics,

$$\begin{bmatrix} \varphi_{k+1} \\ \mathbf{u}_k \end{bmatrix} = \begin{bmatrix} \mathbf{A}_\xi & \mathbf{B}_\xi \\ \mathbf{0} & \mathbf{I} \end{bmatrix} \begin{bmatrix} \varphi_k \\ \mathbf{u}_{k-1} \end{bmatrix} + \begin{bmatrix} \mathbf{B}_\xi \\ \mathbf{I} \end{bmatrix} \Delta \mathbf{u}_k$$

The unconstrained optimal policy is defined with respect to a steady state, φ^r , that minimizes the steady state input magnitude and satisfies $\mathbf{C}_\theta \varphi^r = y^r$. Where \mathbf{C}_θ is generated with the inaccurate parameters. In terms of the state above, the resulting tracking stage cost for (3.19) is

$$\|\mathbf{y}_k - \mathbf{y}^r\|_{\mathbf{Q}}^2 + \|\Delta \mathbf{u}_k\|_{\mathbf{R}}^2 = \|\varphi_k - \varphi^r\|_{\mathbf{Q}_\theta}^2 + \|\Delta \mathbf{u}_k\|_{\mathbf{R}}^2, \quad \mathbf{Q}_\theta = \mathbf{C}_\theta^\top \mathbf{Q} \mathbf{C}_\theta.$$

With the transition dynamics and the cost matrices above, an infinite-horizon LQ policy is obtained. Without output feedback, the state is determined exclusively by the input record while the optimal policy is only updated by a shift in the reference output. A limitation of this approach is that it will have a tracking offset under model mismatch as shown in Figure 3.4. By replacing the model dynamics with the filtered version, measurement feedback is enabled. Two unconstrained policies were presented. The infinite horizon tracking policy (3.23), shown in Figure 3.5, and the extended state policy (3.22). In contrast to the unfiltered case, there is no need to compute the GOBF vector steady state as the model definition handles the output reference directly. In addition to measurement feedback, the extended model policy introduces a known disturbance that appends the future reference at the end of the finite horizon which is set at $N = 10$. The profile for this case is illustrated in Figure 3.6.

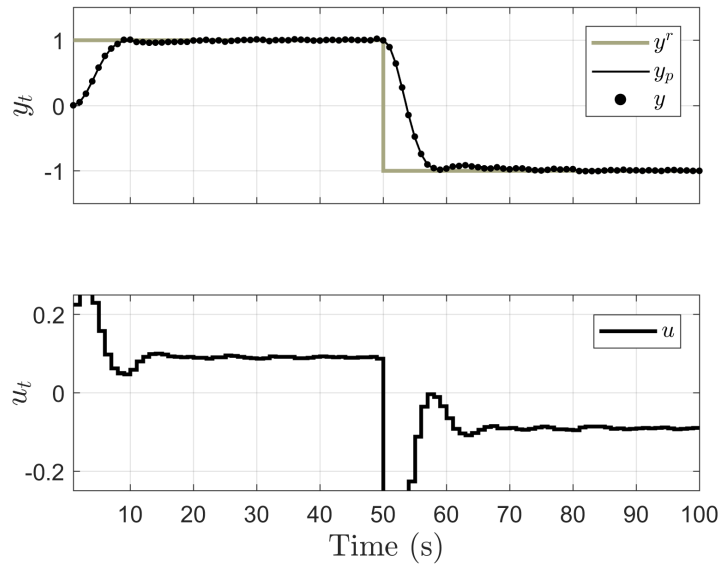


Figure 3.5: Infinite-Horizon Tracking Policy, Approximate Model

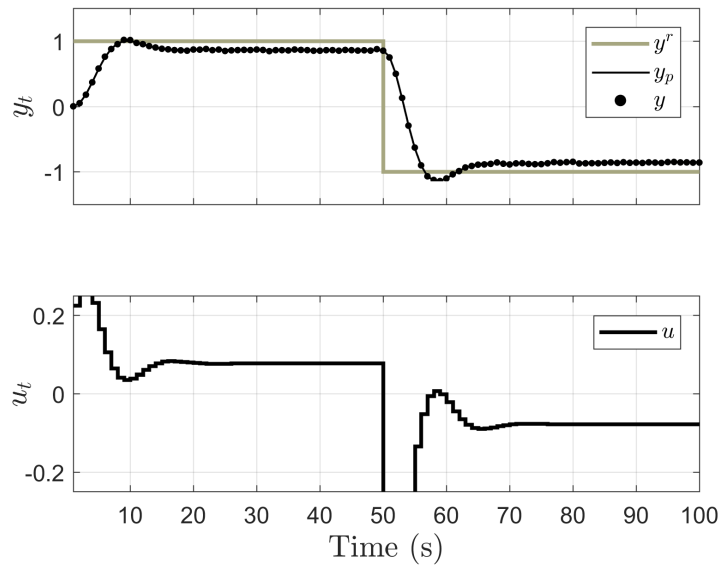


Figure 3.4: Unfiltered LQ Policy, Approximate Model

3.6 SUMMARIZING EXAMPLE

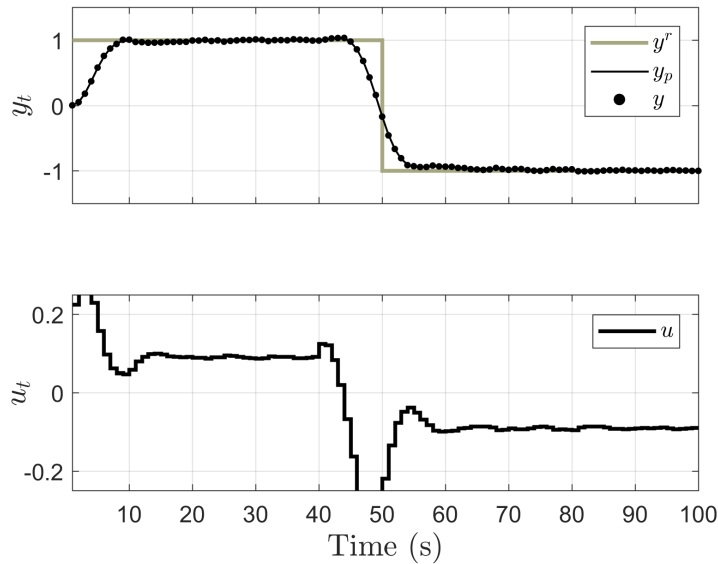


Figure 3.6: Extended State Tracking Policy, Approximate Model

Compared to the control profile obtained with the unfiltered dynamics, the feedback policies provide superior tracking performance. As seen in the figures above, the unconstrained feedback policies are identical initially, and only differ once the output reference changes. The extended model offers the ability to anticipate the shift and adjust the optimal input profile accordingly. This feature can be particularly useful for tracking reference profiles that are not piece-wise constant. Also, note that the input profile obtained from the extended model policy has a less aggressive control moves as a result.

3.6.3 Robust Reformulation

Constraints handling could be achieved by the iterative or preemptive adjustment of the cost matrices. Instead, the robust formulation circumvents this by the explicit declaration

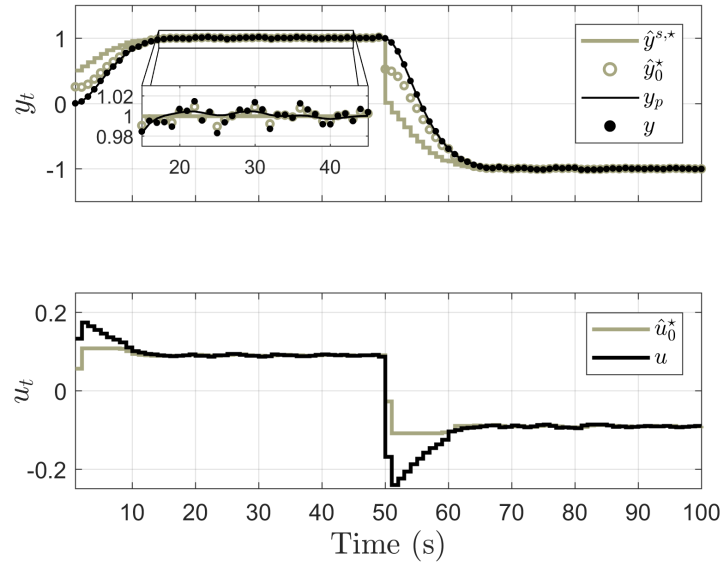


Figure 3.7: Robust Tracking Policy, Perfect Model

of the constraints in the associated optimal control problem (3.33). The system is now subject to the constraints,

$$0.25 \leq u \leq 0.25$$

$$-1.5 \leq y \leq 1.5,$$

which are violated by the profiles obtained from the unconstrained policies above. In order to illustrate the robust features, the ancillary gain and error bounds are computed such that the steady states for the desired output references are near the boundary of the tightened constraints. The offset cost is given by $T = 2Q$. The system input/output profiles along with their related optimization variables are displayed for both models in the Figures 3.7 and 3.8.

Under model mismatch, the tracking performance deteriorates slightly. With respect to the perfect models, as one would expect, the settling times for the artificial steady

3.6 SUMMARIZING EXAMPLE

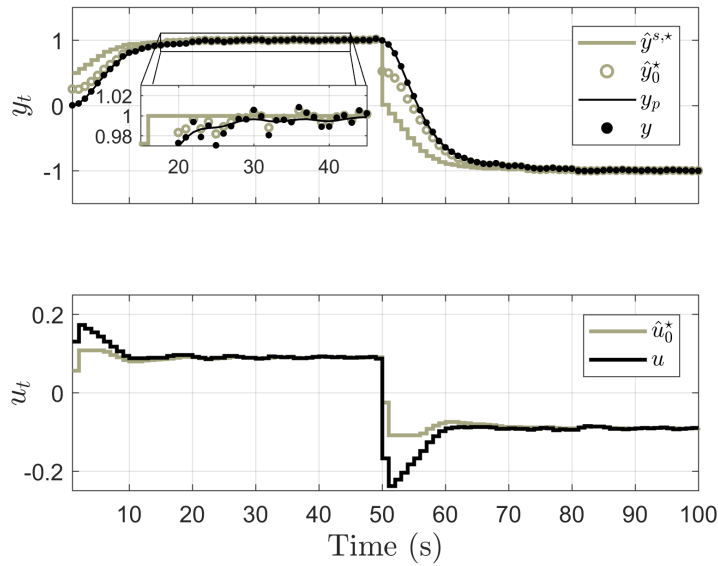


Figure 3.8: Robust Tracking Policy, Approximate Model

state and the plant output increase. In Figure 3.9, the descent of the objective function under a constant reference for the approximate model is illustrated. The filtered Gaussian measurement noise and the overall output disturbance, including the model error, is displayed in the bottom quadrant.

The effect of the offset cost is illustrated by increasing it with $T = 10Q$. This results in a more aggressive policy as the artificial steady state is pushed towards the reference by the increased cost which results in optimal control actions at the boundary for several sampling instances after the reference step change. This is shown in detailed along with the optimized variables in Figure 3.11.

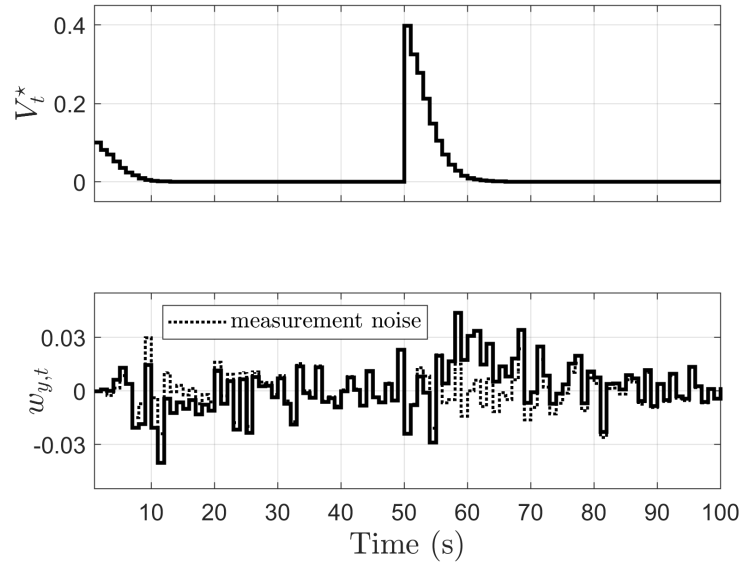


Figure 3.9: Lyapunov Descent and Output Disturbance, Approximate Model

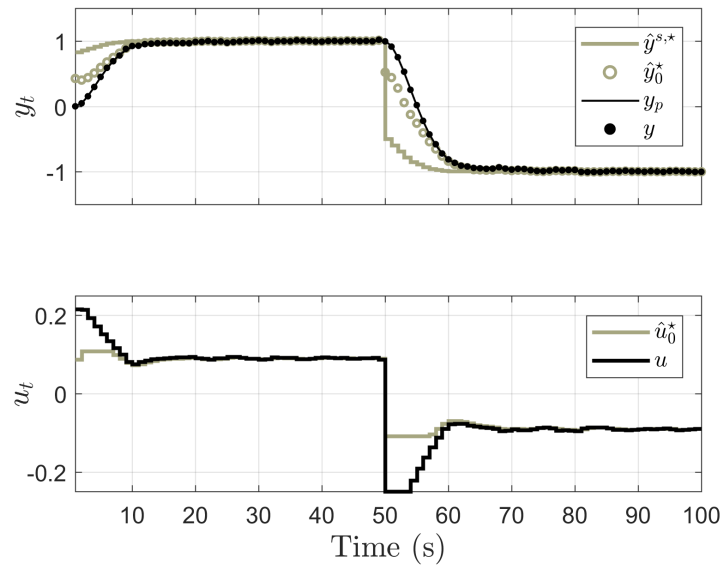


Figure 3.10: Robust Tracking Policy with Higher Offset Cost, Approximate Model

3.6 SUMMARIZING EXAMPLE

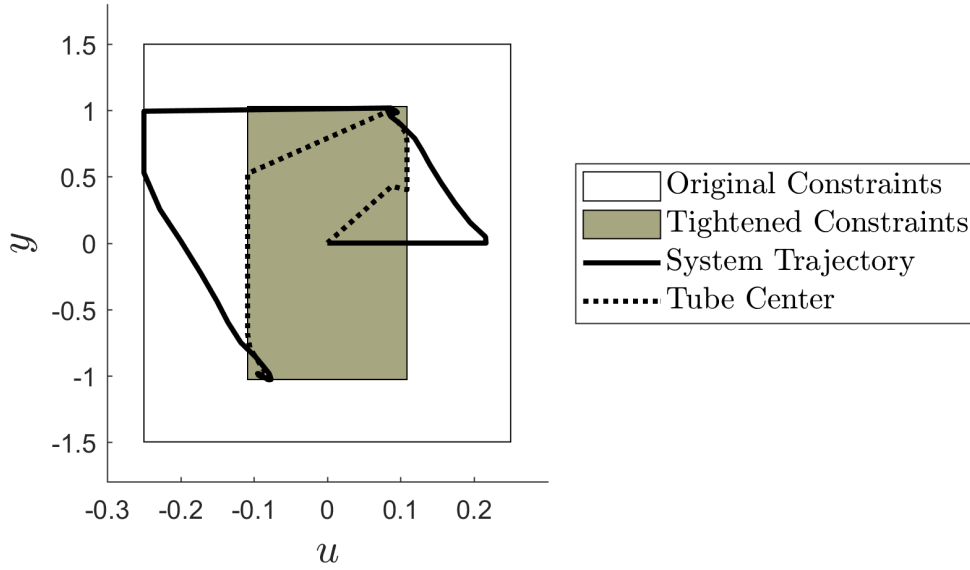


Figure 3.11: Robust Tracking Policy Constraint Enforcement, Approximate Model

Robust Reformulation Remarks

Assuming that the measurement noise component is Gaussian, the model error approaches a constant in expectation for a steady input. [Limon et al. \(2010\)](#) suggest adjusting against it with the aid of a stable estimator. For a given steady state, the following expression is satisfied,

$$\hat{\mathbf{y}} = \mathbf{y} - \mathbf{C}_m (\mathbf{I} - \mathbf{A}_K) \mathbf{w}_m,$$

which follows from the definition of the error and its dynamics. Based on this expression, the adjusted reference is defined,

$$\hat{\mathbf{y}}_t^r := \mathbf{y}_t^r - \mathbf{C}_m (\mathbf{I} - \mathbf{A}_K) \hat{\mathbf{w}}_{m,t}, \quad (3.38)$$

where $\hat{\mathbf{w}}_{m,t}$ is calculated with a suitable model disturbance estimator. For example, a stable first order error filter

$$\hat{\mathbf{w}}_{m,t} = \rho (\mathbf{x}_{m,t} - (\mathbf{A}_m \mathbf{x}_{m,t-1} + \mathbf{B}_m \Delta \mathbf{u}_{t-1})) + (1 - \rho) \hat{\mathbf{w}}_{m,t-1}, \rho \in (0, 1).$$

For a non-negligible measurement noise, a more complex filter may be required. Although this feature could be added to our formulation, this is not necessary as the integral action of the filtered cost takes care of it.

The robust policy presented here is inspired by the work of [Zeilinger et al. \(2014\)](#), in which a suboptimal feasible solution is obtained in limited time. We refer to their manuscript for details on how to extend this formulation to consider limits to the solution time. The most relevant modification required is the inclusion of a stabilizing constraint that turns the current Quadratic Program (QP) formulation into a convex Quadratically Constrained QP (QCQP).

The design criteria for the ancillary gain is more appropriately handled by H_∞ methods in general. This requires the solution of convex Linear Matrix Inequality (LMI) optimization problems. Here, due to the simplicity of the illustrative system, it is specified with an Linear quadratic regulator (LQR) policy. More details regarding this feature are provided in [Limon et al. \(2010\)](#).

4

CERTAINTY EQUIVALENCE ADAPTIVE GOBF-MPC

With the set of MPC policies for a fixed model structure properly defined, we advance into the formulation of the adaptive case. The parameter adaptation method to be followed is derived from the conditional distribution obtained under an idealized characterization of the disturbance signal. Different adjustments and the introduction of new ingredients in the resulting set of equations constitute the field of Recursive Least Squares (RLS) methods. A specific RLS choice, with only a couple of parameters to adjust, is presented and serves as the adaptation component to be included thereafter. The chapter proceeds with a series of illustrative simulation examples for the infinite-horizon tracking control policy applied to the mass-spring minimal SISO system. This is done with the aim to place the focus solely on the effect of the GOBF generating pole set choice. Lastly, a more general certainty equivalence control algorithm that includes signal constraints is introduced. Its performance is illustrated on a quadruple tank MIMO system.

4.1 PARAMETER ADAPTATION

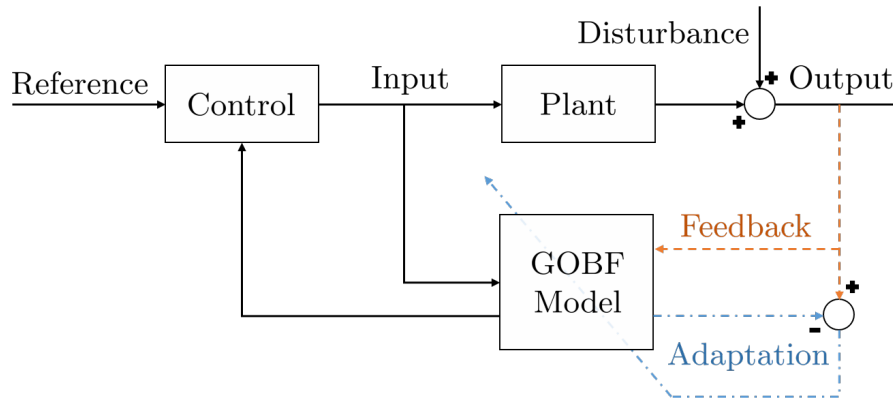


Figure 4.1: Adaptive GOBF MPC

4.1 PARAMETER ADAPTATION

Adaptation can be understood as an indirect output feedback connection to the controller with respect to the existing framework, as shown in Figure 4.1. By changing the coefficients of the GOBF expansions that parametrize the model, the tracking cost evaluation changes accordingly. As a result, the computation of the optimal input changes with the adaptation dynamics. The purpose of the inclusion of this feature is to find parameters that approximate the true system transfer function in the neighborhood of the output reference signal in situations where these are not already known. As noted in Chapter 2, including pole locations into the model structure that are consistent with the true dynamics is important to yield acceptable predictor structures. This was shown to be facilitated by the GOBF structure as it allows multiple locations. The generating pole set can afford inaccurate locations, as long as approximate ones for the dominant features are included.

If an accurate system model is already at hand, there is no need for adaptation and the GOBF parametrization is not required. The inherent assumption of the approach is that only approximate knowledge, expressed by a generating pole set, is available. Since

the exact expansion coefficients may no longer be computed for uncertain dynamics, the problem must be defined in terms of their estimates, conditioned to prior distributions and the available data record.

4.1.1 Conditional Parameter Distribution

The model error signal has been characterized in section 2.4.3 with respect to the structural model error and a stochastic contribution. A necessary¹ simplifying assumption, is to treat each scalar model error signal sequence, corresponding to a single output channel, as *i.i.d.* samples drawn from zero-mean, Gaussian distributions with variance $r_{i,v}$. This simplification leads to the formulation of a least-squares problem for the parameter estimate. Its solution can be expressed with a set of recursions that are equivalent to the Kalman Filter applied to the estimate of an uncertain state with time-varying dynamics. Consider a parameter vector that adheres to the following linear state-space representation,

$$\begin{aligned}\boldsymbol{\theta}_{t+1} &= \mathbf{A}_\theta \boldsymbol{\theta}_t + \mathbf{B}_\theta \hat{\mathbf{u}}_t + \mathbf{w}_t, & \boldsymbol{\theta}_0 &= \boldsymbol{\theta} \\ \mathbf{y}_t &= \mathbf{C}_{\varphi,t} \boldsymbol{\theta}_t + \mathbf{v}_t\end{aligned}\tag{4.1}$$

where $\mathbf{w}_k \sim \mathcal{N}(\mathbf{0}, \mathbf{Q}_w)$, and $\mathbf{v}_k \sim \mathcal{N}(\mathbf{0}, \mathbf{R}_v)$. Note that, unlike the state-transition dynamics, the output matrix, $\mathbf{C}_{\varphi,t}$, is time-varying. For an unmeasured, uncertain vector with known dynamics (4.1), the Kalman Filter specifies the estimate conditioned by an initial Gaussian distribution given by $\hat{\boldsymbol{\theta}}_{0|0}$, $\mathbf{P}_{0|0}$, and the data record \mathbf{Y}_t . The resulting distribu-

¹ For this derivation

4.1 PARAMETER ADAPTATION

tion is also Gaussian and is obtained by the recursions (4.2), derived from the associated least-squares problem.

$$\begin{aligned}
\mathbf{P}_{k|k-1} &= \mathbf{A}_\theta^\top \mathbf{P}_{k-1|k-1} \mathbf{A}_\theta + \mathbf{Q}_w \\
\hat{\boldsymbol{\theta}}_{k|k-1} &= \mathbf{A}_\theta \hat{\boldsymbol{\theta}}_{k-1|k-1} + \mathbf{B}_\theta \hat{\mathbf{u}}_{k-1} \\
\mathbf{L}_k &= \mathbf{P}_{k|k-1} \mathbf{C}_{\varphi,k}^\top (\mathbf{C}_{\varphi,k}^\top \mathbf{P}_{k|k-1} \mathbf{C}_{\varphi,k} + \mathbf{R}_v)^{-1} \\
\hat{\boldsymbol{\theta}}_{k|k} &= \hat{\boldsymbol{\theta}}_{k|k-1} + \mathbf{L}_k (\mathbf{y}_k - \mathbf{C}_{\varphi,k} \hat{\boldsymbol{\theta}}_{k|k-1}) \\
\mathbf{P}_{k|k} &= (\mathbf{I} - \mathbf{L}_k \mathbf{C}_{\varphi,k}) \mathbf{P}_{k|k-1}.
\end{aligned} \tag{4.2}$$

With these difference equations in place, the result below, adjusted from Theorem 7.1 in [Åström & Wittenmark \(2008\)](#), is stated without proof.

Corollary 1. *Conditional Gaussian Parameter Distribution.* Consider a constant, uncertain parameter vector, $\boldsymbol{\theta}$, related to a GOBF MISO system with output, $y_k = \boldsymbol{\varphi}_k^\top \boldsymbol{\theta} + v_k$, $v_k \sim \mathcal{N}(\mathbf{0}, r_v)$. Its estimate distribution at the current time, t , conditioned by the data record, \mathbf{Y}_t and an initial Gaussian distribution $\mathcal{N}(\hat{\boldsymbol{\theta}}_0, \mathbf{P}_{\theta,0})$ is also Gaussian, and satisfies the following difference equations

$$\mathbf{L}_t = \mathbf{P}_{\theta,t-1} \boldsymbol{\varphi}_t (\boldsymbol{\varphi}_t^\top \mathbf{P}_{\theta,t-1} \boldsymbol{\varphi}_t + r_v)^{-1} \tag{4.3a}$$

$$\hat{\boldsymbol{\theta}}_t = \hat{\boldsymbol{\theta}}_{t-1} + \mathbf{L}_t (y_t - \boldsymbol{\varphi}_t^\top \hat{\boldsymbol{\theta}}_{t-1}) \tag{4.3b}$$

$$\mathbf{P}_{\theta,t} = (\mathbf{I} - \mathbf{L}_t \boldsymbol{\varphi}_t^\top) \mathbf{P}_{\theta,t-1} \tag{4.3c}$$

where,

$$\hat{\boldsymbol{\theta}}_t = \mathbb{E}[\boldsymbol{\theta} | \mathbf{Y}_t]$$

$$\mathbf{P}_{\theta,t} = \mathbb{E}[(\boldsymbol{\theta} - \hat{\boldsymbol{\theta}}_t)(\boldsymbol{\theta} - \hat{\boldsymbol{\theta}}_t)^\top | \mathbf{Y}_t].$$

with initial condition $\hat{\theta}_0, P_{\theta,0}$.

The expressions in Corollary 1 follow directly from the application of the Kalman Filter (4.2) with the assignments below with respect to the time-varying general system (4.1).

$$A_{\theta} = I, B_{\theta} = \mathbf{0}, C_{\varphi,t} = \varphi_t^{\top}$$

$$\hat{\theta}_{t|t} = \hat{\theta}_t, P_{t|t} = P_{\theta,t}$$

$$Q_w = \mathbf{0}, R_v = r_v$$

The conditional subscript notation has been eliminated for simplicity since this particular case allows it. At each sample instance, the vector φ_k is obtained from the known, deterministic transition dynamics defined by the GOBF model. Note that the result has been given in terms of MISO systems. With the working model definition, these recursions apply independently for each input channel and their respective information vector. This simplifies the inverse in (4.3a) to a scalar operation. In relation to predictive control methods, the immediate consequence of this distribution characterization is that it allows the evaluation of the analytical expectation of the tracking cost one step into the future, conditioned to the data record and a given input vector, $E[\|y_{t+1} - y^r\|_Q^2 | Y_t, u_t]$. This result cannot be easily extended into the subsequent stages in the objective function, as the required future output realizations in (4.3b) are not available. A Certainty Equivalence (CE) assumption corresponds to treating the current estimate as if it were the true parameter, and make deterministic predictions accordingly.

4.1 PARAMETER ADAPTATION

4.1.2 Recursive Least Squares Estimator

The Kalman Filter equations (4.3) are at the heart of Recursive Least Squares Methods. In practice, a variety of adjustment are made. Here, we will follow a slightly more general form given by,

$$\mathbf{L}_t = \mathbf{P}_{\theta,t-1} \boldsymbol{\varphi}_t (\boldsymbol{\varphi}_t^\top \mathbf{P}_{\theta,t-1} \boldsymbol{\varphi}_t + \lambda r_v)^{-1} \quad (4.4a)$$

$$\hat{\boldsymbol{\theta}}_t = \hat{\boldsymbol{\theta}}_{t-1} + \delta_t \mathbf{L}_t (y_t - \boldsymbol{\varphi}_t^\top \hat{\boldsymbol{\theta}}_{t-1}) \quad (4.4b)$$

$$\mathbf{P}_{\theta,t} = \lambda^{-1} (\mathbf{I} - \delta_t \mathbf{L}_t \boldsymbol{\varphi}_t^\top) \mathbf{P}_{\theta,t-1}. \quad (4.4c)$$

Only two modifications with respect to (4.3) have been included in the (4.4). First, an exponential forgetting factor, $\lambda \in (0, 1]$ has been introduced. As its name indicates, this parameter effectively imposes a higher weight in the most recent error signal contribution to the least-squares loss function, fading the effect of past data as time advances. The second adjustment corresponds to a basic dead-zone supervision method. This feature aims to detect and limit the effect of small errors that may accumulate and corrupt the parameter estimate. The implementation of this supervision is achieved by defining the following switch variable for each output channel,

$$\delta_t = \begin{cases} 1, & \text{if } (y_t - \hat{\boldsymbol{\theta}}_{t-1}^\top \boldsymbol{\varphi}_t)^2 \geq \epsilon_\delta \\ 0, & \text{otherwise} \end{cases} \quad (4.5)$$

where ϵ_δ is a small positive real number chosen in relation to the noise to signal ratio. We refer the interested reader to the work of [Dozal-Mejorada \(2008\)](#) for a more detailed discussion on the selection of these parameters.

4.2 CE ADAPTIVE INFINITE-HORIZON TRACKING

The simplest adaptive policy that adheres to the structure shown in [Figure 4.1](#) is defined with respect to the infinite-horizon cost of the filtered tracking state as defined below.

$$\hat{k}_{\infty,t}^*(\hat{\theta}_t, \mathbf{x}_{tr,t}) = \mathbf{u}_{t-1} + \hat{\mathbf{K}}_{\infty,t} \mathbf{x}_{tr,t}, \quad \mathbf{x}_{tr,t} := \begin{bmatrix} \Delta \varphi_t \\ \mathbf{y}_t - \mathbf{y}^r \end{bmatrix}. \quad (4.6)$$

The corresponding transition dynamics can be obtained from the filtered extended model with as shown in [Section 3.2.2](#). Note that both, the policy, and the gain are now denoted with a hat accent and the subscript t . This notation indicates that the policy is computed with the current parameter estimate, $\hat{\theta}_t$, given by the RLS estimator [\(4.4\)](#) at time t . The policy is updated online by solving the associated DARE for a given estimate realization that parametrizes the output matrix \mathbf{C}_θ . In conjunction with the fixed GOBF state transition pair, $\{\mathbf{A}_\xi, \mathbf{B}_\xi\}$, these elements define the filtered tracking state dynamics. It follows from the stability of the GOBF dynamics that there exist a solution to this DARE at each time, for a suitable pair of cost matrices $\{\mathbf{Q}, \mathbf{R}\}$, irrespectively of the parameter realization.

4.2.1 SISO Mass-Spring Example

A series of simulations under the policy (4.6), applied to the minimal mass-spring example for different GOBF model structures are presented. The physical parametrization of the model is identical to the base case in Chapter 2. The motivation of this study is to contextualize the introduction of parameter adaptation into our working GOBF MPC framework. The simplifying policy choice, focuses the attention to the effect of the model structure and assumes the system is unconstrained. The scalar cost parameters are set to $Q = 0.1$ and $R = 10$. The RLS estimator is set to its basic form (4.3), with $P_{\theta,0} = 10^2 \mathbf{I}$, $\lambda = 1$ and $\epsilon_\delta = 0$.

Different model choices with varying order, n , and generating pole structure are evaluated. The sequence of simulations is presented with increasing level of detail for the model specification, illustrating the value of the GOBF approach. The tracking signal for the output is set at a constant value of $y^r = 1$. The system is set to be initially motionless, at its equilibrium point. A common Gaussian noise sequence, small in relation to the reference signal, $|v_t| < 0.1 \forall t$, is added to the system output in all simulations. The parameter vector is updated recursively with close-loop data. Its elements are initialized with $\hat{\theta}_{k,0} = 1$ for the first four elements, and $\hat{\theta}_{k,0} = 0$ for higher order contributions.

The results for the varying cases studied are displayed in figure pairs that display the profiles for the input-output signals and the parameter estimates for the first four elements of $\hat{\theta}_t$. The first set of simulations is made with FIR models of varying order. The results shown in Figure 4.2 illustrate an improvement on the control performance as the model order increases. Once the output stabilizes, the parameters start drifting as shown in Figure 4.3. This effect is more pronounced for the model with the lowest order. The

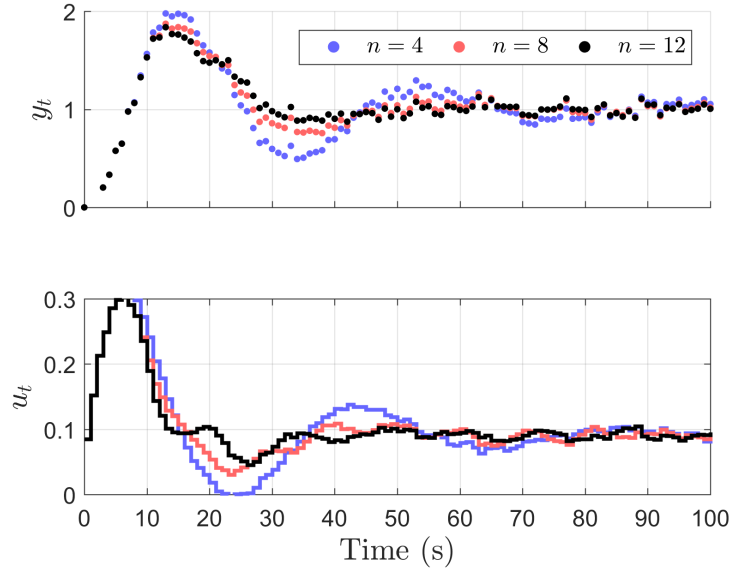


Figure 4.2: FIR Control

second set corresponds to a one-pole Laguerre modeling choice. With respect to the FIR approach, this option offers an additional degree of freedom for control design with the choice of generating pole, ξ . First, the order remains fixed at $n = 4$ while the generating pole varies. The results in Figure 4.4 show that it is possible to obtain significantly better performance to the highest order FIR model above with any of the simulated pole choices. Among these options, the best performance is obtained by $\xi = 0.6$.

Additional simulations with one-pole Laguerre models with higher order and a generating pole location at $\xi = 0.8$ were also tested. These profiles yield a conflicting result to the observations made with FIR models. The performance actually deteriorates with higher order contributions. In an effort to clarify this behavior, the estimation profiles for parameters of higher order contributions, $\hat{\theta}_{4,t} - \hat{\theta}_{8,t}$, are displayed in Figure 4.8. Note that parameters of matching order among all three cases have a similar trajectory as displayed in Figure 4.7 and Figure 4.8. Also, higher order contributions display more chattering

4.2 CE ADAPTIVE INFINITE-HORIZON TRACKING

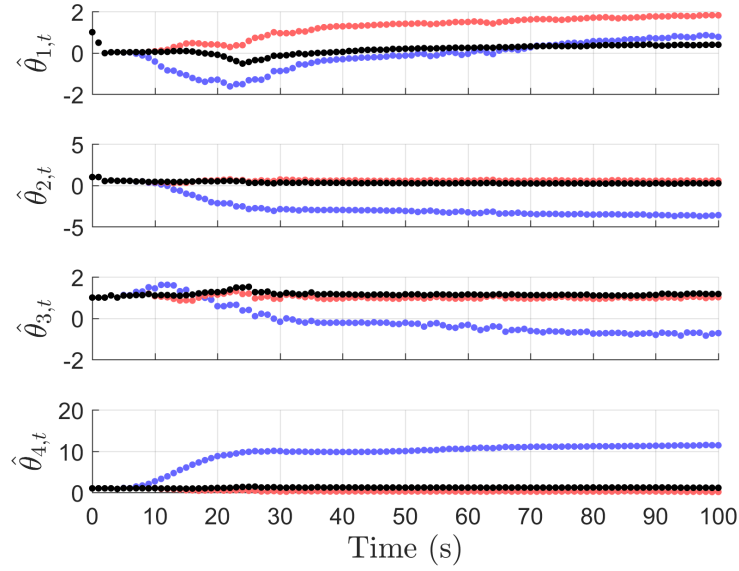


Figure 4.3: FIR Estimation

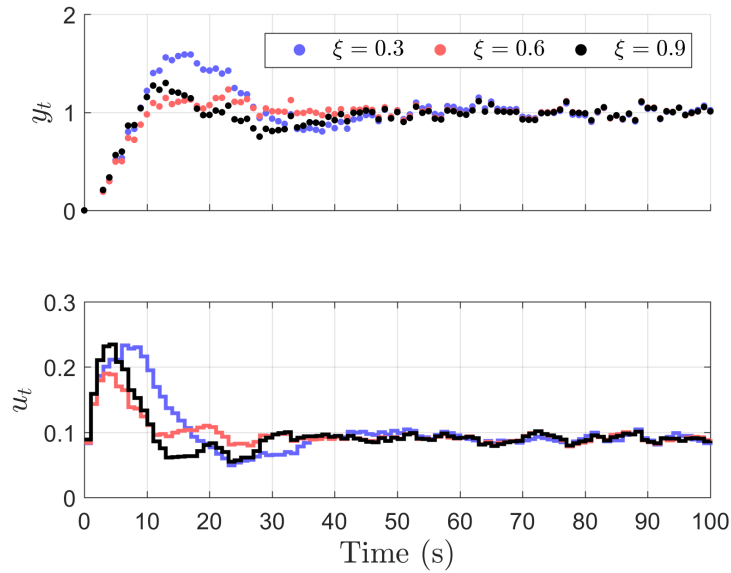
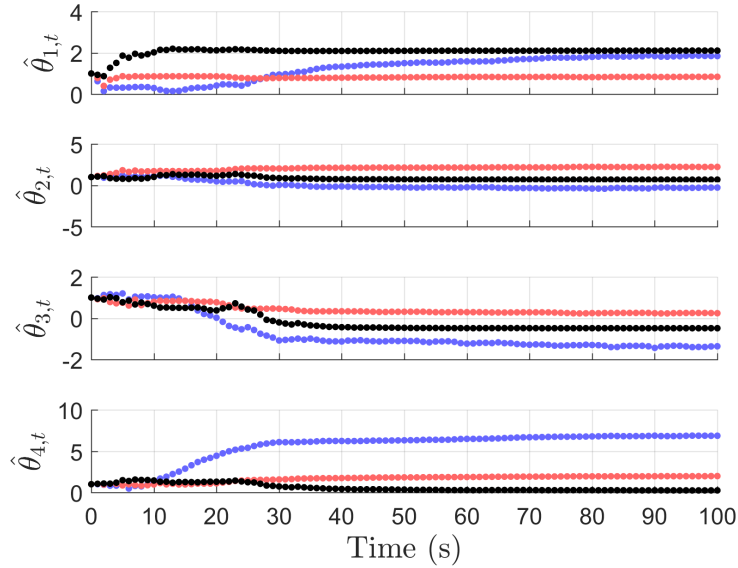


Figure 4.4: Laguerre Control with $n = 4$

Figure 4.5: Laguerre Estimation with $n = 4$

than the leading counterparts. This could be attributed to the poor conditioning of the recursive least-squares problem for that region of the parameter space. These features of the estimation process introduce variance in the related state element contributions to the output prediction. Ultimately, this is reflected in undesirable variations for the optimal control signal. Ideally, with a proper choice for the generating pole, this could be avoided, since the required expansion order is lower as a consequence.

Next, three different GOBF models that include a Kautz building block in their construction are studied. In a similar fashion to the simulations in Chapter 2, these are design to illustrate the effect of inaccurate generating pole set. The GOBF pole locations in the unit disk are displayed in Figure 4.9 for each model along with those for the system. These pole choices were made to feature increasing levels of accuracy with respect to prior knowledge about the true dynamics. The first model, GOBF_1 , results from the all-pass cascading using Algorithm 2.1 with two FIR blocks of order one and a Kautz

4.2 CE ADAPTIVE INFINITE-HORIZON TRACKING

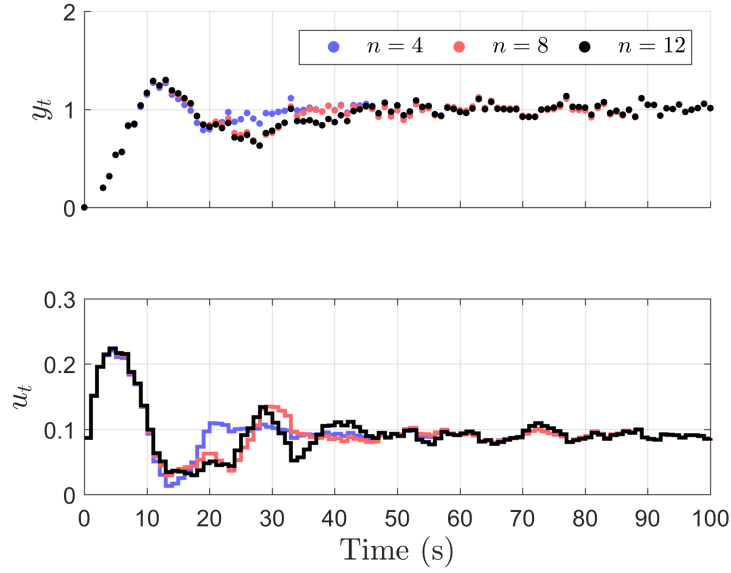


Figure 4.6: Laguerre Control with $\xi = 0.8$

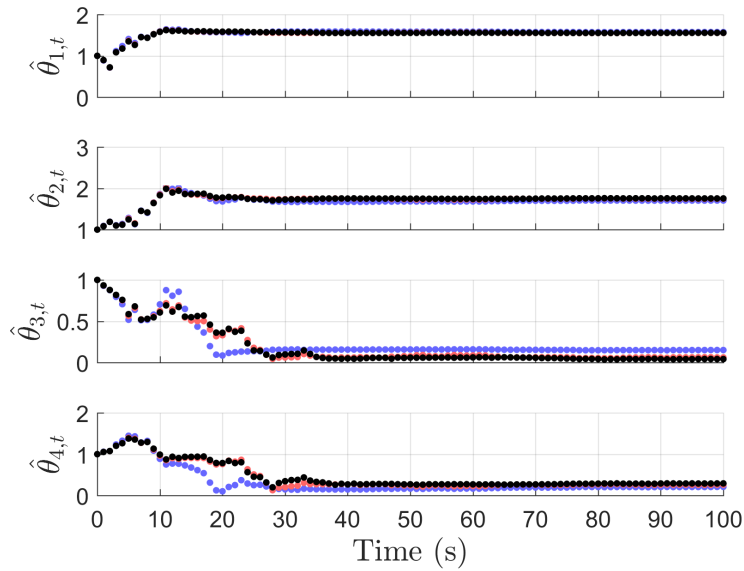
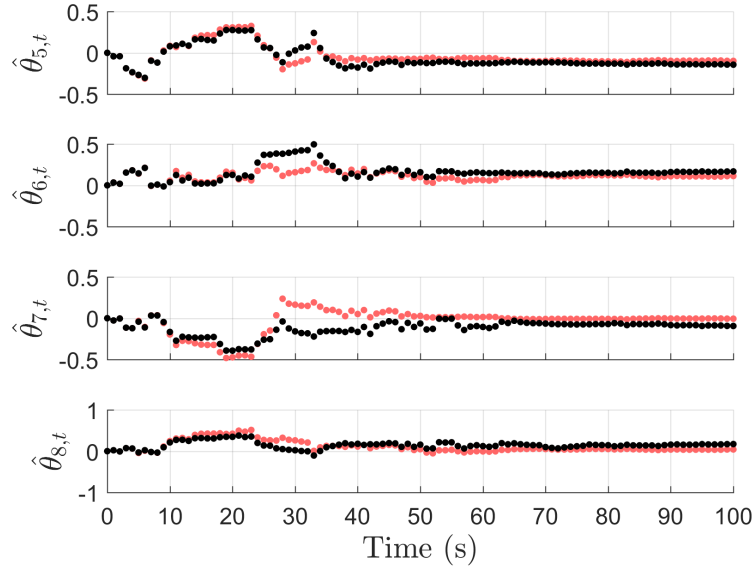


Figure 4.7: Laguerre Estimation with $\xi = 0.8$

Figure 4.8: Laguerre Higher Order Estimation with $\xi = 0.8$

block in between with $\xi = \{0, 0.7 \pm 0.2i, 0\}$. The intermediate model replaces the leading block with a Laguerre contribution with a pole in the vicinity of the plant poles, $\xi_1 = 0.8$. GOBF₃ matches the plant poles to the nearest decimal, $\xi = \{0.9, 0.6 \pm 0.5i, 0.7\}$. Not surprisingly, as shown in Figure 4.10, the latter model representation yields the best tracking control while the first one performs worst. On the other hand, the intermediate case is only marginally worse with respect to the accurate model.

To conclude this section, we examine the advantages of the GOBF model structure compared to a fixed denominator model. The specific purpose of these simulations is to determine whether accuracy in the system poles, without the orthonormal structure, is sufficient to obtain good control performance under adaptation. This quality assessment is made in terms of the evolution of the reciprocal condition number of the accumulated information matrix. The fixed denominator model structure is similar to the GOBF ap-

4.2 CE ADAPTIVE INFINITE-HORIZON TRACKING

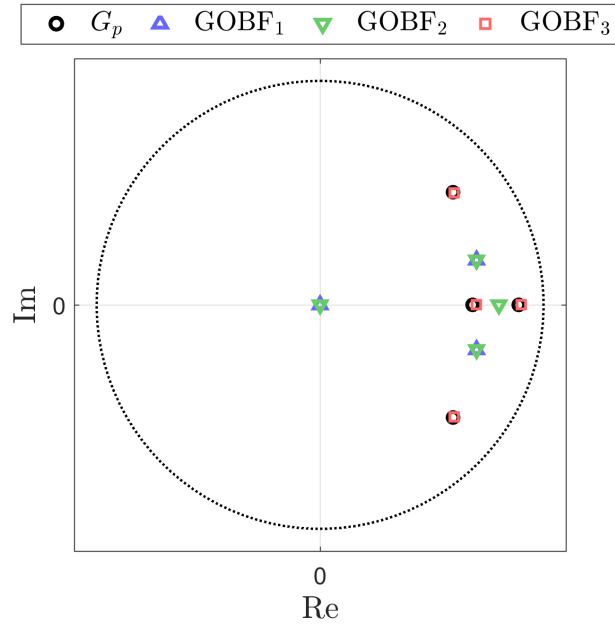


Figure 4.9: GOBF Pole Locations

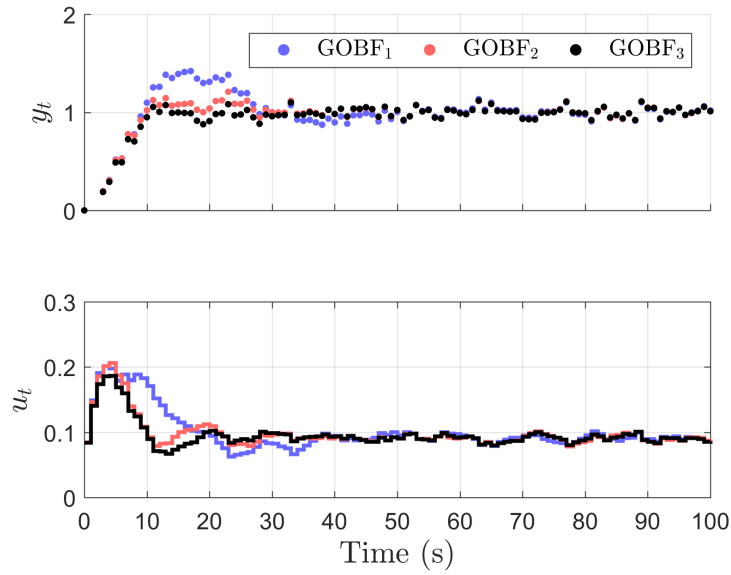
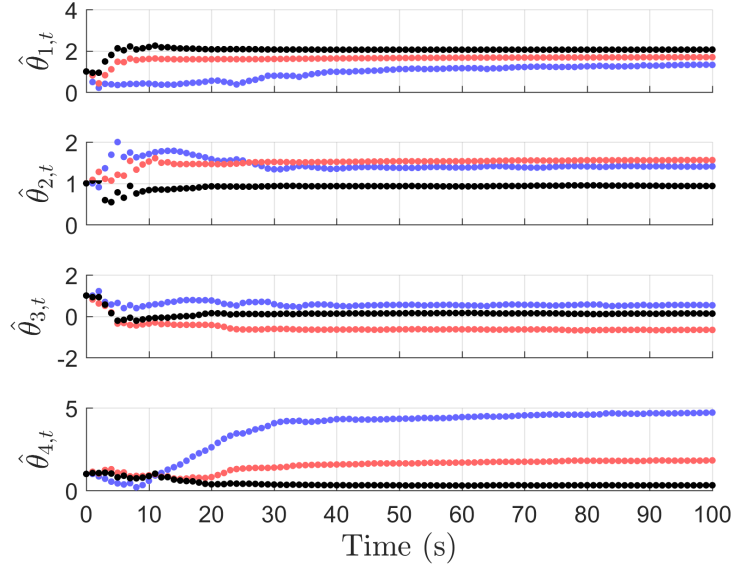


Figure 4.10: GOBF Control with $n = 4$

Figure 4.11: GOBF Estimation with $n = 4$

proach in that it is generated by a fixed choice of poles. These poles define a polynomial that is set as the fixed denominator of a filter applied to the input,

$$\begin{aligned} \psi_{i,t} &= \frac{q^{n-i}}{D(q)} u_t, \quad i = \mathbb{I}_{1:n}, \quad D(q) := \prod_{i=1}^n (q - \xi_i) \\ &= \frac{q^{n-i}}{1 + d_1 q^{-1} + \dots + d_n q^{-n}} u_t \end{aligned}$$

In a similar fashion to an FIR model, the output is modeled as a linear combination of the elements of a recorded sequence of the leading element of ψ_t ,

$$\begin{aligned} \hat{y}_t &= G_D(q; \boldsymbol{\theta}) u_t \\ &= \boldsymbol{\theta}^\top \boldsymbol{\psi}_t \end{aligned}$$

where,

$$G_D(q; \boldsymbol{\theta}) := \sum_{i=1}^n \theta_i \frac{q^{n-i}}{D(q)}$$

$$\boldsymbol{\psi}_t := \left[\psi_{1,t} \quad \psi_{2,t} \quad \dots \quad \psi_{n,t} \right]^\top = \left[\psi_{1,t} \quad \psi_{1,t-1} \quad \dots \quad \psi_{1,t-n+1} \right]^\top$$

the associated state transition dynamics are given by,

$$\boldsymbol{\psi}_{t+1} = \begin{bmatrix} -d_1 & -d_2 & \dots & \dots & -d_n \\ 1 & 0 & \dots & \dots & 0 \\ 0 & \ddots & \ddots & \ddots & \vdots \\ \vdots & \ddots & \ddots & \ddots & \vdots \\ 0 & \dots & 0 & 1 & 0 \end{bmatrix} \boldsymbol{\psi}_t + \begin{bmatrix} 1 \\ 0 \\ \vdots \\ \vdots \\ 0 \end{bmatrix} u_t.$$

Similarly to the one-pole Laguerre model, with all poles at the origin this structure also yields the FIR state transition pair. A fixed denominator model is constructed with the pole set labeled as GOBF₃ in Figure 4.9. The simulated profiles, using the same control design and experiment definition above, are shown in Figure 4.12 and 4.13. The simulations show that the improved estimation provided by the GOBF model structure is also important. Compared with all the preceding cases, the fixed denominator results are only definitively superior to the FIR models. Even some of the low-order one-pole Laguerre cases studied seem to outperform this case despite the accuracy of the model poles with respect to the mass-spring system.

In order to determine the value of input balanced realizations, these results should be compared to the GOBF model generated with the same poles, GOBF₃, shown in figures 4.10 and 4.11. The output signal settling time to the tracking reference to noise level is roughly doubled with the fixed denominator model. In an adaptive setting, it is important

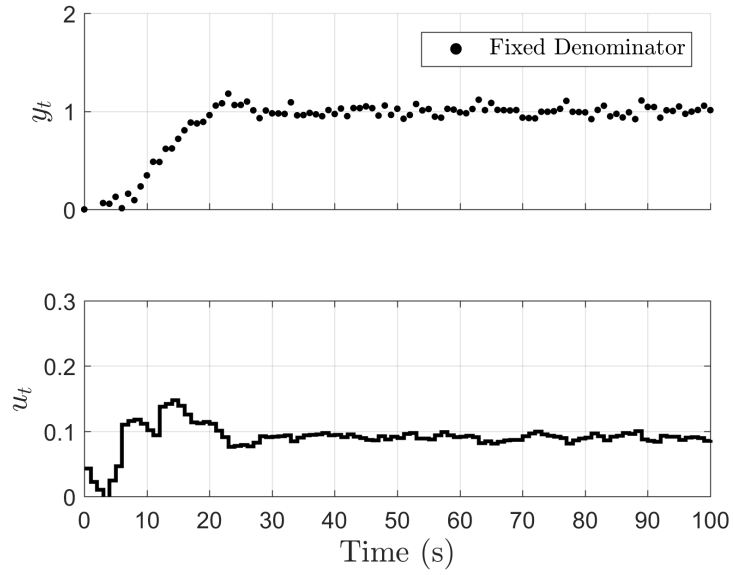


Figure 4.12: Fixed Denominator Control

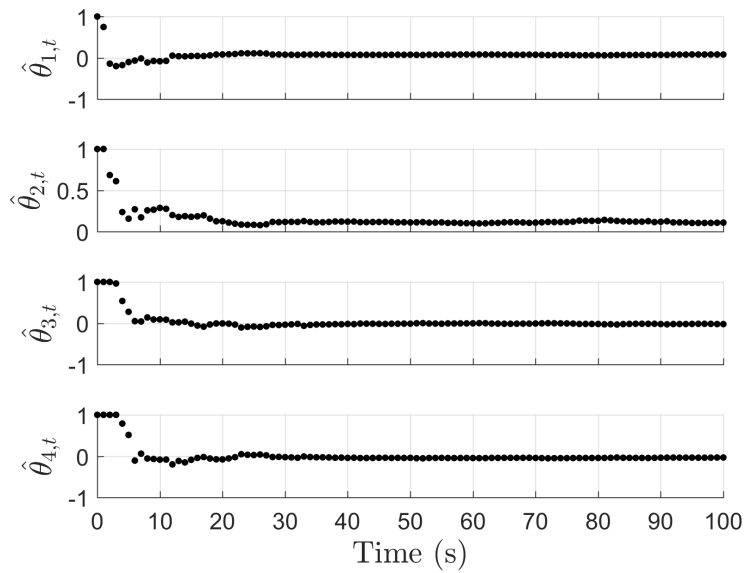


Figure 4.13: Fixed Denominator Estimation

to maximize the extraction of information from signal transients. Once the system reaches a steady state, the error-driven estimation process either stabilizes or drifts as seen in the figures above. The information aspect will be examined in more detail in the next chapter. For now, we limit the exposition to the fact that the quality of the least-squares estimation process is related to the conditioning of the inverse of the information matrix for a given model,

$$\begin{aligned} \mathbf{P}_{\theta,t}^{\varphi} &:= \left(\sum_{k=1}^t \boldsymbol{\varphi}_k \boldsymbol{\varphi}_k^{\top} \right)^{-1} + \mathbf{P}_{\theta,0} \\ \mathbf{P}_{\theta,t}^{\psi} &:= \left(\sum_{k=1}^t \boldsymbol{\psi}_k \boldsymbol{\psi}_k^{\top} \right)^{-1} + \mathbf{P}_{\theta,0}. \end{aligned}$$

As noted above, the matrix $\mathbf{P}_{\theta,0}$ is a parameter of the RLS estimator related to the certainty level for $\hat{\boldsymbol{\theta}}_0$. The reciprocal condition number, $1/\kappa$, for a matrix \mathbf{P} is specified by,

$$\frac{1}{\kappa} := \frac{1}{\|\mathbf{P}^{-1}\|_1 \|\mathbf{P}\|_1} \quad (4.7)$$

where the pseudo-inverse is used in place of the inverse for singular matrices. The profiles displayed in Figure 4.14 were computed according to equation (4.7) with the recorded information state transitions for each model. The effect of the initial covariance is removed by including only the recorded information, *i.e.* the reciprocal condition number is computed for $\mathbf{P}_{\theta,t}^{\varphi} - \mathbf{P}_{\theta,0}$ and its fixed denominator counterpart.

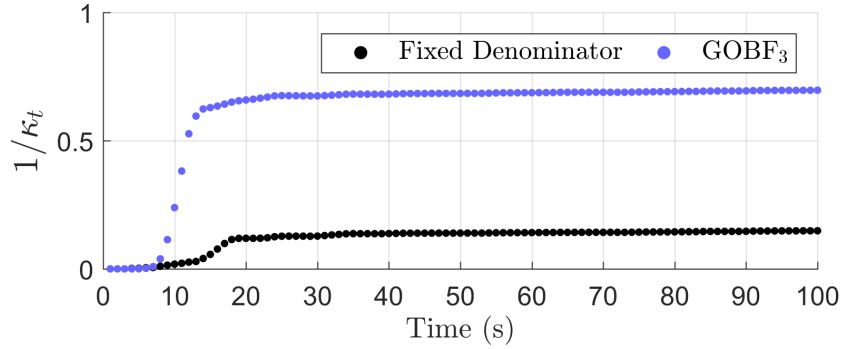


Figure 4.14: Information Inverse Conditioning

A reciprocal condition number close to one is preferable than close to zero as it leads to numerical robustness of the estimation process. It is evident, that even under a limited amount of data from a short closed-loop transient, the input-balanced transition for the GOBF model is far superior in this respect. After 10 samples, the reciprocal condition number for the GOBF model is higher than the final value for the fixed denominator case.

4.3 CERTAINTY EQUIVALENCE ADAPTIVE MPC

The observations in the previous section highlighted the importance of a proper GOBF selection. In addition to this point, it was shown how the orthonormality property, built into the model definition, is beneficial to the parameter estimation process. The performance of the control and the coupled adaptation processes is only as good as the model permits.

In this section we introduce a more general adaptive control algorithm, applicable to constrained systems. In its definition, some of the features of the robust formulation in Chapter 3 will be included. However, by adopting an adaptive approach, we have im-

explicitly acknowledged that a proper characterization of the error bound is not available. Without a description of the error bounding set, the constraint tightening and other measures taken against the disturbance cannot be made. This is aggravated by the fact that as the model is updated, those measures would also have to be modified accordingly. Here, we will assume that the satisfaction of an available constraint set for the input signal will be sufficient. There is nothing that prevents output constraints to be included in the formulation, but any satisfaction guarantees in this regard have been lost.

4.3.1 Optimal Control Problem

The extended state notation in Chapter 3 for the MPC optimization variables will be readopted hereinafter. Again, we will limit the extended state definition with the first backward difference filter, Δ . As a result, the vector $\hat{\mathbf{x}}_k$ denotes the stacking of the filtered information vector, $\hat{\mathbf{x}}_{\varphi,k} := \Delta\hat{\varphi}_k$, the predicted output signal $\hat{\mathbf{x}}_{y,k} := \hat{\mathbf{y}}_k$, and the preceding input, $\hat{\mathbf{x}}_{u,k} := \hat{\mathbf{u}}_{k-1}$ in the finite horizon,

$$\hat{\mathbf{x}}_k = \begin{bmatrix} \hat{\mathbf{x}}_{\varphi,k} \\ \hat{\mathbf{x}}_{y,k} \\ \hat{\mathbf{x}}_{u,k} \end{bmatrix}.$$

Without an error bounding set, the variables of the first stage are fixed at the current measurements. The time-varying state transition dynamics for this extended state are given by the following model representation,

$$f_t(\hat{\mathbf{x}}_k, \hat{\mathbf{u}}_k) := \mathbf{A}_t \hat{\mathbf{x}}_k + \mathbf{B}_t(\hat{\mathbf{u}}_k - \hat{\mathbf{x}}_{u,k}) \quad (4.8)$$

where,

$$\mathbf{A}_t := \begin{bmatrix} \mathbf{A}_{m,t} & \mathbf{0} \\ \mathbf{0} & \mathbf{I} \end{bmatrix}, \quad \mathbf{B} := \begin{bmatrix} \mathbf{B}_{m,t} \\ \mathbf{I} \end{bmatrix}$$

$$\mathbf{A}_{m,t} := \begin{bmatrix} \mathbf{A}_\xi & \mathbf{0} \\ \hat{\mathbf{C}}_{\theta,t} \mathbf{A}_\xi & \mathbf{I} \end{bmatrix}, \quad \mathbf{B}_{m,t} := \begin{bmatrix} \mathbf{B}_\xi \\ \hat{\mathbf{C}}_{\theta,t} \mathbf{B}_\xi \end{bmatrix}.$$

Observe that the time-varying aspect of the dynamics is expressed solely in the output matrix $\hat{\mathbf{C}}_{\theta,t}$, which is updated with the latest available parameter estimate realization. For a MIMO plant, each MISO subsystem has a lower-dimensional component of the overall vector assigned to it. This collection of vectors, $\hat{\boldsymbol{\theta}}_{i,t}$ for $i = 1, \dots, n_y$ are updated by individual estimation processes according to (4.4) and arranged as entries in $\hat{\mathbf{C}}_{\theta,t}$ according to the overall model structure.

The inclusion of an artificial steady state is kept, along with the associated steady-state equations in the constraint set. However, the constraints on the steady-state input are dropped. In the robust case, the artificial steady-state input signal, $\hat{\mathbf{u}}^s$, is relevant as the offset cost can be extended to penalize large deviations from it. This rationale is only applicable to an accurate model. Here, the achievable steady inputs change with each parameter update. Therefore, this portion of the problem definition is relaxed to avoid infeasible problems. In the adaptive case, this could occur for a poorly parametrized model realization. The artificial reference provides the problem flexibility in terms of its time-varying set of admissible initial conditions. On the other hand, the steady-state input variable, along with its matching information vector, $\hat{\boldsymbol{\varphi}}^s$, are treated as auxiliary variables to impose the steady-state output under the current model. They are indirectly bounded by the output constraint imposed on $\hat{\mathbf{y}}^s$, which is kept.

The optimal control problem for the adaptive CE algorithm, as described above, is denoted by $\mathcal{P}_{ce,N}(\mathbf{x}, \mathbf{y}^r)$ and specified in (4.9). The extended state constraint set, \mathcal{X} , is defined to contain the input and output constraints,

$$\mathcal{X} := \{\mathbf{x} \mid \mathbf{x}_y \in \mathcal{Y}, \mathbf{x}_u \in \mathcal{U}\}.$$

For similar reasons of the exclusion of the artificial steady state input variable, the terminal constraint set (4.9d) is not included explicitly in the problem formulation. Instead, it is assumed to hold for the optimized artificial output reference and a sufficiently large finite horizon size, N . In all the simulations to follow, \mathcal{X} is defined by simple box constraints on the input and output signal variables. The filtered information states are implicitly constrained as a result.

$$\mathcal{P}_{ce,N}(\mathbf{x}, \mathbf{y}^r) : \min_{\mathbf{u}, \hat{\mathbf{y}}^s} J_{N,t}(\hat{\mathbf{x}}_0, \mathbf{u}, \hat{\mathbf{x}}_m^s) + J_{s,t}(\hat{\mathbf{y}}^s, \mathbf{y}^r) \quad (4.9)$$

$$\text{s.t. } \hat{\mathbf{x}}_0 = \mathbf{x} \quad (4.9a)$$

$$\hat{\mathbf{x}}_{k+1} = f_t(\hat{\mathbf{x}}_k, \hat{\mathbf{u}}_k), \quad k \in \mathbb{I}_{0:N-1} \quad (4.9b)$$

$$\hat{\mathbf{x}}_k \in \mathcal{X}, \quad k \in \mathbb{I}_{1:N-1} \quad (4.9c)$$

$$\hat{\mathbf{x}}_N \in \mathcal{X}_f(\hat{\mathbf{y}}^s) \quad (4.9d)$$

$$\begin{bmatrix} \mathbf{A}_\xi - \mathbf{I} & \mathbf{B}_\xi \\ \mathbf{C}_\theta & \mathbf{0} \end{bmatrix} \begin{bmatrix} \hat{\boldsymbol{\varphi}}^s \\ \hat{\mathbf{u}}^s \end{bmatrix} = \begin{bmatrix} \mathbf{0} \\ \hat{\mathbf{y}}^s \end{bmatrix} \quad (4.9e)$$

$$\hat{\mathbf{y}}^s \in \mathcal{Y} \quad (4.9f)$$

The time dependence of the CE control problem is denoted by the subscript, t , on the finite horizon portion. This cost function is parametrized by the time-varying dynamics (4.8). For more details on the definition of this object and other elements of the optimization, we refer to the fixed model counter-parts description provided in the preceding chapter. Overall, the CE adaptive approach for constrained systems is summarized in the pseudo-code presented in Algorithm 4.1.

Algorithm 4.1 CE Adaptive Control Action

Require:

Current measured state, \mathbf{x}_t

Parameter estimate distribution at previous sampling time $\{\hat{\boldsymbol{\theta}}_{t-1}, \mathbf{P}_{\theta,t-1}\}$

GOBF state transition matrices $\{\mathbf{A}_\xi, \mathbf{B}_\xi\}$

Cost parameters $\{\mathbf{Q}, \mathbf{R}, \mathbf{T}\}$

Ensure:

Control action \mathbf{u}

- 1: Update parameter distribution with RLS (4.4), to get $\{\hat{\boldsymbol{\theta}}_t, \mathbf{P}_{\theta,t}\}$
 - 2: Update state-transition model (4.8) with $\hat{\boldsymbol{\theta}}_t$
 - 3: Solve filtered model DARE to obtain terminal cost matrix $\mathbf{P}_{f,t}$
 - 4: Solve $\mathcal{P}_{ce,N}(\mathbf{x}, \mathbf{y}^r)$ in (4.9)
 - 5: Extract optimal control element, $\hat{\mathbf{u}}_0^* = \hat{\mathbf{x}}_{u,1}^*$
 - 6: $\mathbf{u} \leftarrow \hat{\mathbf{u}}_0^*$
-

4.3.2 *Quadruple Tank MIMO Plant Example*

A computational model for a quadruple-tank system, as shown in Figure 4.15, is presented next. Liquid flows into each unit from a set of feed lines. The specific flow for each line is determined by the action of a pump and a routing valve that splits the pump output into two. Each tank has an orifice at the bottom that results in a flow that feeds either the tank below or the feed reservoir. The MIMO structure that defines the system of interest is given by the measurement of the heights for the lower tanks as model outputs and the voltage assigned to the pumps as inputs.

The model dynamics are derived from the coupled mass balances using Bernoulli's law for the orifice flows in (4.10).

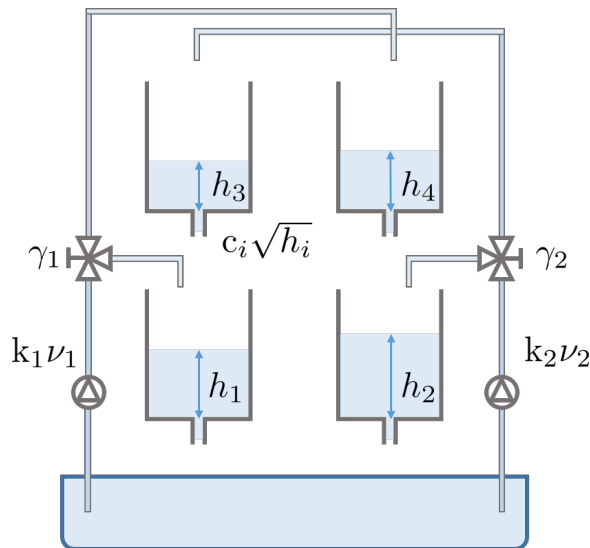


Figure 4.15: Quad-Tank System Diagram

$$\begin{aligned}
\frac{dh_1}{dt} &= -\frac{a_1}{a_T} \sqrt{2gh_1} + \frac{a_3}{a_T} \sqrt{2gh_3} + \frac{\gamma_1 k_1}{a_T} \nu_1 \\
\frac{dh_2}{dt} &= -\frac{a_2}{a_T} \sqrt{2gh_2} + \frac{a_4}{a_T} \sqrt{2gh_4} + \frac{\gamma_2 k_2}{a_T} \nu_2 \\
\frac{dh_3}{dt} &= -\frac{a_3}{a_T} \sqrt{2gh_3} + \frac{(1-\gamma_1)k_1}{a_T} \nu_1 \\
\frac{dh_4}{dt} &= -\frac{a_4}{a_T} \sqrt{2gh_4} + \frac{(1-\gamma_2)k_2}{a_T} \nu_2
\end{aligned} \tag{4.10}$$

A full description of the system and its properties is given in (Johansson 2000). A discrete linear state-space model is generated using a standard first order approximation around an operating steady state and its subsequent zero-order hold discretization with sampling time of one second. It is important to note that this model is used only as a control design tool and all the subsequent simulations for the system are obtained by the numerical integration of the nonlinear dynamics (4.10). The nominal parametrization of the model is obtained with the values in Table 4.1.

Table 4.1: Quad-Tank Model Nominal Parameters

Name	Symbol	Value	Units
Orifice Areas	$\{a_1, a_2, a_3, a_4\}$	$\{0.48, 0.52, 0.26, 0.28\}$	cm^2
Cross-Sectional Area	a_T	10	cm^2
Steady-State Heights	$\{h_1^o, h_2^o, h_3^o, h_4^o\}$	$\{9.0, 9.0, 12.0, 11.8\}$	cm
Steady-State Voltages	$\{\nu_1^o, \nu_2^o\}$	$\{13.3, 13.3\}$	V
Split Fractions	$\{\gamma_1, \gamma_2\}$	$\{0.36, 0.4\}$	–
Pump Constants	$\{k_1, k_2\}$	$\{5, 5\}$	$\text{cm}^3 / (\text{V} \cdot \text{s})$
Gravity Constant	g	980	cm/s^2

The values for the nominal upper level tank heights and the pump voltages are rounded to the nearest decimal and are determined by fixing the remaining elements of the physical parameter set. This system offers a set of interesting features in relation to the GOBF model representation. To elaborate on this point, consider the MIMO matrix filter description of the linear model,

$$\mathbf{y}_t = \mathbf{G}_p(\theta, q)\mathbf{u}_t, \quad \mathbf{G}_p = \begin{bmatrix} G_{1,1}(\theta, q) & G_{1,2}(\theta, q) \\ G_{2,1}(\theta, q) & G_{2,2}(\theta, q) \end{bmatrix} \quad (4.11)$$

where,

$$\mathbf{y}_t = \begin{bmatrix} h_{1,t} - h_1^o \\ h_{2,t} - h_2^o \end{bmatrix}, \quad \mathbf{u}_t = \begin{bmatrix} \nu_{1,t} - \nu_1^o \\ \nu_{2,t} - \nu_2^o \end{bmatrix}.$$

At a given operation point, the time constants of the system are inversely proportional to the square root of the height and the ratio of the tank and orifice areas,

$$\tau_i := \frac{a_i}{a_T} \sqrt{\frac{g}{2h_i}}$$

These time constants are expressed in the matrix filter (4.11) as the real pole locations of its scalar components as shown in Figure 4.16.

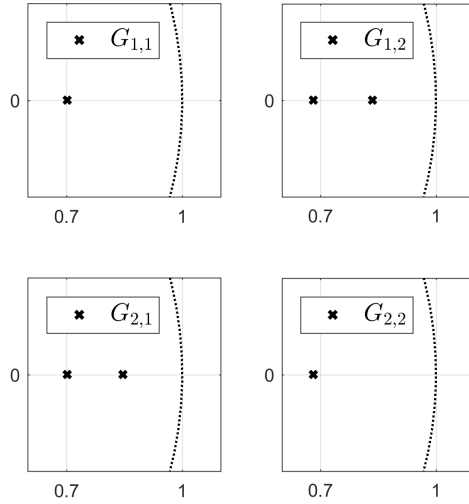


Figure 4.16: Linearized Quad-Tank Model Pole Locations

The rationale behind the variety of the physical model values selected for the nominal case in Table 4.1 is to induce different pole locations for the first and second order transfer function relationships that compose \mathbf{G}_p . By setting the flow split fractions such that most of the flow is directed to the top level, the gain of the off-diagonal second order elements is higher with respect to the first order diagonal counterparts.

4.3.3 Quad-Tanks CE Adaptive MPC Results

We can now test the CE adaptive control strategies in terms of the relationship of the linear approximation and the model structure definition, comprised of a MIMO set of generating poles, and an initial parameter estimate distribution. Comparisons are made to fixed-model versions of each simulation under identical conditions other than adaptation with the RLS estimator (4.4). Since the system dynamics shift at different reference points, it is

appropriate to activate the forgetting factor of the estimator with a value of $\lambda = 0.99$. The dead-zone feature is also enabled with $\epsilon_\delta = 2 \times 10^{-4}$.

The tracking objective and off-set costs functions are defined by the horizon size $N = 20$ and the matrices $\mathbf{Q} = \mathbf{I}$, $\mathbf{R} = 0.1\mathbf{Q}$, and $\mathbf{T} = 10^2\mathbf{Q}$. The same bounded white noise sequence, $|v_{i,t}| < 0.01 \forall t$, is added to all output measurements. Box constraints specify (4.9c), such that,

$$\begin{aligned} -3.5 &\leq \hat{u}_{i,k} \leq 3.5, \quad \forall k \in \mathbb{I}_{0:N-1}, \quad \forall i \in 1, 2 \\ -1.5 &\leq \hat{g}_{i,k} \leq 1.5, \quad \forall k \in \mathbb{I}_{1:N-1}, \quad \forall i \in 1, 2. \end{aligned}$$

The experiment is divided in four periods of 100 seconds each. For the first and final intervals, the reference corresponds to the nominal heights. For the second and third, it is updated with $\mathbf{y}^r = \begin{bmatrix} 1 & -1 \end{bmatrix}^\top$ and $-\mathbf{y}^r$ respectively.

The generating pole set structure, and the initial parameter estimate covariance, where applicable, are also common for all cases. The former is matched exactly with the nominal linear model as shown in Figure 4.16, while the latter is set at $\mathbf{P}_{\theta,0} = 10^3\mathbf{I}$. The experiment is repeated for three different initial means, $\hat{\boldsymbol{\theta}}_{\theta,0}$, for the parameter estimate distribution. The different values are given in Table 4.2 below.

Table 4.2: Initial Model Parameterization for CE Adaptive Control Experiments

Instance	y_1 MISO Parameter, $\hat{\boldsymbol{\theta}}_{1,0}$	y_2 MISO Parameter, $\hat{\boldsymbol{\theta}}_{2,0}$
Model 1	$[0.2128, 0.1156, 0.1644]^\top$	$[0.1191, 0.1683, 0.2269]^\top$
Model 2	$[0.30, 0.15, 0.15]^\top$	$[0.15, 0.15, 0.30]^\top$
Model 3	$[0.40, 0.20, 0.30]^\top$	$[0.20, 0.30, 0.40]^\top$

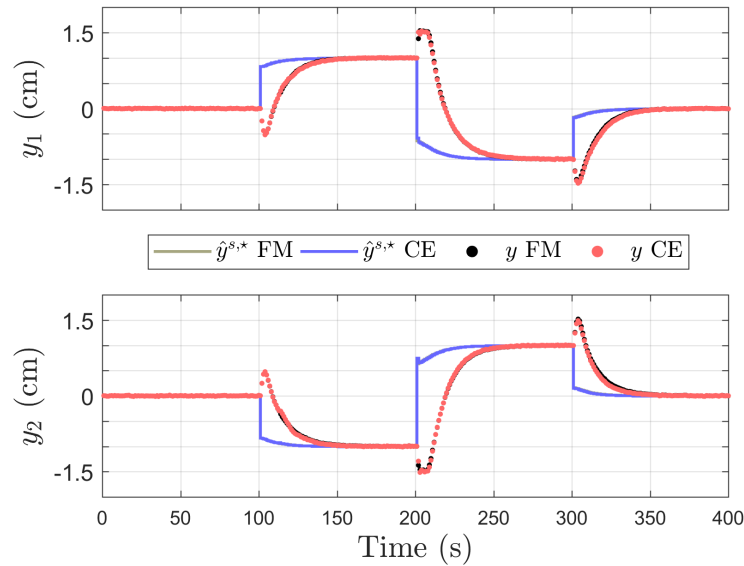


Figure 4.17: Quad-Tank Model 1 Output Profiles

The parameter set for Model 1 is derived analytically from the inner product expressions that define the exact GOBF truncation coefficients. Model 2 and 3 are parametrized to yield model error proportional to their difference with respect to Model 1. The simulated input-output profiles are given in Figures 4.17-4.22. The fixed model and CE adaptive profiles are labeled with FM and CE respectively.

For the exact GOBF representation of the linear model, the policies obtained are nearly identical. For fixed inaccurate models, as expected, the MPC feedback action takes longer to bring the system to the desired reference. The adaptive versions converge to the same policy shortly after the onset of the second constant reference interval. With the specified parameters, models 1 and 2 effectively overestimate the gain of the diagonal transfer

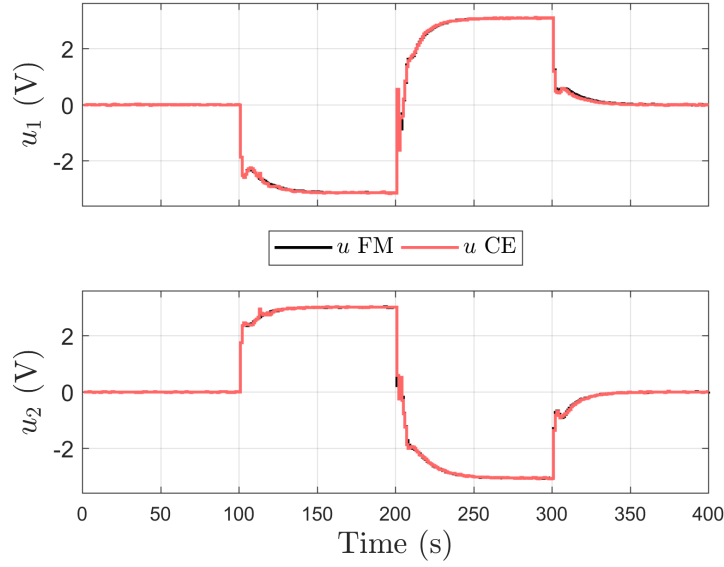


Figure 4.18: Quad-Tank Model 1 Input Profiles

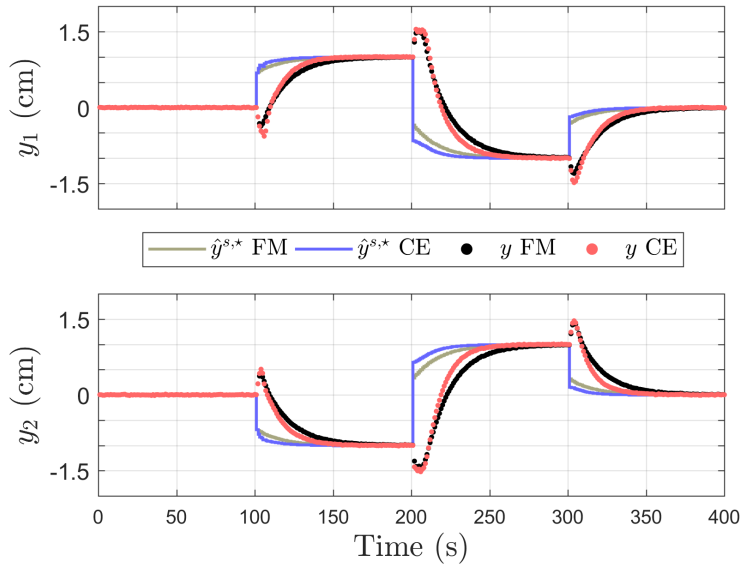


Figure 4.19: Quad-Tank Model 2 Output Profiles

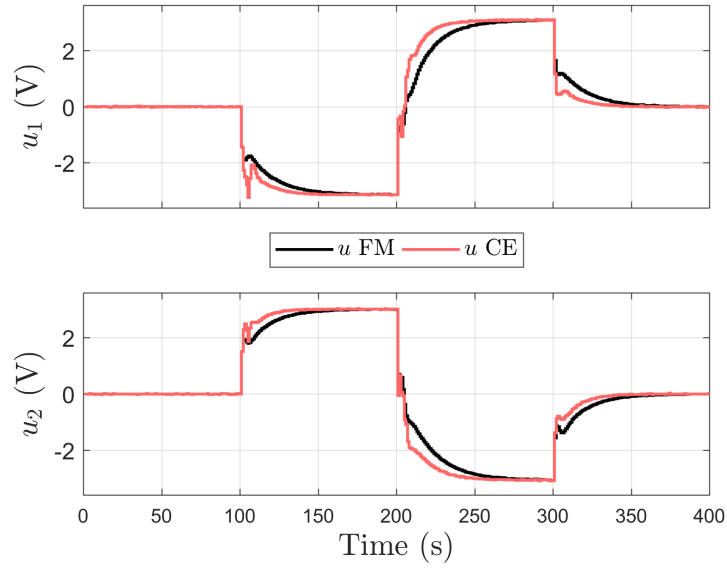


Figure 4.20: Quad-Tank Model 2 Input Profiles

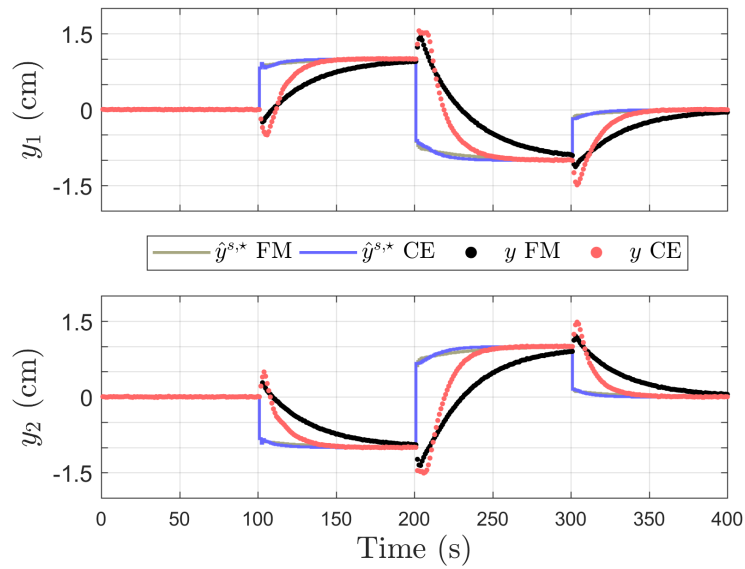


Figure 4.21: Quad-Tank Model 3 Output Profiles

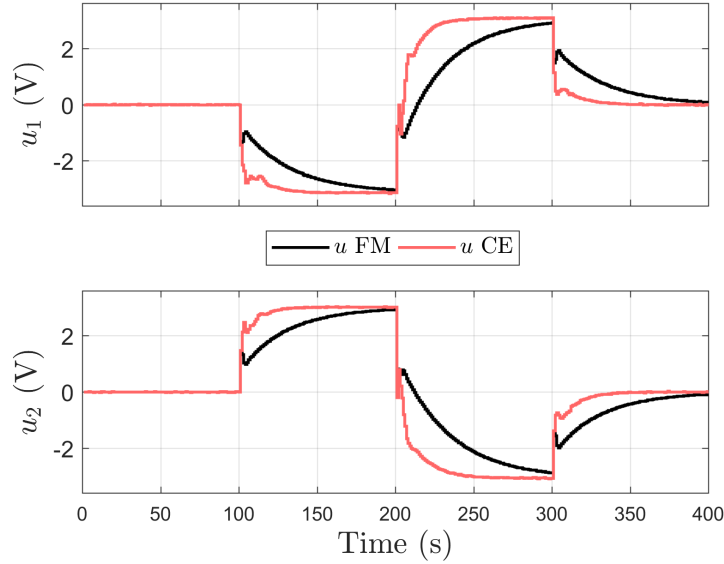


Figure 4.22: Quad-Tank Model 3 Input Profiles

function. It takes longer to reach the reference as a result. To illustrate the effect of the model error, define the following measure,

$$\epsilon_{\Delta} := \|\Delta(\mathbf{y}_t - \mathbf{C}_{\theta}\varphi_t)\|. \quad (4.12)$$

This measure is related to the disturbance from the point of view of the filtered model that defines each MPC optimization. The closed-loop error signal for each of the specified models is displayed in Figure 4.23. For both formulations, the error grows in between reference steps but adjusts as the input stabilizes and the filtered information contribution vanishes. Under the adaptive formulation, the control algorithm has the tools to bring the error towards the origin quicker by adjusting the parameters. A common feature observed in adaptive control formulations is the shattering of the input signal due to the

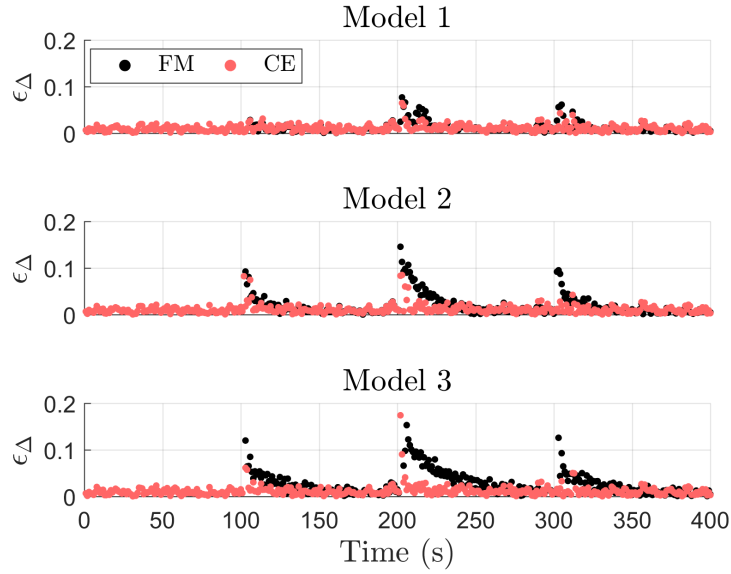


Figure 4.23: Quad-Tank Filtered Error for Models 1-3

adaptation transients. Here, this aspect is not significant enough to impact the output profiles.

The adaptive cases are capable of providing the desired tracking, irrespectively of the initial mean for the parameter distribution. This is a good indication in terms of the consistency of the estimation process. The parameter estimate transients for the adaptive cases are displayed in Figure 4.24. The action of the dead-zone supervisor is expressed in the constant periods for the parameter estimate elements. Note that the RLS estimator has converged to an alternative representation for the system. This can be inferred by the convergence of elements $\hat{\theta}_1$ and $\hat{\theta}_6$ to smaller values. These parameters correspond to the diagonal transfer function elements in (4.11). While the pairs $\hat{\theta}_2, \hat{\theta}_3$ and $\hat{\theta}_4, \hat{\theta}_5$ parametrize $G_{1,2}$ and $G_{2,1}$ respectively. The adaptive controller is effectively treating each lower tank height output mainly as a separate second order transfer function, which corresponds to the independent stacking of two tanks. This will be an appropriate representation for a

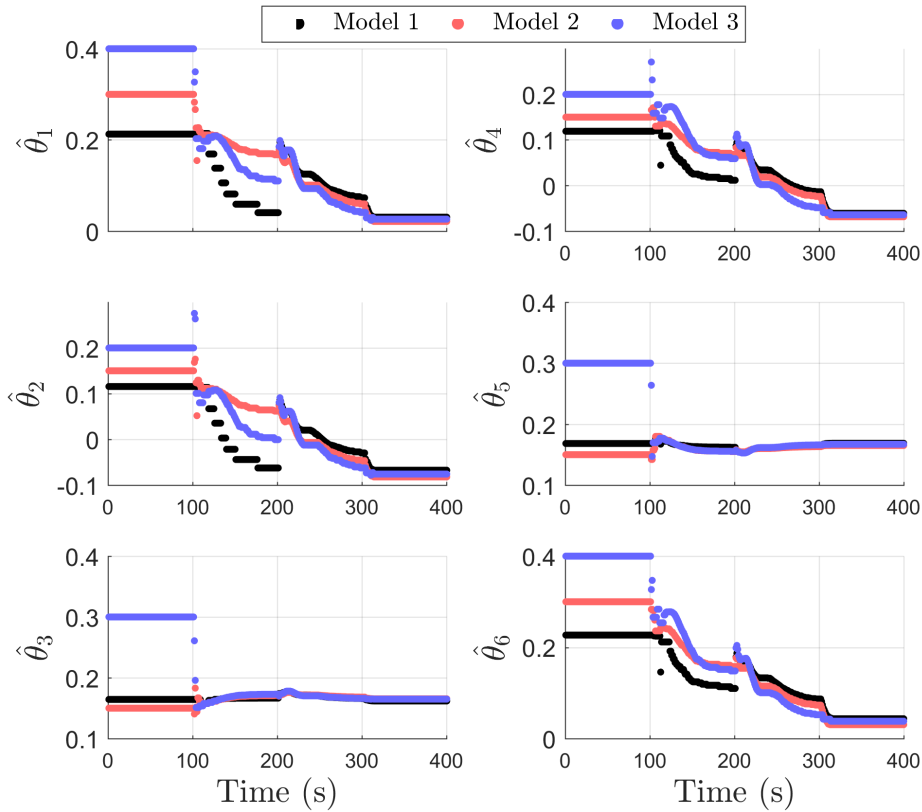


Figure 4.24: Quad-Tank Parameter Estimation

perfectly symmetrical system. The small contribution from the diagonal elements adjusts for the discrepancy as the system is not exactly symmetrical. If this type of solution should be avoided, a constrained estimator can be easily incorporated into the framework.

The overall evaluation of the simulation set obtained with the triad of initial models reassure the idea that, generating poles consistent with the plant enable the estimation process to provide parameters that translate into good tracking performance.

4.4 CONCLUSIONS

Two different CE adaptive control strategies have been presented in this chapter. The infinite-horizon policy is incorporated into the more general version with constraints as its time-varying terminal policy. This is achieved by appending a recursive on-line estimator into the working framework. The mass-spring minimal SISO system was studied to test the effect of varying orthonormal truncations in the context of the simpler, infinite-horizon policy. This case study was extended to show the effect of the defining orthonormality property of the GOBF model in the conditioning of the estimation. This is a desirable feature for adaptive control, as it enables the efficient assimilation of the closed-loop signal transients.

The artificial reference, from the robust formulation in the previous chapter, has been kept with a few modifications. This inclusion expands the admissible set of feasible initial conditions. This is important in the context of adaptation as it provides the controller with additional degrees of freedom to find feasible solutions when the model is poorly parametrized. The system description of a minimal MIMO quad-tank model has been outlined. This tool was used to outline a general method to define the generating pole set from a linear model related to the plant. A set of simulation results indicate that a suitable selection of the poles with respect to the region of references to be tracked lead to good control performance despite poor selection of the initial GOBF expansion coefficients.

5

INFORMATION CONSTRAINTS FOR GOBF MODELS

In this chapter, information constraints are incorporated into the CE adaptive control strategy. Such constraints, benefit the estimation process for the uncertain uncertain vector, $\hat{\theta}$, that parametrizes the predictor model. This modification leverages the structural properties of the GOBF model and the CE adaptive control algorithm. Prior to defining the proposed strategy, a summarizing overview of three relevant methods for including this type of constraints that have been proposed in the literature will be provided. By discussing the advantages and limitations of these alternatives, the guiding principles for the design of our method will become evident. The induction of exploratory features through a constraint set instead of additional modifications to the objective function is intended ot keep the focus on the control action. After the proper introduction of the overall approach, simulation examples with an illustrative scenario applied to the quad-tank system are presented.

The proposed approach has a direct interpretation in the scope of Dual Control Theory (Feldbaum 1960) as introduced in Chapter 1. The trade-off between the action and investigation risks is balanced by the enforcement of information constraints that enhance the

5.1 INFORMATION PRELIMINARIES

estimation process while optimizing a tracking CE objective that recursively adapts to the informative closed-loop signals.

5.1 INFORMATION PRELIMINARIES

A few important concepts, related to the simultaneous estimation process in an adaptive formulation are presented next. The discussion is carried through the scope of our GOBF modeling framework, facilitating the subsequent exposition of relevant strategies. Since the estimation problem has been decomposed into MISO subsystems, all claims will be made pertaining this simplified structure unless noted otherwise.

5.1.1 *Anticipated Information*

[Heirung et al. \(2017\)](#) proposed the definition of anticipated information for uncertain SISO systems. The concept is applicable to state-space model representations with known state-transition dynamics. Our model structure, as defined in Chapter 2, fits this description with the minor modification of multidimensional input record elements. The equivalent definition is given by,

$$\begin{aligned}\mathbf{Y}_{k|t} &:= \{\mathbf{u}_{k-1|t}, \mathbf{Y}_t\} \quad \text{for } k > t \\ \mathbf{u}_{k-1|t} &:= \{\mathbf{u}_{k-1}, \dots, \mathbf{u}_t\} \\ \mathbf{Y}_t &:= \{y_t, \dots, y_0, \mathbf{u}_{t-1}, \dots, \mathbf{u}_0\},\end{aligned}\tag{5.1}$$

for a system with the a GOBF state-space representation of the following form,

$$\begin{aligned}\boldsymbol{\varphi}_{t+1} &= \mathbf{A}_\xi \boldsymbol{\varphi}_t + \mathbf{B}_\xi \mathbf{u}_t \\ y_t &= \boldsymbol{\theta}^\top \boldsymbol{\varphi}_t + v, \quad v \sim \mathcal{N}(\mathbf{0}, r_v),\end{aligned}\tag{5.2}$$

where the vector $\boldsymbol{\theta}$ is uncertain. The current estimate distribution, $\{\hat{\boldsymbol{\theta}}_t, \mathbf{P}_{\boldsymbol{\theta},t}\}$, is assumed to be updated with RLS as outlined in the previous chapter. This characterization is made in order to introduce a modified expectation evaluation that simplifies the prediction of future estimates for the parameter estimate distribution beyond one step.

Corollary 1. *Anticipated Parameter Covariance for GOBF MISO Systems.* Consider system (5.2) as described above. The parameter covariance matrix conditioned to the anticipated information,

$$\mathbf{P}_{\boldsymbol{\theta},k|t} := \mathbb{E}[(\boldsymbol{\theta} - \hat{\boldsymbol{\theta}}_t)(\boldsymbol{\theta} - \hat{\boldsymbol{\theta}}_t)^\top | \mathbf{Y}_{k|t}],$$

evolves deterministically for a sequence of anticipated control actions according to

$$\boldsymbol{\varphi}_{k|t} = \mathbf{A}_\xi \boldsymbol{\varphi}_{k-1|t} + \mathbf{B}_\xi \mathbf{u}_{k-1}\tag{5.3a}$$

$$\sigma_{y,k|t}^2 = \boldsymbol{\varphi}_{k|t}^\top \mathbf{P}_{\boldsymbol{\theta},k-1|t} \boldsymbol{\varphi}_{k|t} + r_v\tag{5.3b}$$

$$\mathbf{P}_{\boldsymbol{\theta},k|t} = \mathbf{P}_{\boldsymbol{\theta},k-1|t} - (\sigma_{y,k|t}^2)^{-1} \mathbf{P}_{\boldsymbol{\theta},k-1|t} \boldsymbol{\varphi}_{k|t} \boldsymbol{\varphi}_{k|t}^\top \mathbf{P}_{\boldsymbol{\theta},k-1|t}\tag{5.3c}$$

where, $k > t$, $\mathbf{P}_{\boldsymbol{\theta},t|t} := \mathbf{P}_{\boldsymbol{\theta},t}$, $\boldsymbol{\varphi}_{t|t} := \boldsymbol{\varphi}_t$, and the pair $\{\mathbf{A}_\xi, \mathbf{B}_\xi\}$ is given by a known GOBF MISO structure.

The recursions in (5.3) follow from the application of Theorem 1 in (Heirung et al. 2017) to the GOBF state-space system (5.2) and the unmodified RLS covariance update. The

5.1 INFORMATION PRELIMINARIES

useful property that this result provides is that the covariance matrix associated with a GOBF model, $\mathbf{P}_{\theta,k|t}$, evolves independently of future output realizations.

5.1.2 Information Matrix

Note that (5.3b) and (5.3c) are equivalently obtained by applying the Matrix Inversion Lemma to the inverse of the parameter covariance, $\bar{\mathbf{I}}_{\theta,k|t} := \mathbf{P}_{\theta,k|t}^{-1}$,

$$\bar{\mathbf{I}}_{\theta,k|t} = \bar{\mathbf{I}}_{\theta,k-1|t} + \frac{1}{r_v} \boldsymbol{\varphi}_{k|t} \boldsymbol{\varphi}_{k|t}^\top. \quad (5.4)$$

The observed information matrix, $\bar{\mathbf{I}}_{\theta,t|t} := \bar{\mathbf{I}}_{\theta,t}$, and its anticipated extension are equivalently derived from the prediction error parameter sensitivities, defined by the log-likelihood function for the Gaussian observations,

$$\bar{\mathbf{I}}_{\theta,t} = \bar{\mathbf{I}}_{\theta,0} + \frac{1}{r_v} \sum_{k=1}^t \left(\frac{\partial \varepsilon_k}{\partial \boldsymbol{\theta}} \right) \left(\frac{\partial \varepsilon_k}{\partial \boldsymbol{\theta}} \right)^\top$$

where,

$$\frac{\partial \varepsilon_k}{\partial \boldsymbol{\theta}} = \frac{\partial}{\partial \boldsymbol{\theta}} \left(y_k - \boldsymbol{\theta}^\top \boldsymbol{\varphi}_k \right) = -\boldsymbol{\varphi}_k.$$

Since the error sensitivities are not functions of the parameter estimate realizations, the anticipated information matrix contributions in (5.4) can be computed explicitly for a sequence of inputs, $\mathbf{u}_{k-1|t}$, leading to an equivalent result to Corollary 1.

5.1.3 *Information Maximization*

If the goal was to reduce the uncertainty of the parameter vector estimate, an optimal system identification experiment could be derived in terms of the anticipated information matrix. The related problem maximizes a suitable objective function, $J : \mathbb{S}_+^n \rightarrow \mathbb{R}$. A common choice is the smallest eigenvalue of the generated information matrix, $\bar{\mathbf{I}}_{\theta,k|t} \in \mathbb{S}_+^n$. The general form for such a problem is given, in broad terms, by

$$\begin{aligned} \max_{\mathbf{u}_{N-1|t}} \quad & J(\bar{\mathbf{I}}_{\theta,N|t}) \\ \text{s.t.} \quad & \text{power constraints} \\ & \text{amplitude constraints} \end{aligned}$$

Different optimality criteria (*e.g.* A,D,E-optimality) are defined by the particular form of the objective function (Ljung 1999). The common feature for any of the available choices, is that the solution defines a sequence of inputs that optimally reduce the volume of the ellipsoidal confidence region associated with the parameter covariance estimate. Figure 5.1 illustrates the defining idea behind the optimization problem. The darkest ellipse represents an initial confidence region for a hypothetical system with two parameters. Each of the dashed ellipses with sequentially decreasing size correspond to the effect of the information gain of individual inputs. Overall, the input sequence leads to the optimized region associated to the maximized information measure. Noting that a single control action can only yield a rank-1 information gain, adjacent elliptical volume reductions are depicted accordingly.

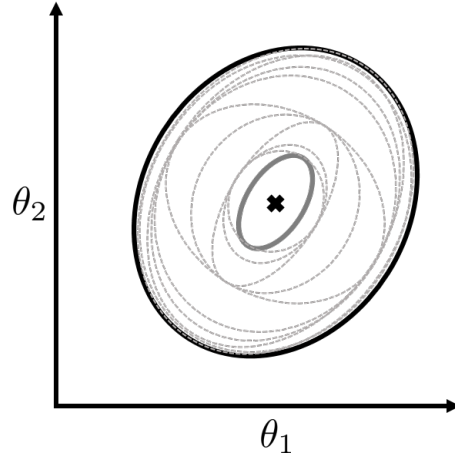


Figure 5.1: Ellipsoidal Parameter Confidence Region Transient

For a complete description of a this problem and detailed strategies to solve subproblems under different constraint sets, under a similar modeling approach, we refer to the work of [Manchester \(2010\)](#). Here, we limit the discussion to the type of mathematical structures that arise in the problem. The dynamics (5.3a) can be equivalently expressed by,

$$\varphi_{k|t} = A_{\xi}^{k-t} \varphi_t + \sum_{i=t}^{k-1} A_{\xi}^{i-t} B_{\xi} \mathbf{u}_{k-1-i+t}.$$

A finite sum of rank-1 contributions, $\varphi_{k|t} \varphi_{k|t}^{\top}$, constitute the anticipated information. From the expression above, it is clear that this is a bilinear matrix function in terms of the vector formed by stacking the series of inputs in $\mathbf{u}_{k-1|t}$. In order to avoid the introduction

of more variables, we will refer to this vector with the same notation. The anticipated information in (5.4) is expressed in the following standard bilinear matrix form,

$$\begin{aligned}\bar{\mathbf{I}}_{\theta,k|t} &= \bar{\mathbf{I}}_{\theta,t} + \frac{1}{r_v} \sum_{j=t+1}^k \varphi_{j|t} \varphi_{j|t}^\top \\ &= \mathbf{F}_0 + \sum_{i=1}^{kn_u} \mathbf{u}_i \mathbf{F}_i + \sum_{i=1}^{kn_u} \sum_{j \geq i}^{kn_u} \mathbf{u}_i \mathbf{u}_j \mathbf{H}_{ij},\end{aligned}\tag{5.5}$$

in terms of the scalar elements, $\mathbf{u}_i \in \mathbb{R}$, of $\mathbf{u}_{k-1|t} \in \mathbb{R}^{kn_u}$. The matrices $\mathbf{F}_0, \mathbf{F}_i, \mathbf{H}_{ij} \in \mathbb{S}_+^n$ are implicitly defined in the expressions above.

Bilinear functions appear in many relevant optimization problems. Solution methods often rely on relaxations obtained with linear approximations. For (5.5), by introducing a symmetric positive semidefinite matrix variable, \mathbf{U} , the last term on the right hand side of the expression above can be reformulated to,

$$\sum_{i=1}^{kn_u} \sum_{j \geq i}^{kn_u} \mathbf{U}_{ij} \mathbf{H}_{ij}, \quad \mathbf{U}_{ij} = \mathbf{u}_i \mathbf{u}_j.$$

The overall result obtained from these treatment is the ability to formulate anticipated information optimization problems a linear matrix function coupled with a set of non-convex scalar equalities. Relaxations can be defined with the aid of McCormick envelopes (Castro 2015) or Linear Matrix inequalities (Shor 1987) in terms of the latter.

5.2 REVIEW OF INFORMATIVE MPC FORMULATIONS

5.1.4 Persistent Excitation

A variety of defining conditions for persistent excitation can be found in standard literature of adaptive filtering (e.g. [Goodwin & Sin \(1984\)](#)). We use the following time domain expression which applies directly to the information matrix.

Definition 2. *GOBF MISO State Persistent Excitation.* The vector $\varphi_t \in \mathbb{R}^n$ is said to be persistently exciting of order n , if there exists an integer m and positive real constants, ρ , and $\bar{\rho}$ such that for all t ,

$$\rho \mathbf{I} \preceq \sum_{i=1}^m \varphi_{t+i} \varphi_{t+i}^\top \preceq \bar{\rho} \mathbf{I}.$$

In practical terms, the existence of the lower bound guarantees an invertible information matrix obtained from a finite sum of rank 1 gains. Therefore, it follows that $m \geq n$ must hold. The upper bound is not a main concern given that, under the assumption of inherent BIBO stability of the system dynamics, this will always exist as long as the input is kept bounded by the controller. In relationship to the covariance illustration in [Figure 5.1](#), persistent excitation can be understood as a non-zero tightening of the ellipsoidal confidence region in all directions over the interval specified by m .

5.2 REVIEW OF INFORMATIVE MPC FORMULATIONS

We are now ready to present three different MPC formulations recently proposed in the literature ([Heirung et al. 2017](#); [Larsson et al. 2016](#); [Marafioti et al. 2014](#)) which are derived from the ideas presented in the previous section. Beyond describing the defining characteristics for each of these strategies, we aim to adapt the applicable features to

our method. The exposition is intended to highlight the limitations and advantages that motivate our proposed alternative. As such, it is meant to be instructional rather than comprehensive.

5.2.1 Dual Adaptive MPC (Heirung et al. 2017)

Provided with the result in Theorem 1, the expectation and variance for the tracking component of the stage cost, conditioned to the anticipated information, yield the following deterministic expression,

$$\mathbb{E}[(y_k - y^r)^2 | \mathbf{Y}_{k|t}] = (\hat{\boldsymbol{\theta}}_t^\top \boldsymbol{\varphi}_{k|t} - y^r)^2 + \sigma_{y,k|t}^2. \quad (5.6)$$

A derivation of these results can be found as Corollaries 3 and 4 in (Heirung et al. 2017). The key observation is that, under this conditioning, the expected value for the parameter vector at all times $k \geq t$ remains fixed at the current estimate, $\hat{\boldsymbol{\theta}}_t$, whereas its actual future expectation, $\hat{\boldsymbol{\theta}}_k$, depends on unrevealed stochastic output realizations. The conditioning on the anticipated information can be understood as the approximation of distributions $\mathcal{N}(\hat{\boldsymbol{\theta}}_k, \mathbf{P}_{\theta,k})$ with $\mathcal{N}(\hat{\boldsymbol{\theta}}_t, \mathbf{P}_{\theta,k|t})$. For the GOBF model structure, or any other model for which the information gains can be propagated deterministically through known dynamics, $\mathbf{P}_{\theta,k} = \mathbf{P}_{\theta,k|t}$.

The proposed method reduces to appending the anticipated expected variance cost to some or all the stages of the finite horizon portion of the objective function. This requires the inclusion of additional decision variables and constraints associated with the recursions in (5.3). As discussed previously, the nonlinear equations (5.3b) and (5.3c) are

an alternative representation of the quadratic equality (5.4). With either formulation a set of nonconvex equalities is obtained. The authors present a Quadratically Constrained Quadratic Program (QCQP) reformulation by the introduction of an auxiliary variable,

$$z_{j|t} := \frac{1}{r_v} \mathbf{P}_{\theta, j-1|t} \boldsymbol{\varphi}_{j|t}.$$

This allows the expression of the sum of anticipated variance contributions in (5.6) as a bilinear function of the new variable and the information state,

$$\begin{aligned} \sum_{j=t}^k \sigma_{y,j|t}^2 &= \sum_{j=t}^k \left(\boldsymbol{\varphi}_{j|t}^\top \mathbf{P}_{\theta, j-1|t} \boldsymbol{\varphi}_{j|t} + r_v \right) \\ &= r_v \sum_{j=t}^k \left(\boldsymbol{\varphi}_{j|t}^\top z_{j|t} + 1 \right). \end{aligned} \quad (5.7)$$

Adopting the MPC notation for the finite horizon control vector, \mathbf{u} , and the accent ($\hat{\cdot}$) for optimization variables predicted with the current model, the cost and constraint set to be appended to a CE adaptive optimal control problem is given in (5.8). To have an effect in the MPC problem, the dual cost horizon, N_d , must satisfy, $2 \leq N_d \leq N$.

$$J_{d,N}(\boldsymbol{\varphi}_t, \bar{\mathbf{I}}_{\theta,t}, \mathbf{u}) := r_v \sum_{k=1}^{N_d-1} \hat{\boldsymbol{\varphi}}_k^\top \hat{\mathbf{z}}_k \quad (5.8)$$

$$\hat{\boldsymbol{\varphi}}_0 = \boldsymbol{\varphi}_t \quad (5.8a)$$

$$\hat{\mathbf{I}}_{\theta,0} = \bar{\mathbf{I}}_{\theta,t} \quad (5.8b)$$

$$\hat{\boldsymbol{\varphi}}_k = \mathbf{A}_\xi \hat{\boldsymbol{\varphi}}_{k-1} + \mathbf{B}_\xi \hat{\mathbf{u}}_{k-1}, \quad k \in \mathbb{I}_{1:N_d-1} \quad (5.8c)$$

$$\hat{\boldsymbol{\varphi}}_k = r_v \hat{\mathbf{I}}_{\theta, k-1} \hat{\mathbf{z}}_k, \quad k \in \mathbb{I}_{1:N_d-1} \quad (5.8d)$$

$$\hat{\mathbf{I}}_{\theta,k} = \hat{\mathbf{I}}_{\theta, k-1} + \frac{1}{r_v} \hat{\boldsymbol{\varphi}}_k \hat{\boldsymbol{\varphi}}_k^\top, \quad k \in \mathbb{I}_{1:N_d-1} \quad (5.8e)$$

The variance cost for the first stage, $\hat{\varphi}_0^\top \hat{z}_0$, and the measurement noise, $N_d r_v$, have been excluded from the definition since they are constants and do not affect the cost optimization.

The scalar elements of the symmetric matrix variable, (5.8e), grow quadratically with the dimension of the parameter vector. On the other hand, the number of stage contributions, N_d , cause the constraint set to grow linearly. This problem defines the optimal compromise between the estimation and tracking aspects of the problem. However, MIMO systems of practical importance may require both large horizon windows and models with high-dimensional parameter vectors. Reported solution times of the associated MPC problem take up to a few seconds in some instances for a low-dimensional FIR SISO system under no structural model mismatch and a local nonlinear solver. Global optimality is desired, since control actions corresponding to local solutions are not guaranteed to induce the desired properties. This further deteriorate the applicability of the method as larger sets of non-convex inequalities make the branching routines, inherent of global solvers, increasingly complex.

5.2.2 MPC with Experiment Constraint (Larsson et al. 2016)

The dual variance cost is given by the interrelated evolution of the GOBF state vector and the covariance matrix variables as shown in (5.3). Its non-negative value can be driven to zero by regulating the vector, maximizing information, or a combination of both. The preceding dual formulation is intended to accomplish whichever is optimal in relation to the simultaneous tracking task, but practical limitations may prevent it success. Information maximization is intrinsically contrary to the tracking task, while regulation

is only desired if the reference is zero. One could, instead, define a bounding measure for the information matrix obtained in the closed loop, and impose progress towards it onto the MPC problem. This is, in very general terms, the approach proposed by Larsson et al. (2016).

Instead of explicitly minimizing an appended cost to the objective, the problem is constrained such that the finite horizon control sequence causes the tightening of the hyper-ellipsoidal confidence regions related to the parameter covariance matrix. The associated experiment design constraint requires two defining parameters. A reference information matrix, $\bar{\mathbf{I}}_\theta^r$, and the number of steps to reach it, $T_{\mathbf{I}}$. The former is determined by a probabilistic constraint on a cost related to the MPC application. The latter is chosen with respect to the relative importance of the control deterioration and the time it takes to satisfy the reference information matrix. We refer to (Larsson 2014) for a detailed description of the theoretical development of the approach and its components. Here, we omit the formal declaration of all the built-in assumptions and approximations by treating these parameters as off-line design elements, fixed by the user, and declare the constraint directly,

$$\bar{\mathbf{I}}_{\theta,0} + \frac{1}{r_v} \sum_{k=1}^{T_{\mathbf{I}}} \varphi_k \varphi_k^\top \succeq \bar{\mathbf{I}}_\theta^r. \quad (5.9)$$

Assuming that the importance of the control deterioration prevails when choosing $T_{\mathbf{I}}$, one can afford to distribute the information gain over a number of steps larger than the MPC finite horizon size, N . Instead of extending the MPC horizon (and the number of optimization variables), an equivalent constraint is formulated with the declaration of a

shorter information horizon, $N_{\mathbf{I}}$, and a deterministic nondecreasing sequence for a scaling factor, κ_t , that satisfy

$$\begin{aligned} n &\leq N_{\mathbf{I}} < N, \\ 0 &\leq \kappa_0 < 1, \kappa_t \rightarrow \infty. \end{aligned}$$

The modified constraint (5.10) is a semidefinite Bilinear Matrix Inequality (BMI), in terms of the MPC optimization variables.

$$\bar{\mathbf{I}}_{\theta,t} + \frac{1}{r_v} \sum_{k=1}^{N_{\mathbf{I}}} \hat{\varphi}_k \hat{\varphi}_k^{\top} \succeq \kappa_t \bar{\mathbf{I}}_{\theta}^r. \quad (5.10)$$

The number of steps for the reference information constraint to be satisfied is implicitly specified by this pair. For example, the sequence can be set to increase linearly with time, $\kappa_t = \frac{t}{T_{\mathbf{I}}}$. Increments on the information horizon size, $N_{\mathbf{I}}$, distribute the specified gain, $\kappa_t \bar{\mathbf{I}}_{\theta}^r - \bar{\mathbf{I}}_{\theta,t}$, among a greater number of stages in the control horizon, resulting in less aggressive excitation. This is done with the risk of obtaining optimal solutions that sequentially postpone excitation, since only the first stage control element is actually applied. It is important to note that the proposed method is originally presented for a more general linear modeling approach, where some of the uncertain parameter vector elements define the state transition dynamics. The cost of this generality is that an adaptive controller is more challenging to define, as the prediction error sensitivities become explicit functions of the parameters. This implies that each time the parameter estimate is updated, the information matrix has to be recomputed with the data record. Due to this limitation, the estimate, $\hat{\theta}$, is only updated after a period of closed loop experimentation, terminated by the satisfaction of (5.9).

In terms of the implementation, the solution of an MPC problem subject to (5.10) remains challenging since BMIs are in general non-convex (VanAntwerp & Braatz 2000). As shown in the previous section, this can be reformulated to a convex linear matrix inequality (LMI) coupled with a set of bilinear equalities. Without further modification, the optimal control problem raises the same concerns of the dual variance cost formulation. Relevant methods that can handle BMI constraints rely on LMI relaxations (Dinh et al. 2012; Manchester 2010). Exact solutions of the original problem formulation require the iteration through several LMI subproblems. As an alternative, the authors propose the addition of a white noise component weighted by a matrix derived from the LMI relaxation solution. This means that the applied control is not optimal with respect to the original problem and only feasibility can be guaranteed.

The relationship to persistent excitation is clear by comparing (5.10) with the expression in Definition 2. The main contribution of this approach is enforcing excitation in a directed fashion, through the reference information matrix. Ideally, the covariance tightening occurs in the directions that matter the most for the problem at hand. This represents another challenge, as the application cost must be defined by deviations of the parameter estimate from those belonging to a good representation of the actual system. The authors propose the computation of an application cost and the associated reference information matrix via off-line simulations with current parameter estimates. One could argue, that when performed with significant inaccuracies, this approach loses its validity. On the other hand, if the parameters already give a good representation, the value of introducing excitation is questionable. For this scenario, it could be sufficient to rely on the information gathered passively with a conventional CE formulation.

5.2.3 Persistently Exciting MPC ([Marafioti et al. 2014](#))

The last approach to be discussed is similar to the previous in terms of the BMI form of the constraint to be included in the MPC formulation. Instead of enforcing the excitation directly in terms of future information gains, $\hat{\varphi}_k \hat{\varphi}_k^\top$, it is implemented indirectly through the first stage control action, $\mathbf{u}_t = \hat{\mathbf{u}}_0$, and a finite sequence of past inputs $\{\mathbf{u}_{t-1}, \mathbf{u}_{t-2}, \dots\}$. So far, the discussion in this chapter has been presented in terms of MISO models since the working model structure follows the diagonal stacking of MISO components for a MIMO system. This enables the segregated treatment of the information/covariance matrices for each output channel. For this method, it is favorable to take a step back and look at the SISO case since the key idea to be borrowed is derived with this simplified treatment.

A few concepts, adapted from the original statements in ([Marafioti et al. 2014](#)), are required for the development. The original definitions are made in the context of models forms with regression vectors given explicitly by the data record (*e.g.* ARX). Their equivalent counterparts for the SISO GOBF model structure are presented here. For ease of notation, the past input record vector, \mathbf{p}_k , is introduced,

$$\mathbf{p}_k = \begin{bmatrix} u_k \\ u_{k-1} \\ \vdots \\ u_{k-n+1} \end{bmatrix} \in \mathbb{R}^n. \quad (5.11)$$

From the inherent controllability of the SISO GOBF model, it follows that any state $\varphi \in \mathbb{R}^n$ is reachable from a finite sequence of inputs that can be expressed in terms of \mathbf{p}_k . This allows the declaration of a related condition to persistent excitation, sufficient richness

(SR) of the input. The SR condition can be interpreted as an indirect measure of the information matrix.

Definition 3. *Sufficiently Richness Condition.* Consider a GOBF SISO system of order n . The scalar input signal, u_k , is sufficiently rich with respect to the SISO state vector if there exists an integer $m \geq n$ and positive real constants, ρ , and $\bar{\rho}$ such that for all t ,

$$\rho \mathbf{I} \preceq \sum_{k=0}^{m-1} \mathbf{p}_{t-k} \mathbf{p}_{t-k}^\top \preceq \bar{\rho} \mathbf{I}. \quad (5.12)$$

Theorem 4. *GOBF SISO Persistent Excitation from SR Inputs.* A necessary and sufficient condition for the state vector associated to a GOBF SISO model to be persistently exciting over the interval $[t+1-n, t+m]$ is that the input signal satisfies the SR condition over the interval $[t+1, t+m]$.

The result above, allows persistent excitation for the vector φ to be induced by the SR condition applied on the input signal. From the implementation point of view, it is not clear what has been gained since the constraint is also a BMI. However, provided with a prior input sequence that satisfies the SR condition at time $t-1$, the BMI has a special form that can be reformulated to a quadratic scalar inequality in terms of u_t .

For the general case with multiple inputs, an equivalent treatment unfolds into a BMI in the dimension of the input signal. This is normally much lower than the state dimension. Nonetheless, the problem solution remains challenging for the same reasons discussed previously. The difficulty is aggravated by the fact that the task of specifying SR sequences for multi-input systems, required for initialization, is not an easy task on its own. The detailed derivation of the scalar input case is given below, with the appropriate modifications for the GOBF approach.

5.3 INFORMATIVE GOBF MPC

The discussion for the three strategies presented in the preceding section exposed a set of features to be considered in the design of an alternative strategy. The direct optimization of the dual variance cost, introduces a large set of non-convex equality constraints. This set grows quadratically with the dimension of the uncertain parameter vector. In place of explicit optimization, the problem can be posed such that the optimal control action is constrained to yield sequential non-zero information matrix gains that in turn cause the variance cost to decrease. The associated constraints of this indirect approach are, in general, semidefinite BMIs in terms of the MPC control variables.

Persistent excitation can be induced by a sufficiently rich input signal as long as reachability with respect to the information state vector holds. For a SISO GOBF component, this is the case and it can be simplified to a scalar quadratic constraint. Overall, it is desired to introduce excitation in a directed fashion pertinent to the deterioration of the control task. Regardless of the approach, dealing with non-convex quadratic expressions inherent of the least squares estimation problem seems unavoidable.

The PE inducing SR input condition can be adapted and generalized to a scalar filtered GOBF signal. Similarly to the single input case, dealing with its filtered scalar version, *i.e.* a GOBF state, vastly simplifies the computational burden of the required constraints, as the SR condition can be reformulated to a scalar quadratic inequality. Furthermore, it should be intuitive that enforcing persistent excitation for a smaller subspace than that corresponding to the overall MIMO structure, should be simpler. Recall that the state-space construction method in Chapter 2, generates the overall structure through diagonal stacking of state-space SISO components. This approach, may not be the most efficient in

terms of the state dimension representing the system. However, it offers the opportunity to define SISO-specific informative constraints.

Each scalar transfer function component has its own independent GOBF state transition dynamics and corresponding parameter vector. Therefore, we can direct the generation of constraints to those subcomponents that need it the most. The definition and subsequent enforcement of an SR condition with the order of the largest SISO vector for each input channel, should induce persistent excitation for all other subcomponents related to that input.

Including a set of SISO SR inequalities to the unmodified CE adaptive MPC problem as presented in the previous chapter could still be inefficient from a computational point of view. It will be shown that a simplifying choice for the objective function, allows the reformulation of the problem into a much more tractable QCQP. The control law switches between the solution of the full CE problem and that of a reduced size informative formulation. The non-convex features are only present in the latter, with variable and constraint set sizes bounded by the dimension of the control signal.

The SR constraint definition will first be presented for the general case of an arbitrary scalar GOBF information state element. The input version, as proposed originally, follows as a special case. In order to determine which state elements generate the constraint set, a heuristic measure, related to the dual variance cost, is introduced subsequently, as a guiding tool for a selection procedure.

5.3.1 SR GOBF State Constraint

Assume that for the j^{th} input channel, a SISO system with index ij , and a scalar element of its information vector have been selected. The matching state transition dynamics $\{\mathbf{A}_{ij,\xi}, \mathbf{b}_{ij,\xi}\}$ and current vector-valued signal $\varphi_{ij,t} \in \mathbb{R}^{n_{ij}}$ are extracted from the overall model. In order to facilitate the treatment of the expressions below, the ij index is dropped.

Let the l^{th} element of the vector φ_t be the scalar signal specified by the selection procedure. Recall from Chapter 2, that φ_t is determined by a vector filter object according to,

$$\varphi_t = \begin{bmatrix} F_1(q) \\ \vdots \\ F_l(q) \\ \vdots \\ F_n(q) \end{bmatrix} u_t = \mathbf{F}_n u_t.$$

The reachability of φ_t holds equivalently with respect to a finite sequence of any of the filtered GOBF state scalar components. By filtering the vector \mathbf{p}_k in (5.11), through the basis function for the l^{th} element and the backward difference operator, we get

$$\Delta F_l(q) \mathbf{p}_{k+1} = \begin{bmatrix} \Delta \varphi_{l,k+1} \\ \phi_{l,k} \end{bmatrix} \in \mathbb{R}^n, \quad \phi_{l,k} := \Delta \begin{bmatrix} \varphi_{l,k} \\ \varphi_{l,k-1} \\ \vdots \\ \varphi_{l,k-n+2} \end{bmatrix} \in \mathbb{R}^{n-1}.$$

Partitioning the filtered vector in this way facilitates the mathematical treatment below. The index have been moved one sampling forward, since GOBF filters, as specified, are

strictly proper. Note that this allows the application of Theorem 4 to obtain an equivalent SR condition in terms of the filtered information states.

Corollary 5. *GOBF SISO Persistent Excitation from SR States.* A necessary and sufficient condition for the state vector associated to a GOBF SISO model to be persistently exciting over the interval $[t + 1 - n, t + m]$ is that one of its scalar filtered elements satisfies the SR condition over the interval $[t + 1, t + m]$ with $m > n$.

$$\sum_{k=0}^{m-1} \begin{bmatrix} \Delta\varphi_{l,t+1-k} \\ \phi_{l,t-k} \end{bmatrix} \begin{bmatrix} \Delta\varphi_{l,t+1-k} \\ \phi_{l,t-k} \end{bmatrix}^{\top} \succeq \rho \mathbf{I}. \quad (5.13)$$

The upper bound is disregarded for the same reasons discussed previously. Note that the lower bound in equation (5.12) is not necessarily the same as ρ above. Declaring the SR condition directly in terms of these filtered GOBF states is useful since the tracking problem is defined around the origin. This allows the initialization of the SR constraints for arbitrary output reference signals with the same sequence, also centered around the origin. Next, we adjust the derivation in (Marafioti et al. 2014) to obtain the GOBF scalar quadratic inequality. Define the following matrix,

$$\Omega_t := \sum_{k=0}^{m-1} \phi_{l,t-k} \phi_{l,t-k}^{\top}$$

and rewrite (5.13),

$$\left[\begin{array}{c|c} (\Delta\varphi_{l,t+1})^2 + \sum_{k=1}^{m-1} \varphi_{l,t+1-k}^2 - \rho & \Delta\varphi_{l,t+1} \phi_{l,t}^{\top} + \sum_{k=1}^{m-1} \Delta\varphi_{l,t+1-k} \phi_{l,t-k}^{\top} \\ \hline \Delta\varphi_{l,t+1} \phi_{l,t} + \sum_{k=1}^{m-1} \Delta\varphi_{l,t+1-k} \phi_{l,t-k} & \Omega_t - \rho \mathbf{I} \end{array} \right] \succeq 0.$$

All the elements in the expression above are determined by variables available prior to defining the control action at time t , except $\Delta\varphi_{l,t+1}$. This scalar element is a function of the associated SISO vector $\Delta\varphi_t$ and the input move Δu_t , related by the state-transition pair $\{\mathbf{A}_\xi, \mathbf{b}_\xi\}$.

$$\Delta\varphi_{l,t+1} = \mathbf{a}_{l,\xi}^\top \Delta\varphi_t + b_{l,\xi} \Delta u_t,$$

where the vector $\mathbf{a}_{l,k}$ is defined as the transpose of the l^{th} row of \mathbf{A}_ξ , and $b_{l,\xi}$ denotes the l^{th} element of the input to state vector \mathbf{b}_ξ . Using the expression above and the Schur Complement Lemma, the semidefinite BMI (5.13) is equivalently enforced by the following pair,

$$\boldsymbol{\Omega}_t - \rho \mathbf{I} \succ 0 \quad (5.14a)$$

$$\alpha_t (\Delta u_t)^2 + 2\beta_t \Delta u_t + \gamma_t > 0 \quad (5.14b)$$

where,

$$\alpha_t = b_{l,\xi}^2 \left(1 - \boldsymbol{\phi}_{l,t}^\top (\boldsymbol{\Omega}_t - \rho \mathbf{I})^{-1} \boldsymbol{\phi}_{l,t} \right) \quad (5.15a)$$

$$\boldsymbol{\omega}_t = (\mathbf{a}_{l,\xi}^\top \Delta\varphi_t) \boldsymbol{\phi}_{l,t} + \sum_{k=1}^{m-1} \Delta\varphi_{l,t+1-k} \boldsymbol{\phi}_{l,t-k} \quad (5.15b)$$

$$\beta_t = b_{l,\xi} \left(\mathbf{a}_{l,\xi}^\top \Delta\varphi_t - \boldsymbol{\omega}_t^\top (\boldsymbol{\Omega}_t - \rho \mathbf{I})^{-1} \boldsymbol{\phi}_{l,t} \right) \quad (5.15c)$$

$$\gamma_t = (\mathbf{a}_{l,\xi}^\top \Delta\varphi_t)^2 + \sum_{k=1}^{m-1} \Delta\varphi_{l,t+1-k}^2 - \boldsymbol{\omega}_t^\top (\boldsymbol{\Omega}_t - \rho \mathbf{I})^{-1} \boldsymbol{\omega}_t - \rho \quad (5.15d)$$

The semidefinite inequality (5.14a) holds automatically if (5.13) holds strictly at $t - 1$. This is easily shown by noting that the SR condition shifted back by one sampling time,

$$\sum_{k=0}^{m-1} \begin{bmatrix} \Delta\varphi_{l,t-k} \\ \phi_{l,t-1-k} \end{bmatrix} \begin{bmatrix} \Delta\varphi_{l,t-k} \\ \phi_{l,t-1-k} \end{bmatrix}^\top = \sum_{k=0}^{m-1} \begin{bmatrix} \phi_{l,t-k} \\ \Delta\varphi_{l,t-n+1-k} \end{bmatrix} \begin{bmatrix} \phi_{l,t-k} \\ \Delta\varphi_{l,t-n+1-k} \end{bmatrix}^\top \succ \rho \mathbf{I}$$

can also be expressed as,

$$\left[\begin{array}{c|c} \Omega_t - \rho \mathbf{I} & \sum_{k=0}^{m-1} \Delta\varphi_{l,t-n+1-k} \phi_{l,t-k} \\ \hline \sum_{k=0}^{m-1} \Delta\varphi_{l,t-n+1-k} \phi_{l,t-k}^\top & \sum_{k=0}^{m-1} (\Delta\varphi_{l,t-n+1-k})^2 - \rho \end{array} \right] \succ 0.$$

As a principal sub-matrix, (5.14a) also holds. Provided with a feasible initialization, the SR condition is satisfied at all future times by the recursive, strict satisfaction of (5.14b). Persistent excitation is successfully introduced in the actual trajectory only if this is achieved by a sequence over the interval $[t_0 + 1 - n, t + m]$, where t_0 denotes the initialization time. In the event of an infeasible problem, the CE solution is applied, and the constraint set is reinitialized at the subsequent sampling time.

The conventional SISO SR input condition (5.12), and its scalar constraint as originally proposed, can be obtained by defining the 0^{th} filtered scalar information vector $\varphi_{0,t} := q^{-1}u_t$. The appropriate scalar dynamics are given by $\alpha_{0,k} = \mathbf{0}$ and $b_{0,\xi} = 1$.

5.3.2 *Informative Optimal control Problem*

A simplification of the CE MPC objective function is formulated based on the following observations. First, the transients between reference signals are usually informative without modification. Imposing information gains is only desired when the closed loop does not provide them. Second, the objective function of the CE problem in a region around the reference is equivalent to the terminal policy by construction. If the artificial reference variable has stabilized to \mathbf{y}^r , and this is sufficiently far away from the bounds imposed by the box constraints, the CE adaptive infinite-horizon tracking policy and the control derived from $P_{ce,N}(\mathbf{x}, \mathbf{y}^r)$ yield the same control move. Incorporating these remarks on the design, we define a region around \mathbf{y}^r , based on the terminal cost, that serves as an indicator for the activation of the informative control problem.

$$\delta_{sr,t} = \begin{cases} 1, & \text{if } \|\mathbf{x}_{m,t} - \mathbf{x}_m^r\|_{\mathbf{P}_{f,t}}^2 < \epsilon_{sr}, \text{ and } y_t \in \mathcal{Y} \\ 0, & \text{otherwise} \end{cases} \quad (5.16)$$

The indicator $\delta_{sr,t}$ signals whether the control aspect has been sufficiently met and active learning through the enforcing of (5.14b) can be afforded. Recall that the tracking steady state is given by,

$$\mathbf{x}_m^r = \begin{bmatrix} \mathbf{0} \\ \mathbf{y}^r \end{bmatrix}$$

When $\delta_{sr,t} = 1$, the SR optimal informative control problem (5.17), denoted by $\mathcal{P}_{sr}(\mathbf{x}, \mathbf{y}^r)$ is solved instead of $\mathcal{P}_{ce,N}(\mathbf{x}, \mathbf{y}^r)$.

$$\mathcal{P}_{sr}(\mathbf{x}, \mathbf{y}^r) : \min_{\Delta \hat{\mathbf{u}}_0} J_{f,t}(\hat{\mathbf{x}}_{m,1}, \mathbf{x}_m^r) \quad (5.17)$$

$$\text{s.t. } \hat{\mathbf{x}}_0 = \mathbf{x} \quad (5.17a)$$

$$\hat{\mathbf{x}}_{m,1} = \mathbf{A}_{m,t} \hat{\mathbf{x}}_{m,0} + \mathbf{B}_{m,t} \Delta \hat{\mathbf{u}}_0 \quad (5.17b)$$

$$\hat{\mathbf{x}}_1 \in \mathcal{X} \quad (5.17c)$$

$$\alpha_{j,t} \Delta \hat{u}_{j,0}^2 + 2\beta_{j,t} \Delta \hat{u}_{j,0} + \gamma_{j,t} > 0, \quad j \in \mathbb{I}_{1:n_u} \quad (5.17d)$$

The objective function is the square of a quadratic norm defined by the terminal cost matrix, $\mathbf{P}_{f,t} \succeq 0$, computed for the full MIMO model with the latest estimate mean vector, $\hat{\boldsymbol{\theta}}_t$.

$$J_{f,t}(\hat{\mathbf{x}}_{m,1}, \mathbf{x}_m^r) = \|\hat{\mathbf{x}}_{m,1} - \mathbf{x}_m^r\|_{\mathbf{P}_{f,t}}^2$$

Other elements of (5.17) retain the description provided in the CE problem definition, found in Chapter 4. Note that the unconstrained solution corresponds to the CE adaptive, infinite-horizon tracking policy. The optimizing argument of (5.17), defines the admissible input move that minimizes the deviation from the terminal policy infinite-horizon cost, while enforcing the SR constraint set. The objective function is quadratic and convex. On the other hand, the SR constraints are, in general, non-convex. Although only feasibility is strictly required, it is also desired to obtain a global solution. In comparison to the dual cost formulation (5.8), the size of the problem is significantly lower, which makes its implementation in real time more plausible.

5.3.3 Parameter Selection Heuristic

With the constraint set and optimal control problem properly introduced, the only missing element for the overall algorithm is the guiding criteria for selecting the scalar state elements that define the SR constraint set. Ideally, this should be simple to check in real time but at the same time relevant to the control performance. We begin its derivation by assuming a diagonal cost matrix, \mathbf{Q} . The following decomposition for the tracking cost expectation, conditioned to one anticipated input, is made

$$\mathbb{E}[\|\mathbf{y}_{t+1} - \mathbf{y}^r\|_{\mathbf{Q}}^2 \mid \mathbf{Y}_{t+1|t}] = \sum_{i=1}^{n_y} Q_i \left((\hat{\boldsymbol{\theta}}_{i,t}^\top \boldsymbol{\varphi}_{i,t+1|t} - y_i^r)^2 + \boldsymbol{\varphi}_{i,t+1|t}^\top \mathbf{P}_{\theta_i,t} \boldsymbol{\varphi}_{i,t+1|t} + r_{v_i} \right).$$

The intermediate term of the sum contributions should be the target of the informative constraint.

Consider a scalar element φ_l of the vector, $\boldsymbol{\varphi}$. Its contribution to the dual cost is proportional to its own magnitude under a given reference signal, its variance, and the covariance interactions with the other scalar elements. The input defines how these interactions change from one sampling time to the next. A simplified indicator candidate, neglecting the covariance and input interactions, is the square of the current state vector element weighted by its variance. To see its relationship with the overall contribution, define the following scalar function for a pair $\{\mathbf{P}_\theta, \boldsymbol{\varphi}\}$,

$$\psi(\mathbf{P}_\theta, \boldsymbol{\varphi}) := \max_l (\boldsymbol{\varphi} \odot \text{diag}(\mathbf{P}_\theta) \odot \boldsymbol{\varphi}),$$

where $\varphi \in \mathbb{R}^n$, and \odot indicates the element-wise product. The operators $\text{diag}(\cdot)$, and $\max_l(\cdot)$ yield the diagonal vector of a matrix and the maximum scalar element for $l \in \mathbb{I}_{1:n}$ respectively. Let $\psi_{ij,t}$ denote the cost indicator function evaluation for the SISO variables corresponding to the i^{th} output and j^{th} input at time t , weighted by Q ,

$$\psi_{ij,t} := Q_i \psi(\mathbf{P}_{\theta_{ij,t}}, \varphi_{ij,t}) \quad (5.18a)$$

$$l_{ij,t} := \arg \max_l (\varphi_{ij,t} \odot \text{diag}(\mathbf{P}_{\theta_{ij,t}}) \odot \varphi_{ij,t}). \quad (5.18b)$$

The parameters $\{\psi_{ij,t}, l_{ij,t}\}$ can be updated cheaply at each sampling time. On the other hand, the constraint set should only be updated periodically, allowing the completion of sufficiently rich transients. When such an event takes place, for each j^{th} input, the new SR inequality is generated in terms of the l^{th} element of the ij^{th} SISO system with the largest $\psi_{ij,t}$,

$$\bar{\psi}_j := \max_i (\psi_{ij,t}) \quad (5.19)$$

5.3.4 Initialization

An important aspect of the approach is that the initialization of the SR constraint parameters must be consistent with the model. This is important as we intend to switch between two modes for the control action, and the effective initialization is required at the onset of the informative regime. Not every scalar sequence that satisfies the SR condition will necessarily lead to the desired recursive feasibility. The initialization sequence must match the frequency, determined by the generating pole set, in order to facilitate it. Fortunately, this is something that can be easily achieved off-line, as part of the control design.

First, a set of artificial input sequences that satisfy the original SR condition (5.12) with a lower-bound defined by ρ_u are generated. These could come from a white noise generator or a more elaborate input design method. The same sequence can be used for all input channels, or dedicated assignments can be made. At this point, the record window size, m , is also defined. By adjusting these parameters the introduced excitation can be customized. With a longer information window size, the rank-1 gains are distributed among more sampling times, resulting in less informative individual inputs for a fixed ρ_u . For a fixed m , the bounding constant indicates the size of the desired shrinking of the ellipsoidal covariance confidence regions for an SR cycle.

The set of input sequences are then filtered through the model dynamics. The final adjustment is made by iteratively reducing, as necessary, the original bounding ρ_u until (5.13) is satisfied. Once all these steps have been completed, the initial set of quadratic inequality coefficients $\{\alpha, \beta, \gamma\}$ are generated for each information state element, φ , and stored in memory with its respective sequence and bounding constant ρ . For large models, the initialization can be simplified by selecting at least one state for each SISO object. We now present a summarizing account of the steps for the proposed method including the common features with the CE Adaptive Control algorithm as presented in the preceding chapter.

5.4 IMPLEMENTATION

Assume that all the quadratic inequality coefficients have been successfully initialized according to the procedure outlined above and the system is at a sampling time at which the information indicator switch, $\delta_{sr,t}$, activates.

Algorithm 5.1 Informative CE Adaptive Control Action

Require:

- Current measured state, \mathbf{x}_t ▷ $\Delta\varphi_t, \mathbf{y}_t, \mathbf{u}_{t-1}$
- Prior parameter estimate distribution $\{\hat{\boldsymbol{\theta}}_{t-1}, \mathbf{P}_{\theta,t-1}\}$
- GOBF state transition matrices $\{\mathbf{A}_\xi, \mathbf{B}_\xi\}$, Cost parameters $\{\mathbf{Q}, \mathbf{R}, \mathbf{T}\}$
- SR parameters $\{\alpha_{j,t}, \beta_{j,t}, \gamma_{j,t}\}$ for $j \in \mathbb{I}_{1:n_u}$ ▷ Selection by (5.18)-(5.19)

Ensure:

- Control action \mathbf{u}
- 1: Update parameter distribution to get $\{\hat{\boldsymbol{\theta}}_t, \mathbf{P}_{\theta,t}\}$
 - 2: Update state-transition model with $\hat{\boldsymbol{\theta}}_t$
 - 3: Solve filtered model DARE to obtain terminal cost matrix $\mathbf{P}_{f,t}$
 - 4: **while** $\delta_{sr,t} = 1$ **do**
 - 5: Solve $\mathcal{P}_{sr}(\mathbf{x}, \mathbf{y}^r)$ in (5.17) ▷ Update SR selection periodically
 - 6: $\hat{\mathbf{u}}_0^* \leftarrow \Delta\hat{\mathbf{u}}_0^* + \mathbf{x}_u$
 - 7: Compute $\{\alpha_{j,t+1}, \beta_{j,t+1}, \gamma_{j,t+1}\}$ for $j \in \mathbb{I}_{1:n_u}$ with (5.15)
 - 8: **end while**
 - 9: Solve $\mathcal{P}_{ce,N}(\mathbf{x}, \mathbf{y}^r)$ ▷ Use Algorithm 4.1
 - 10: $\mathbf{u} \leftarrow \hat{\mathbf{x}}_{u,1}^*$
-

The modified certainty equivalence control algorithm with SR information constraints is specified in Algorithm 1. The periodic state element selection in line 5 should be performed with a frequency that allows at least two SR cycles for a given set.

5.4.1 Quad-Tank Simulation Results

Resuming the analysis of the quad-tank minimal example, recall that, with an appropriate choice for the pole generating set, the conventional CE formulation was successful in recovering the policy obtained with an accurate model regardless of the initial mean for the parameter estimate. For that case, the passive learning introduced by the reference step changes is sufficient to provide good parameter estimates, that in turn yield good control performance. This motivates the study of a different type of scenario for the SR formulation, where this does not occur. Assume that the pole and order of the system is only approximately known. A model structure is generated with poles distributed in the region where accurate pole locations are believed to be located. The off-diagonal SISO filters are modeled with third order GOBF truncations with generating pole set $\xi = \{0.90, 0.80, 0.70\}$. The diagonal elements, corresponding to the direct interaction of the pump flows to the lower tanks, are constructed with second order filters and $\xi = \{0.75, 0.65\}$. These regions contain the poles of the linearized model around the nominal steady-state. Overall, there are 10 parameter coefficients distributed according to this structural description. The truncation scalar components that constitute the mean estimate, $\hat{\theta}$, are initialized uniformly with $\hat{\theta} = 0.15$.

For all the results below, the SR constraint initialization was performed with input-specific scalar sequences that satisfy the SR condition with $\rho_u = 0.01$, $m = 10$, and $n = 3$. These parameters are appropriate to induce persistent excitation on all the SISO components for the model as specified. The constraint activation indicator (5.16) is defined with $\epsilon_{sr} = 0.1$. All other applicable MPC parameters and problem specifications remain identical to the simulations in Chapter 4, unless noted otherwise.

5.4 IMPLEMENTATION

In the first experiment, we take a step back in order to illustrate what has been accomplished in terms of parameter estimation. The reference is set at zero, which corresponds to the nominal steady state for the tank system. Additionally, the dead-zone supervisory feature of RLS is removed. With this set up, we have isolated the analysis to the effect of the SR constraint with state selection. Four different versions of the CE controller are implemented:

- (i) CE Constrained Adaptive MPC (Chapter 4)
- (ii) Version (i), with input SR constraints
- (iii) Version (i), with GOBF SR constraints, fixed state choice
- (iv) Proposed approach. GOBF SR constraints and state selection every 50s

Figure 5.2 displays the evolution of the trace of the parameter estimate covariance matrix, $P_{\theta,t}$. This function is a good indicator of the quality of the estimation process. A lower value indicates a higher level of certainty with respect to current mean estimate $\hat{\theta}_t$. It is observed that the proposed approach outperforms all the other alternatives under this measure. The CE passive approach is the first to cease decreasing significantly. This should not be surprising since there is nothing in the problem definition that asks for such behavior. In general the initial descent of the GOBF versions is much more consistent than the input version. The proposed approach departs from the fixed state version after the first 50 second interval and continues decreasing, reaching a value roughly two orders of magnitude lower at the end of the experiment. A zoomed portion of the input profiles generated with these methods is shown in Figure 5.3. At some time between 200 and 300 seconds, the fixed direction SR constraints appear to enter a cyclic profile which could

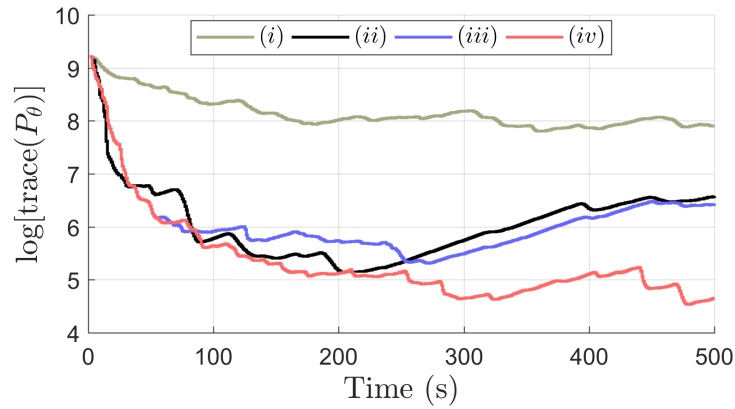


Figure 5.2: Quad-Tank Adapted Parameter Covariance with SR Constraints

explain the increment in the covariance trace, as the excitation introduced is not enough to compete with the effect of the exponential forgetting factor. In other words, the new information generated is the same that is continuously fading. This does not happen with the state selection feature, as the small excitation pulses remain irregular throughout the experiment.

The parameter estimation transient for two representative elements of the overall estimate mean vector are shown in Figure 5.4. It is observed that the improved estimation features discussed above are reflected on the stability of the transients for the parameters. As discussed in Chapter 4, the orthonormality of the GOBF transfer functions results in improved conditioning of the covariance. The main motive of the proposed constraints is to introduce excitation in varying directions that matches the frequency of the model components to further enhanced this aspect of the adaptive control problem.

For the second experiment, we repeat the reference step changes studied in Chapter 4 under the new model definition with approximate plant knowledge. The fixed GOBF state version, (iii), is not included for this part. The dead-zone feature is reincorporated

5.4 IMPLEMENTATION

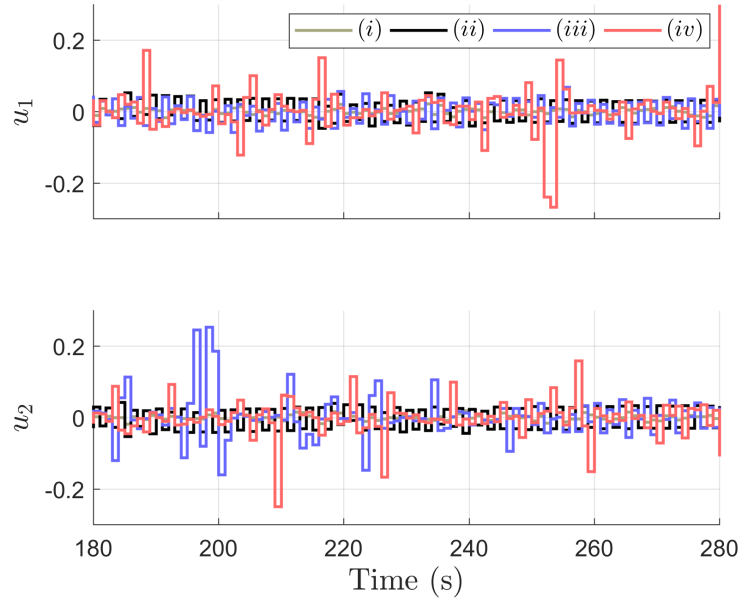


Figure 5.3: Quad-Tank Regulation SR Input Detailed Profiles

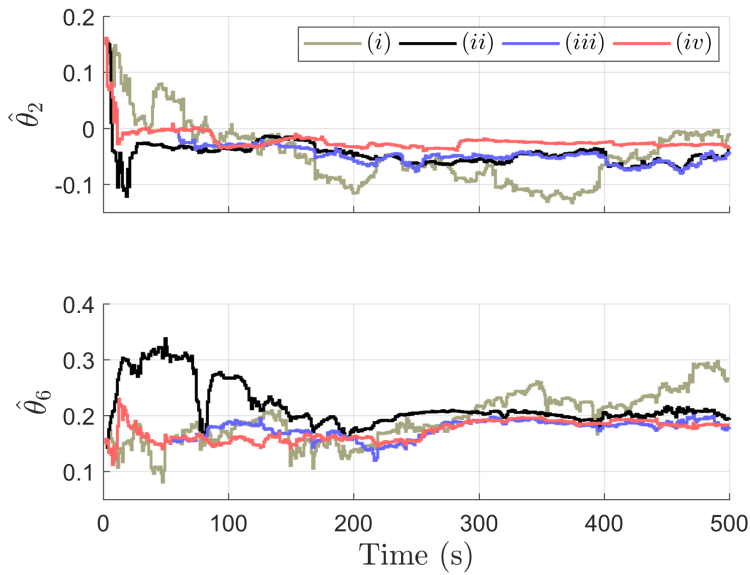


Figure 5.4: Quad-Tank Regulation SR Parameter Estimation

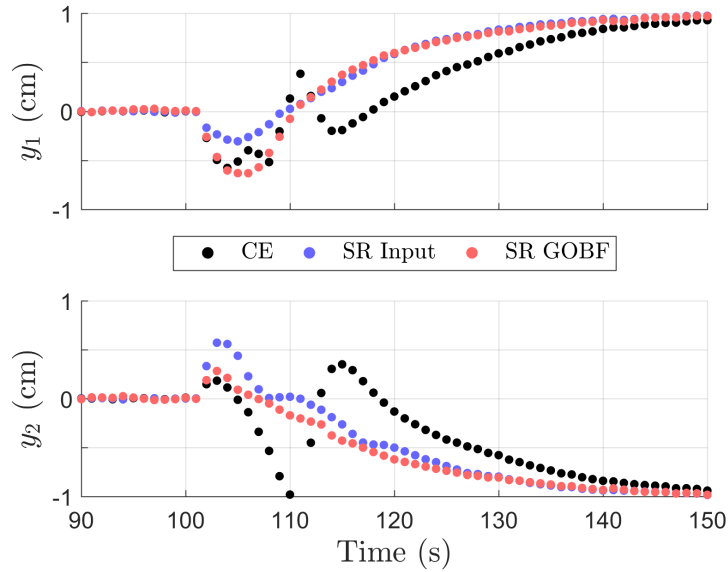


Figure 5.5: Quad-Tank Output Profile Reference Intervals 1-2

in the RLS estimator to avoid parameter drifting that may render the problem infeasible when the reference signal changes. The output transient between the first and second reference intervals is illustrated in Figure 5.5. The magnitude of the excitation induced by the SR constraints and their activation are illustrated in Figures 5.6 and 5.7 respectively. Note that the large oscillations induced by the low quality of the estimation process does not have a proportional adverse effect in the output profile. These spikes on the input are buffered by the upper level tanks, which receive most of the flow. The overall input-output profile is given in Figures 5.9 and 5.8. Both, the CE and input SR formulations display large bursting episodes. Unlike the small information bursts induced by the proposed method, these are not intentional and their magnitude is unpredictable.

The dead-zone feature of the RLS estimator, is intended to remove the shattering observed in the first experiment as shown in Figure 5.4. Note that the improved estimation

5.4 IMPLEMENTATION

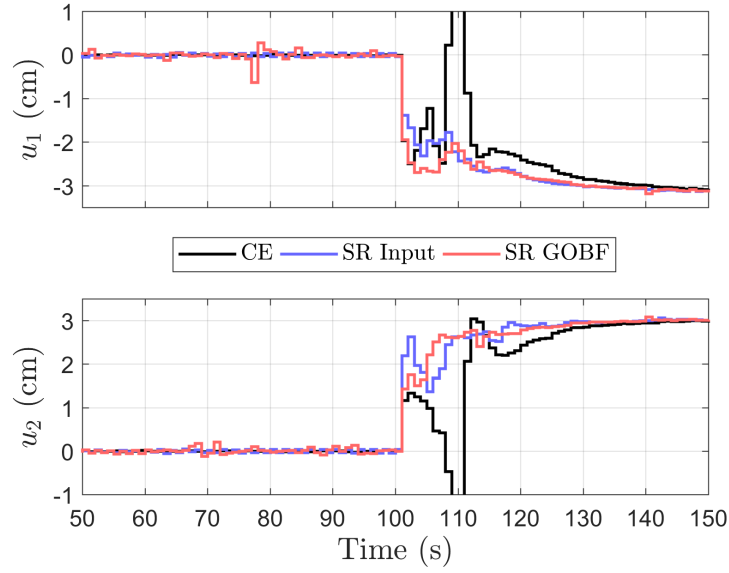


Figure 5.6: Quad-Tank Input Profile Reference Intervals 1-2

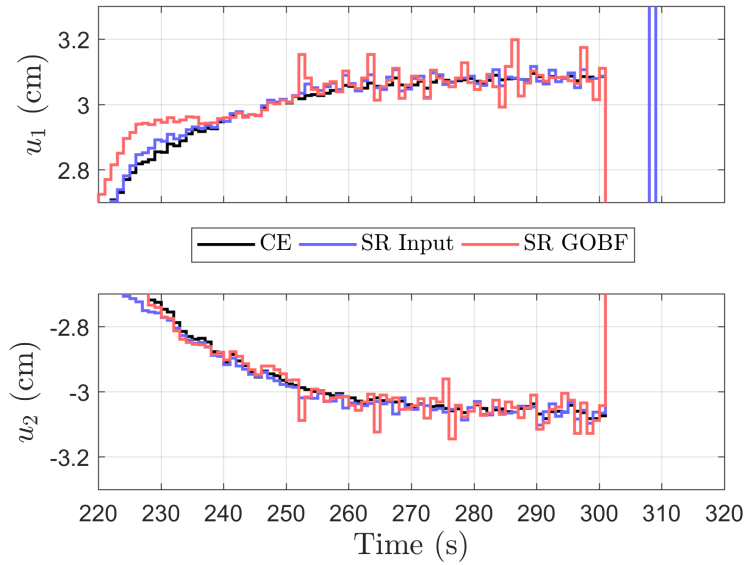


Figure 5.7: Quad-Tank SR Activation

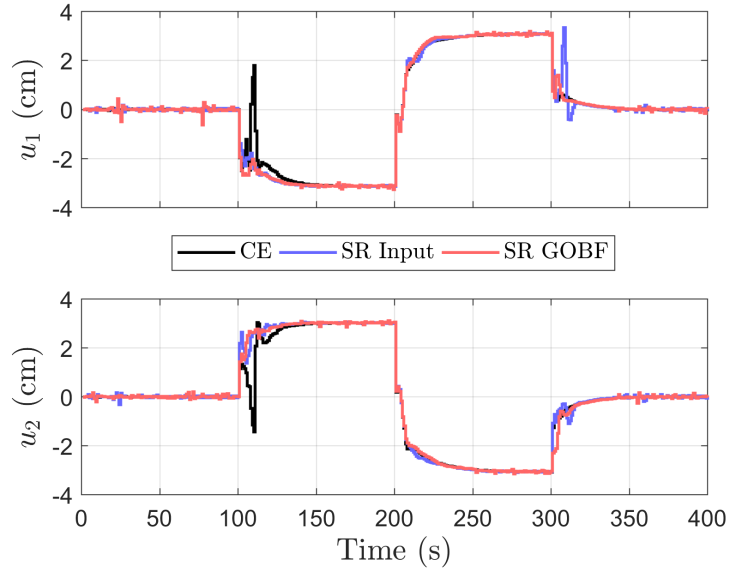


Figure 5.8: Quad-Tank Control Output Profiles

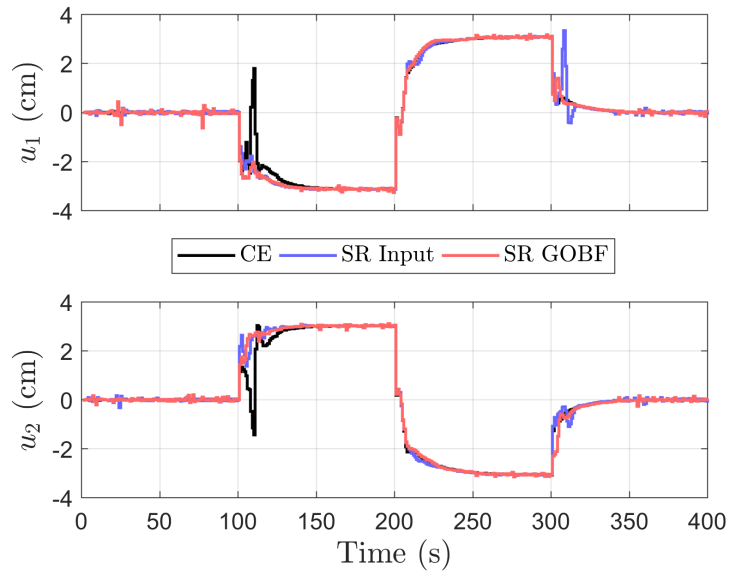


Figure 5.9: Quad-Tank Control Input Profiles

provided by the SR GOBF constraints is also evident in the parameter estimate profiles in Figure 5.10, under this estimator feature.

The state selection procedure based on the variance cost indicator (5.19), is set to act every 40 seconds. The chosen sequence is listed in Table 5.1 for the 10 different periods at which the SR constraint set is updated. State indexes 1-2 and 9-10 correspond to the direct interactions of pumps 1 and 2 with their adjacent lower level tanks respectively. Indexes 3-5 and 6-8 belong to the higher order indirect cross-interaction through the upper level tanks. Elements from all SISO subcomponents are selected, dominated by the leading coefficient of the higher order off-diagonal filters. This is consistent with the model as the system routing valves are set divert most of the flow through the upper level, and these state contributions are expected to be more significant to the tracking task.

Table 5.1: SR GOBF State Selection Index

SR Interval	1	2	3	4	5	6	7	8	9	10
u_1	6	2	2	6	6	6	6	6	7	7
u_2	3	10	3	10	3	3	3	10	4	4

In computational terms, the related optimization problem for this illustrative model reduces to a nonconvex QCQP of dimension 2 which is solved with BARON 17.8.9 (Tawarmalani & Sahinidis 2005). For a representative experiment with the GOBF formulation, the SR constraint set is activated 260 of the 400 sampling instances with no infeasible problems. Out of these, BARON reaches the imposed maximum time of one CPU second 16 times on a standard laptop computer. The average solution time for all QCQP instances is 0.43 seconds.

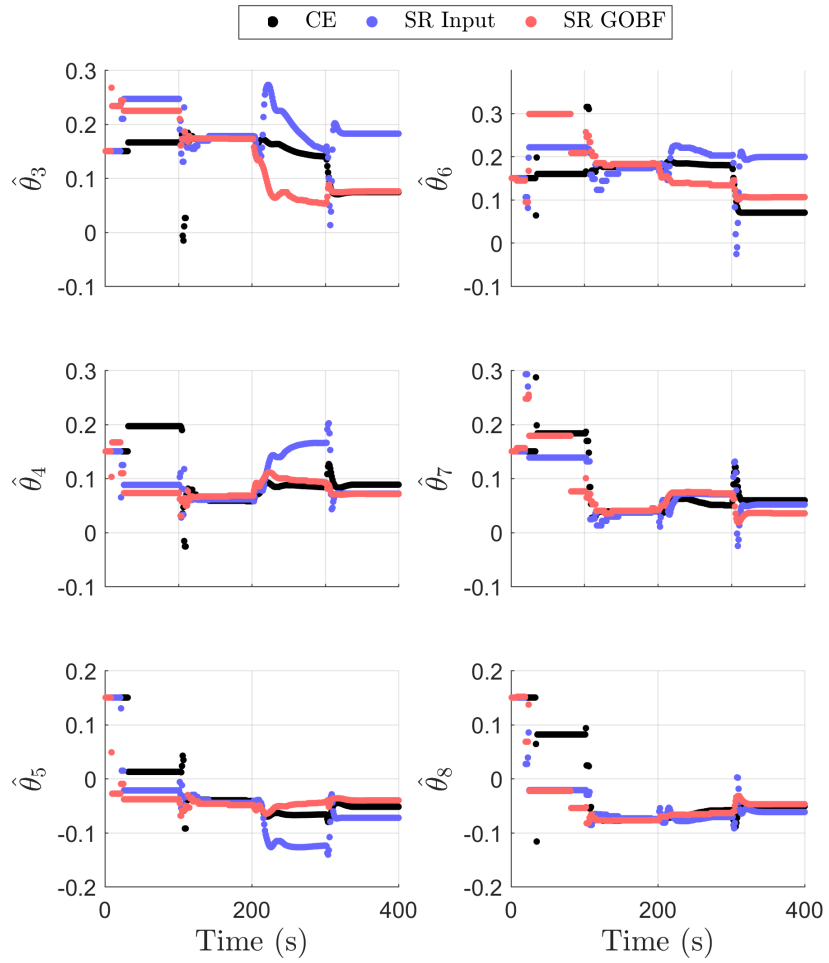


Figure 5.10: Off-Diagonal SISO Filters Parameter Estimation

5.5 CONCLUSIONS

5.5 CONCLUSIONS

The motivation and practical considerations of the inclusion of informative features in the CE Adaptive MPC control problem with GOBF models has been presented. Alternatives proposed in the literature have been framed into this modeling structure. Instead of relying on linear relaxations or the direct optimization of the expected output variance, we have proposed an indirect method that stems from the induction of persistent excitation through sufficiently rich input signals. The working model structure enables the enforcement of this condition in terms of the filtered GOBF state elements instead of the raw input signal. In turn, this opens the doors for a new element in the constraint formulation. Namely, the state selection procedure through the dual cost targeting function. With the intent of obtaining faster solution times, the SR constraints are not applied directly to the full-size constrained MPC problem. Instead, an indicator function that activates when the system is near the tracking steady state was introduced. The activated optimal control problem is consistent with the model and MPC cost definition. Different aspects of the method were illustrated by its application on the illustrative MIMO Quad-Tank System.

CONCLUSIONS AND FUTURE WORK

6.1 CONCLUSIONS

We have presented the GOBF modeling approach as a compelling choice for adaptive model predictive control. Several aspects have been discussed. There are two notable benefits. First, the enhancement of the identification enabled by the orthonormal, input balanced state-space realizations. Second, the inherent controllability properties that allow the definition of infinite-horizon tracking terminal cost functions and convex parameter estimation problems that can be handled with unmodified RLS methods.

In Chapter 3, a variety of non-adaptive MPC policies were presented. The introduction of output feedback that eliminates tracking offsets when the model is not exact was introduced through the modification of the original MIMO model as presented in Chapter 2 with backwards difference filters. The importance of model representations that lead to bounded error signals was demonstrated by the constraint tightening approach in the robust formulation.

6.1 CONCLUSIONS

The adaptive MPC formulation was motivated with a series of orthonormal basis representations. The improvement of the conditioning of the least-squares parameter estimation problem was demonstrated by a comparison to a fixed denominator structure, representative of other linear approaches in this regard. A more general constrained certainty equivalence MPC method was presented. The problem definition includes an artificial reference optimization variable and its associated off-set cost. To our best knowledge, this is the first time that this is incorporated in an adaptive MPC approach. The construction of the GOBF MIMO model from an available linear representation for the system was outlined. The recovery of control performance by adaptation from a poorly parametrized original model was demonstrated on the illustrative Quad-Tank system.

The formulation of information constraints with suitable for the Constrained CE adaptive method of Chapter 4 is another notable contribution. The combined approach has dual control characteristics by inducing probing features in the input signal. It is noted that for a tracking control task, the transients between references are already informative. The active probing features through small information gains are enforced only in periods where the traditional certainty equivalence approach would not. The induced persistent excitation with the selection procedure is shown to avoid large unexpected bursting that are observed even with the conventional input SR constraints.

6.1.1 Publications

The contents of Chapters 4 and 5 are currently being modified into a series of two publications.

Adaptive MIMO MPC with Generalized Orthonormal Basis Functions (In Preparation)

Dual Adaptive MPC with Generalized Orthonormal Basis Functions - Persistent Excitation Constraints (In Preparation)

This separation allows a more focused introduction to the features of the MIMO model construction and its associated constrained CE adaptive MPC algorithm, which has many features that have not been proposed in the literature. The second paper is intended to extend the simulation results with other computational case studies that may benefit from the active approach.

6.2 FUTURE WORK

6.2.1 *Integration with Robust Controller*

Based on the observations made this far, it is valid to ask when it is convenient for the adaptation to cease. For systems with time invariant structure, one could envision an approach that switches between adaptive and non-adaptive robust regimes. This requires the definition of adequate measures, related to the evolution of the prediction error that would define the supervisory layer that performs the switch. While adapting, the information constraints can be enabled in the closed-loop as tuning mechanism and disabled as necessary.

6.2 FUTURE WORK

6.2.2 MIQP Reformulation

Since the coefficients of the quadratic constraints are known prior to computing the control action, the convexity and feasibility of each constraint for each input channel can be determined prior to the solution of the optimization. One could then solve specific QP subcases and apply the best solution as shown in the SISO example in (Marafioti et al. 2014). This could also be done relatively simply for the Quad-Tank case since there only two channels and the number of subproblems can only reach 4 when both constraints are non-convex and feasible. As the dimension of the input variable and feasible nonconvex constraint grows, the number of combinations grows exponentially. These structure could be more efficiently framed with the aid of integer variables assigned to each input channel that would define convex MIQPs which could be more efficiently solved. For example, consider a non-convex inequality quadratic constraint for input u with known real roots r_1 and r_2 , such that $r_1 < r_2$, and a large positive constant M . The nonconvex quadratic equality, is equivalently represented by

$$u < r_1 + Mz, \quad u > r_2 - M(1 - z), \quad z \in \{0, 1\}$$

6.2.3 Further Experimental Validation

There are many features of the proposed approach that have not been tested. For instance, although the model was formulated in general for higher order backward difference filters, we limited the control design to the first order. For example, other type of disturbance like signals that have periodic attributes may benefit from a different selection of

this feature of the model. Another aspect that remains unexplored is the incorporation of more sophisticated estimator structures to the problem. For example, the quad-tank analysis could be modified with box constraints and moving horizon estimators that enforce positive gains for all the SISO transfer function elements. This could be compared to simpler projection approaches applied to the recursive least-squares update. In principle, the GOBF approach would also facilitate these estimation modifications compared to other linear model representations.

6.2.4 *Adaptive Control with Physical Constraints*

As it was observed in the Quad-Tank example simulations of Chapter 4, the original system representation corresponding to the linearized nominal model is not recovered by the adaptive estimator, even though the initial and final references coincide. As discussed previously, this is related to the approximate symmetry of the system, but also of the experiment as well. The estimation can then be constrained to constitutive relationships between the predicted outputs of the MIMO system such as mass balances. These constraints could be relaxed during adaptation transients and strictly enforced around steady state operations.

BIBLIOGRAPHY

- Åström, K. & Wittenmark, B. (1973). On self tuning regulators. *Automatica*, 9(2), 185–199.
- Åström, K. & Wittenmark, B. (2008). *Adaptive Control*. Courier Corporation.
- Biegler, L., Yang, X., & Fischer, G. (2015). Advances in sensitivity-based nonlinear model predictive control and dynamic real-time optimization. *Journal of Process Control*, 30, 104–116.
- Bitmead, R., Gevers, M., & Wertz, V. (1990). *Adaptive optimal control: The thinking man's GPC*. Prentice Hall New York.
- Bodin, P., Villemoes, L., & Wahlberg, B. (2000). Selection of best orthonormal rational basis. *SIAM Journal on Control and Optimization*, 38(4), 995–1032.
- Bradtke, S., Ydstie, B., & Barto, A. (1994). Adaptive linear quadratic control using policy iteration. In *American Control Conference, 1994*, volume 3, (pp. 3475–3479). IEEE.
- Castro, P. (2015). Tightening piecewise mccormick relaxations for bilinear problems. *Computers & Chemical Engineering*, 72, 300–311.
- Dinh, Q., Gumussoy, S., Michiels, W., & Diehl, M. (2012). Combining convex–concave decompositions and linearization approaches for solving bmis, with application to static output feedback. *IEEE Transactions on Automatic Control*, 57(6), 1377–1390.
- Dozal-Mejorada, E. (2008). *Adaptive control with supervision*. PhD thesis, Carnegie Mellon University.
- Feldbaum, A. (1960). Dual control theory. i. *Avtomatika i Telemekhanika*, 21(9), 1240–1249.
- Finn, C., Wahlberg, B., & Ydstie, B. (1993). Constrained predictive control using orthogonal expansions. *AIChE Journal*, 39(11), 1810–1826.
- Genceli, H. & Nikolaou, M. (1996). New approach to constrained predictive control with simultaneous model identification. *AIChE journal*, 42(10), 2857–2868.
- Goodwin, G., Ramadge, P., & Caines, P. (1980). Discrete-time multivariable adaptive control. *IEEE Transactions on Automatic Control*, 25(3), 449–456.
- Goodwin, G. & Sin, K. (1984). *Adaptive Filtering Prediction and Control*. Englewood Cliffs, NJ, USA: Prentice Hall.

BIBLIOGRAPHY

- Griffith, D., Zavala, V. M., & Biegler, L. (2017). Robustly stable economic nmPC for non-dissipative stage costs. *Journal of Process Control*, 57, 116–126.
- Heirung, T., Ydstie, B., & Foss, B. (2017). Dual adaptive model predictive control. *Automatica*, 80, 340–348.
- Heuberger, P., van den Hof, P., & Wahlberg, B. (2005). *Modelling and identification with rational orthogonal basis functions*. Springer Science & Business Media.
- Johansson, K. (2000). The quadruple-tank process: A multivariable laboratory process with an adjustable zero. *IEEE Transactions on control systems technology*, 8(3), 456–465.
- Larsson, C. (2014). *Application-oriented experiment design for industrial model predictive control*. PhD thesis, KTH Royal Institute of Technology.
- Larsson, C., Ebadat, A., Rojas, C., Bombois, X., & Hjalmarsson, H. (2016). An application-oriented approach to dual control with excitation for closed-loop identification. *European Journal of Control*, 29, 1–16.
- Lewis, F. & Liu, D. (2013). *Reinforcement Learning and Approximate Dynamic Programming for Feedback Control*, volume 17. John Wiley & Sons.
- Limon, D., Alvarado, I., Alamo, T., & Camacho, E. (2010). Robust tube-based MPC for tracking of constrained linear systems with additive disturbances. *Journal of Process Control*, 20(3), 248–260.
- Ljung, L. (1999). *System Identification (2Nd Ed.): Theory for the User*. Upper Saddle River, NJ, USA: Prentice Hall PTR.
- Manchester, I. (2010). Input design for system identification via convex relaxation. In *Decision and Control (CDC), 2010 49th IEEE Conference on*, (pp. 2041–2046). IEEE.
- Marafioti, G., Bitmead, R., & Hovd, M. (2014). Persistently exciting model predictive control. *International Journal of Adaptive Control and Signal Processing*, 28(6), 536–552.
- Mayne, D. (2014). Model predictive control: Recent developments and future promise. *Automatica*, 50(12), 2967–2986.
- Mayne, D., Rawlings, J., Rao, C., & Socoart, P. (2000). Constrained model predictive control: Stability and optimality. *Automatica*, 36(6), 789–814.
- Mayne, D., Seron, M., & Raković, S. (2005). Robust model predictive control of constrained linear systems with bounded disturbances. *Automatica*, 41(2), 219–224.
- Middleton, R., Goodwin, G., Hill, D., & Mayne, D. (1988). Design issues in adaptive control. *IEEE transactions on automatic control*, 33(1), 50–58.

- Mullis, C. & Roberts, R. (1976). Roundoff noise in digital filters: Frequency transformations and invariants. *IEEE Transactions on Acoustics, Speech, and Signal Processing*, 24(6), 538–550.
- Ninness, B. & Gómez, J. C. (1996). Asymptotic analysis of mimo system estimates by the use of orthonormal bases. In *Proceedings of the 13th IFAC World Congress, San Francisco, USA*, (pp. 363–368).
- Rakovic, S., Kerrigan, E., Kouramas, K., & Mayne, D. (2005). Invariant approximations of the minimal robust positively invariant set. *IEEE Transactions on Automatic Control*, 50(3), 406–410.
- Rathouský, J. & Havlena, V. (2013). Mpc-based approximate dual controller by information matrix maximization. *International Journal of Adaptive Control and Signal Processing*, 27(11), 974–999.
- Rawlings, J. & Mayne, D. (2009). *Model predictive control: Theory and design*. Nob Hill Pub.
- Rawlings, J. B. & Risbeck, M. (2017). Model predictive control with discrete actuators: Theory and application. *Automatica*, 78, 258–265.
- Sbarbaro, . D., Filatov, N., & Unbehauen, H. (1999). Adaptive predictive controllers based on orthonormal series representation. *International Journal of Adaptive Control and Signal Processing*, 13(7), 621–631.
- Shor, N. (1987). Quadratic optimization problems. *Soviet Journal of Circuits and Systems Sciences*, 25.
- Staus, G., Biegler, L., & Ydstie, B. (1996). Adaptive control via non-convex optimization. In *State of the Art in Global Optimization* (pp. 119–137). Springer.
- Sutton, R. & Barto, A. (1998). *Reinforcement learning: An introduction*, volume 1. MIT press Cambridge.
- Tanaskovic, M., Fagiano, L., Smith, R., & Morari, M. (2014). Adaptive receding horizon control for constrained mimo systems. *Automatica*, 50(12), 3019–3029.
- Tawarmalani, M. & Sahinidis, N. V. (2005). A polyhedral branch-and-cut approach to global optimization. *Mathematical Programming*, 103, 225–249.
- VanAntwerp, J. & Braatz, R. (2000). A tutorial on linear and bilinear matrix inequalities. *Journal of process control*, 10(4), 363–385.
- Zeilinger, M., Raimondo, D., Domahidi, A., Morari, M., & Jones, C. (2014). On real-time robust model predictive control. *Automatica*, 50(3), 683–694.